

University of Windsor

Scholarship at UWindor

Electronic Theses and Dissertations

Theses, Dissertations, and Major Papers

Winter 2014

Synthesis and Characterization of Bis-bispidine-based Tetraazamacrocycles and Their Coordination Studies

Md. Jahirul Islam
University of Windsor

Follow this and additional works at: <https://scholar.uwindsor.ca/etd>

Recommended Citation

Islam, Md. Jahirul, "Synthesis and Characterization of Bis-bispidine-based Tetraazamacrocycles and Their Coordination Studies" (2014). *Electronic Theses and Dissertations*. 5011.
<https://scholar.uwindsor.ca/etd/5011>

This online database contains the full-text of PhD dissertations and Masters' theses of University of Windsor students from 1954 forward. These documents are made available for personal study and research purposes only, in accordance with the Canadian Copyright Act and the Creative Commons license—CC BY-NC-ND (Attribution, Non-Commercial, No Derivative Works). Under this license, works must always be attributed to the copyright holder (original author), cannot be used for any commercial purposes, and may not be altered. Any other use would require the permission of the copyright holder. Students may inquire about withdrawing their dissertation and/or thesis from this database. For additional inquiries, please contact the repository administrator via email (scholarship@uwindsor.ca) or by telephone at 519-253-3000ext. 3208.

**Synthesis and Characterization of Bis-bispidine-based Tetraazamacrocycles and Their
Coordination Studies**

By

Md. Jahirul Islam

A Thesis
Submitted to the Faculty of Graduate Studies
through the Department of **Chemistry and Biochemistry**
in Partial Fulfillment of the Requirements for
the Degree of **Master of Science**
at the University of Windsor

Windsor, Ontario, Canada

2013

© 2013 Md. Jahirul Islam

Synthesis and Characterization of Bis-bispidine-based Tetraazamacrocycles and Their
Coordination Studies

by

Md Jahirul Islam

APPROVED BY:

J. Gagnon
Earth & Environmental Sciences

H. Eichhorn
Department of Chemistry & Biochemistry

Z. Wang, Advisor
Department of Chemistry & Biochemistry

October 10, 2013

Declaration of Co-Authorship / Previous Publications

I. Co-Authorship Declaration

I hereby declare that this thesis incorporates material that is the result of joint research as follows:

This thesis incorporates the outcome of joint research undertaken in collaboration with Erin J. Miller, Jacob S. Gordner and Deep Patel under the supervision of Dr. Zhuo Wang. The collaboration with Erin J. Miller, Jacob S. Gordner and Deep Patel is covered in Chapter 2, section **2.2.3.1** (Synthesis and characterization of **7–9**) of this thesis. The collaboration with Erin J. Miller and Jacob S. Gordner is covered in Chapter 2, section **2.2.4.1** (Synthesis of **10**) of this thesis. My supervisor Dr. Zhuo Wang prepared the manuscript for publication in *Tetrahedron Letters*, **2013**, *54*, 2133. and I have compiled the data for the supporting information.

Single crystal X-ray data of compound **10** and **12** (Chapter 2) and **5** (Chapter 3) were collected and refined by Nicholas Vukotic (graduate student of Dr. Loeb's Group). Prof. C. L. B. Macdonald collected and refined the X-ray data for compound **9** (Chapter 2). Dr. Kelong Zhu collected raw X-ray data for compound **8** (Chapter 2) and I refined the data. Dr. Paul D. Boyle (UWO) collected and refined X-ray data for compound **7** (Chapter 3). All the single crystal X-ray data included in this thesis are unpublished.

I am aware of the University of Windsor Senate Policy on Authorship and I certify that I have properly acknowledged the contribution of other researchers to my thesis, and have obtained written permission from each of the co-author(s) to include the above material(s) in my thesis.

I certify that, with the above qualification, this thesis, and the research to which it refers, is the product of my own work.

II. Declaration of Previous Publication

This thesis includes [1] original paper that has been previously published in peer reviewed journals, as follows:

Thesis Chapter	Publication title/full citation	Publication status
Chapter 2	Effective Synthesis of Bis-Bispidinone and Facile Difunctionalization of Highly Rigid Macrocyclic Tetramines. Islam, M. J. ; Miller, E. J.; Gordner, J. S.; Patel, D.; Wang, Z., <i>Tetrahedron Lett.</i> 2013 , 54, 2133–2136.	Published

I certify that I have obtained written permission from the copyright owner to include the above published material in my thesis. I certify that the above material describes work completed during my registration as graduate student at the University of Windsor.

I declare that, to the best of my knowledge, my thesis does not infringe upon anyone's copyright nor violate any proprietary rights and that any ideas, techniques, quotations, or any other material from the work of other people included in my thesis, published or otherwise, are fully acknowledged in accordance with the standard referencing practices. Furthermore, to the extent that I have included copyrighted material that surpasses the bounds of fair dealing within the meaning of the Canada Copyright Act, I certify that I have obtained written permission from the copyright owner to include such material in my thesis.

I declare that this is a true copy of my thesis, including any final revisions, as approved by my thesis committee and the Graduate Studies office, and that this thesis has not been submitted for a higher degree to any other University or Institution.

Abstract

Bis-bispidine based tetraazamacrocycles can be used to encapsulate metal ions selectively to form highly stable complexes which may have interesting optical and electronic properties. This thesis discusses an effective synthetic pathway which has been used to obtain the desired bis-bispidine-based tetraazamacrocycles (Chapter 2). The synthesis of the macrocycles utilizes *N*-Boc-*N'*-allylbispidinone **4** as the starting material which was subsequently converted to diketal bis(chloroacetamide) **8** and diketal bis(iodoacetamide) **9**. Cyclization of diketal bispidine hydrochloride **7** and bis(iodoacetamide) **9** followed by reduction afforded diketal bis-bispidine tetraazamacrocycle **12**. Cleavage of the ketal groups afforded a versatile bis-bispidinone substrate **13** which was further functionalized to diester **16** and bis-bispidine **17**. The desired bis-bispidine tetraazamacrocycle **17** was also obtained through another synthetic pathway which is discussed in Chapter 2. All the new compounds have been characterized by ¹H, ¹³C NMR, IR, mass spectrometry and some by single crystal X-ray diffraction technique.

Bis-bispidine-based tetraazamacrocycles have been used for coordination studies with metal ions under different reaction conditions and this is discussed in Chapter 3.

Dedication

To my parents, my wife and my daughter

Acknowledgements

First of all, I would like to thank my supervisor Dr. Zhuo Wang for her guidance, support, advice and patience over the last couple of years. Thank you very much for giving me the opportunity to work in your research group. I acknowledge my supervisor for her significant contributions in all aspects of my research.

I would like to thank our past group members: Erin Miller, Jacob Gordner and Deep Patel, Samantha Scalia and Yiting Chen (Emily) for their help and friendship while working in the lab. I would like to thank the newest group members Wilson Luo and Miriam Zaltsman for proofreading my thesis.

I would like to thank Dr. Holger Eichhorn and Dr. Joel Gagnon for being on my committee and their valuable time in reading my thesis. I am also grateful to Dr. Sirinart Ananvoranich for taking her time to attend my defense and read my thesis.

I would like to thank Nicholas Vukotic, Prof. C. L. B. Macdonald, Dr. Kelong Zhu and Dr. Paul D. Boyle (UWO) for their help to collect and refine the single crystal X-ray data. I am very thankful to Dr. Matthew J. Revington for the assistance with NMR experiments, Dr. Janeen Auld for MS analysis, Dr. John Hayward for his help in IR measurement and Sinisa Djurdjevic for his help in melting point measurement.

I also like to thank Dr. James Green, Dr. Holger Eichhorn and Dr. John Hayward for arranging very helpful organic group meetings every week.

I am really grateful to Marlene, Beth and Cathy for their tremendous help and support throughout my graduate studies. I would like to thank the Department of Chemistry and Biochemistry and all the staff at the CCC for their help and cooperation.

I would like to express my heartfelt gratitude to all of my family members for their sacrifices, continuous support and encouragement throughout my entire life. Special thanks to my parents who have been praying from thousands of miles away for my wellbeing and success abroad. I would like to thank my loving wife Shahanara Akter for her endless cooperation, support and encouragement throughout my studies abroad. Many thanks to my little daughter Jemimah, whom was my motivation to work hard and I hope you will always be with me in all of my future endeavors.

Finally, I would like to thank the Natural Sciences and Engineering Research Council (NSERC), Canada Foundation for Innovation (CFI) and the University of Windsor for funding.

Table of Contents

Declaration Co-Authorship/Previous Publications	iii
Abstract	v
Dedication	vi
Acknowledgements	vii
List of Tables	xii
List of Figures	xiii
List of Schemes	xv
List of Appendices	xvi
List of Abbreviations/Symbols	xvii
Chapter 1: Introduction	1
1.1 Macrocycles.....	1
1.2 Importance of macrocyclic ligands.....	1
1.2.1 Chemical aspects.....	2
1.2.2 Biological aspects.....	4
1.3 Types of macrocyclic ligands.....	4
1.3.1 Oxygen-based macrocycles.....	4
1.3.2 Nitrogen-based macrocycles.....	5
1.3.2.1 Polyamine or imine macrocycles.....	5
1.3.2.2 Porphyrins and phthalocyanines.....	8
1.3.2.3 Bis-bispidine-based tetraazamacrocycles.....	9
1.3.3 Macrocycles containing donor atoms other than nitrogen and oxygen.....	13
1.4 Metal-ligand coordination.....	14
1.4.1 Metal ion dependence.....	14
1.4.2 Hole size ligands and its consequence.....	14
1.4.3 Metal-bis-bispidine complexes.....	17
1.5 Scope of this thesis.....	18
Reference.....	19

Chapter 2: Synthesis of Bis-bispidine-based Tetraazamacrocycles	22
2.1 Experimental	22
2.1.1 Materials and methods	22
2.1.2 Synthesis and characterization	23
2.1.3 X-ray crystallography	39
2.1.3.1 General data collection and refinement	39
2.1.3.2 Crystallographic data	39
2.2 Results and discussion	45
2.2.1 Retrosynthetic plan for bis-bispidinone 1	45
2.2.2 Synthesis of bis-bispidine hydrochloride 6	46
2.2.3 Synthesis and characterization of bis(iodoacetamide) 9	48
2.2.3.1 Synthesis and characterization	48
2.2.3.2 Crystallographic data analysis of 8	49
2.2.3.3 Crystallographic data analysis of 9	50
2.2.4 Synthesis and characterization of diketal bis-bispidine 12	51
2.2.4.1 Synthesis and characterization	51
2.2.4.2 Crystallographic data analysis of 10	53
2.2.4.3 Crystallographic data analysis of 12	54
2.2.5 Synthesis and characterization of bis-bispidinone 13	56
2.2.6 Synthesis and characterization of diester 16 and bis-bispidine 17	61
2.2.7 Synthesis and characterization of bispidine hydrochloride 19	62
2.2.8 Synthesis and characterization of bis(iodoacetamide) 21	64
2.2.9 Synthesis and characterization bisamide 22 and bis-bispidine 17	65
2.3 Conclusion	67
Reference	68
Chapter 3: Coordination Studies of Bis-bispidine-based Tetraazamacrocycles	70
3.1 Experimental	70
3.1.1 Materials and methods	70
3.1.2 Synthesis and characterization	70
3.1.2.1 Synthesis of diketal bis-bispidine-copper(II) complexes	70
3.1.2.2 Synthesis of diketal bis-bispidine-nickel(II) complex	71

3.1.2.3	Synthesis of diketal bis-bispidine-cobalt(II) complex	72
3.1.2.4	Synthesis of bis-bispidine-copper(II) complex	72
3.1.2.5	Synthesis of bis-bispidine-nickel(II) complex	74
3.1.2.6	Synthesis of bis-bispidine-cobalt(II) complexes	75
3.1.3	X-ray crystallography	75
3.1.3.1	General data collection and refinement for compound 5	75
3.1.3.2	General data collection and refinement for compound 7	76
3.1.3.3	Crystallographic data	77
3.2	Results and discussion	80
3.2.1	Synthesis towards metal-diketal bis-bispidine complexes	81
3.2.1.1	Attempted synthesis of 4	81
3.2.1.2	Crystallographic data analysis of 5	82
3.2.1.3	Coordination of 1 with Cu ²⁺ , Ni ²⁺ and Co ²⁺ ions	83
3.2.2	Synthesis towards metal-bis-bispidine complexes	84
3.2.2.1	Attempted synthesis of 6	84
3.2.2.2	Crystallographic data analysis of 7	85
3.2.2.3	Coordination of 2 with Cu ²⁺ , Ni ²⁺ and Co ²⁺ ions	87
3.3	Conclusion	89
	Reference	90
	Chapter 4: Conclusion and Future Work	92
4.1	Conclusion	92
4.2	Future work	93
	Appendices	94
Appendix A:	Copyright permission	94
	Vita Auctoris	95

List of Tables

Table 2.1	Crystallographic data for compound 8	39
Table 2.2	Crystallographic data for compound 9	41
Table 2.3	Crystallographic data for compound 10 •CH ₂ Cl ₂	42
Table 2.4	Crystallographic data for compound 12	43
Table 3.1	Crystallographic data for compound 5	77
Table 3.2	Crystallographic data for compound 7	78
Table 3.3	Reaction conditions of 1 with metal ions	84
Table 3.4	Reaction conditions of 2 with metal ions	88

List of Figures

Figure 1.1	Example of representative macrocycles	1
Figure 1.2	Macrocycles capable of binding with radioactive and paramagnetic metal ions	3
Figure 1.3	Example of macrocyclic sensor materials	3
Figure 1.4	Crown ethers of different ring sizes	5
Figure 1.5	Variation of the stability of copper(II) complexes with different tetramines	6
Figure 1.6	Schematic diagram of metal-directed template synthesis	7
Figure 1.7	Structure of porphyrin 15 and phthalocyanine 16	8
Figure 1.8	Example of bis-bispidine tetraazamacrocycles	9
Figure 1.9	Functionalized bis-bispidine-based tetraazamacrocycles 20 and 21	10
Figure 1.10	Example of sulfur-, phosphorous- and selenium-containing macrocycles	13
Figure 1.11	Determination of available cavity size	15
Figure 1.12	Structure of [Na(benzo-15-crown-5)(H ₂ O)]I 35	16
Figure 1.13	Structure of [Na(12-crown-4) ₂][(ClO ₄)] 36	16
Figure 1.14	Structure of [Na(18-crown-6)] ⁺ 37	17
Figure 1.15	Tetramethylbis-bispidine 38 and its copper(II) complex 39	17
Figure 1.16	Electronic spectra of 39 in CH ₃ NO ₂ (a) and in H ₂ O	18
Figure 1.17	Functionalized bis-bispidine-based tetraazamacrocycles 40	18

Figure 2.1	Bis-bispidine-based tetraazamacrocycles	45
Figure 2.2	Crystallographic structure of bis(chloroacetamide) 8	49
Figure 2.3	Crystallographic structure of bis(iodoacetamide) 9	50
Figure 2.4	Crystallographic structure of macrocyclic bisamide 10 •CH ₂ Cl ₂	54
Figure 2.5	Crystallographic structure of diketal tetraazamacrocycle 12	55
Figure 2.6	Molecular view of bis-bispidine tetraazamacrocycle 12 showing channels of the tetraamine cores	56
Figure 2.7	¹³ C NMR sample of (a) a freshly prepared sample of <i>N</i> -Boc- <i>N'</i> -ethoxycarbonylbispidinone 5 in MeOD. (b) the sample after overnight in MeOD. (c) the sample after evaporation of MeOD followed by dissolution in CDCl ₃	59
Figure 2.8	Formation of ketone hydrate 15 in aqueous medium	60
Figure 3.1	Bis-bispidine tetraazamacrocycles 1–3	80
Figure 3.2	Protonated diketal bis-bispidine tetraazamacrocycle 5	82
Figure 3.3	Crystallographic ORTEP plot of protonated diketal bis-bispidine 5	82
Figure 3.4	Protonated bis-bispidine tetraazamacrocycle 7	85
Figure 3.5	ORTEP diagram of protonated cation of 7	86
Figure 3.6	ORTEP drawing for the cation of 7 (major component)	86
Figure 3.7	ORTEP diagram of (a) disordered perchlorate anion of 7 , (b) major component of perchlorate anion	87

List of Schemes

Scheme 1.1	Synthesis of bridged cyclam 12 and cyclen 13	7
Scheme 1.2	Template synthesis of macrocyclic-Ni(II) complex 14	8
Scheme 1.3	Synthesis of dihydroxy bis-bispidine tetraazamacrocycle 20	11
Scheme 1.4	Synthesis of hydroxy bis-bispidine tetraazamacrocycle 21	12
Scheme 2.1	Retrosynthetic plan.	46
Scheme 2.2	Synthesis of <i>N</i> -Boc- <i>N'</i> -ethoxycarbonylbispidinone 5	47
Scheme 2.3	Synthesis of bis(iodoacetamide) 9	48
Scheme 2.4	Synthesis of diketal bis-bispidine tetraazamacrocycle 12	51
Scheme 2.5	Synthesis of bis-bispidinone 13	57
Scheme 2.6	Transformation of <i>N</i> -Boc- <i>N'</i> -ethoxycarbonylbispidinone 5 to dimethyl ketal	58
Scheme 2.7	Synthesis of bis-bispidine diester 16 and bis-bispidine 17	62
Scheme 2.8	Synthesis of bispidine hydrochloride 19	63
Scheme 2.9	Synthesis of bis(chloroacetamide) 20 and bis(iodoacetamide) 21	64
Scheme 2.10	Synthesis of macrocyclic bisamide 22 and bis-bispidine 17	66
Scheme 3.1	Coordination reaction of 1 with copper(II) triflate.	81
Scheme 3.2	Coordination reaction of 2 with copper(II) acetate	84
Scheme 4.1	Proposed synthesis of polymacrocycle 2 and polymetallomacrocycle 3 .	93

List of Appendices

Appendix A : Copyright Permission

94

List of Abbreviations/ Symbols

α	alpha position, or angle label (X-ray crystallography)
Å	angstrom
Anal.	analysis
β	beta position, or angle label(X-ray crystallography)
br	broad (NMR spectra)
^t Bu	tertiary butyl group
(Boc) ₂ O	di- <i>tert</i> -butyl dicarbonate
Calcd	calculated
¹³ C	carbon-13
CDCl ₃	deuterated chloroform
cm	centimetres
cm ⁻¹	wave numbers (reciprocal centimetres)
δ	chemical shift (NMR spectra)
d	doublet (NMR spectra)
dd	doublet of doublets (NMR spectra)
dq	doublet of quartets (NMR spectra)
ddt	doublet of doublet of triplets (NMR spectra)
°	degrees
°C	degrees Celsius
dm	doublet of multiplets (NMR spectra)
D ₂ O	Deuterium oxide
DMSO	dimethyl sulfoxide

DBU	1,8-Diazabicyclo[5.4.0]undec-7-ene
DIBAL	Diisobutylaluminium hydride
Et ₂ O	diethyl ether
EtOH	ethanol
EA	elemental analysis
equiv	equivalents
<i>F</i>	structure factors (X-ray crystallography)
FW	formula weight
g	gram
γ	Gamma position, or angle label (X-ray crystallography)
GOF	Goodness-of-fit (X-ray crystallography)
h	hour(s)
¹ H	proton
HRMS	high resolution mass spectrometry
Hz	Hertz
IR	infrared
ⁱ Pr	Isopropyl
<i>J</i>	coupling constant
λ	Wavelength (X-ray crystallography)
μ	absorption coefficient (X-ray crystallography)
M	central metal atom or molar concentration
M ⁺	parent ion (Mass spectrometry)
m	multiplet

MHz	Megahertz
min	minutes
mL	milliliter
mmol	millimole
mol	mole
MS	mass spectrometry
MW	molecular weight
m/z	mass/charge
μm	micrometer
Me	methyl
MeCN	acetonitrile
MeOD	deuterated methanol
MeOH	methanol
NMR	nuclear magnetic resonance
ORTEP	Oak ridge thermal ellipsoid plot (X-ray crystallography)
Ph	phenyl group
ppm	parts per million
%	percent
θ	theta diffraction/Braggs' angle (X-ray crystallography)
q	quartet (NMR spectra)
<i>R</i>	reliability factor (X-ray crystallography)
SAINT	SAX area-detector integration (SAX-Siemens analytical X-ray)
SADABS	Siemens area detector absorption correction
SMART	Siemens molecular analysis research tool

s	singlet (NMR spectra) or seconds
t	triplet
THF	tetrahydrofuran
TMS	trimethylsilane
TLC	Thin layer chromatography
UV	Ultraviolet
V	unit cell volume (X-ray crystallography)
Z	asymmetric units per unit cell (X-ray crystallography)
H ₂ O	water

Chapter 1: Introduction

1.1 Macrocycles

A 'macrocycle' is a large cyclic molecule comprising a ring of at least nine atoms that includes a minimum of three potential donor atoms.^{1,2} Figure 1.1 illustrates three different examples of representative macrocycles. The donor atoms of a macrocyclic ligand are oriented in such way that they can coordinate to the electron deficient metal ions by donating pairs of electrons.

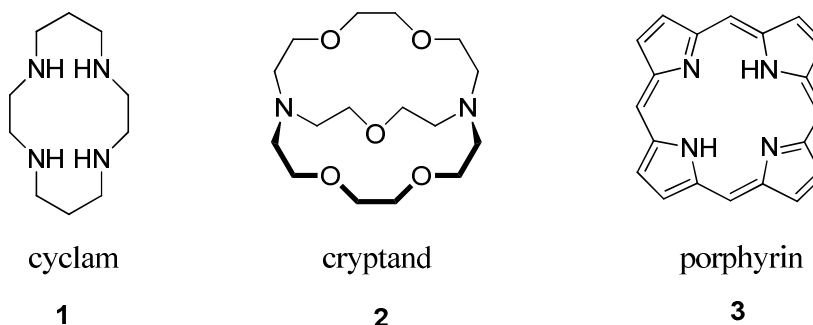


Figure 1.1 Example of representative macrocycles.

1.2 Importance of macrocyclic ligands

In the early 1960s, the development of macrocyclic ligands started with the discovery of the nickel-mediated condensation of tris-ethylenediamine nickel(II) perchlorate and acetone by Busch and Curtis.^{3,4} The early impetus in the synthesis of macrocyclic ligands and their complexes was focused on mimicking naturally occurring macrocycles such as metalloproteins, porphyrins, corrins and cobalamines.^{5,6} Simple synthetic macrocycles can be considered as the structural models for biological molecules. For example, the synthesis and study of porphyrins and their derivatives would provide insights of heme proteins which are responsible in dioxygen-activation and electron-transfer processes.¹

Therefore, a study of the synthetic model compounds would give a better understanding of the naturally occurring biomolecules.¹ The growing attention in this exciting and interesting field can be attributed to the following aspects in chemistry and biology.

1.2.1 Chemical aspects

Metal complexes of macrocyclic ligands are highly stable both thermodynamically and kinetically in comparison to their open chain analogs.^{1,7} Due to the structural resemblance and high stability, some of these complexes could be used in the construction of models for metalloproteins.⁸ For instance, cyclodextrins and their derivatives can bind various molecular substrates which could serve as models for various enzymatic processes.⁸

One of the most important applications of macrocyclic ligands is to extract metal ions selectively. Therefore, conventional 'pyrometallurgy' which involves a high temperature process that emits green-house gases, can be replaced by environmentally friendly hydrometallurgy. The latter technique involves the dissolution of metal ions from the ores in an aqueous solution and extraction of the metal ions of interest using macrocycles in an organic solvent. Recovery of metal ions can lead to pure metal ions of interest.^{1,9}

In addition, macrocyclic ligands and their transition metal complexes have pharmacological properties and are currently being used as therapeutic and diagnostic agents in the biomedical arena. For example, previously lethal metal-overload disorders such as Wilson's disease and thalassaemia, were identified as copper and iron overload, respectively. A successful treatment of these disorders can be achieved by using macrocyclic agents.¹⁰ Due to the chelation property, macrocyclic compounds such as enterobactin and [15]pyN₅ can bind iron and copper ions accumulated in tissues,

respectively, and reduce their quantity significantly.^{11,12} In addition, paramagnetic complexes of Gd^{3+} , Tb^{3+} , Eu^{3+} and Mn^{2+} with macrocyclic ligands such as tetrakis(carboxymethyl)-1,4,7,10-tetraazacyclo-dodecane (DOTA) **4** and 1,4,10,13-tetraoxa-7,16-diaza-cyclooctadecane-7,16-diacetic acid (ODDA) **5** are being used widely as magnetic resonance imaging (MRI) contrast agents (Figure 1.2).^{1,10,13-15}

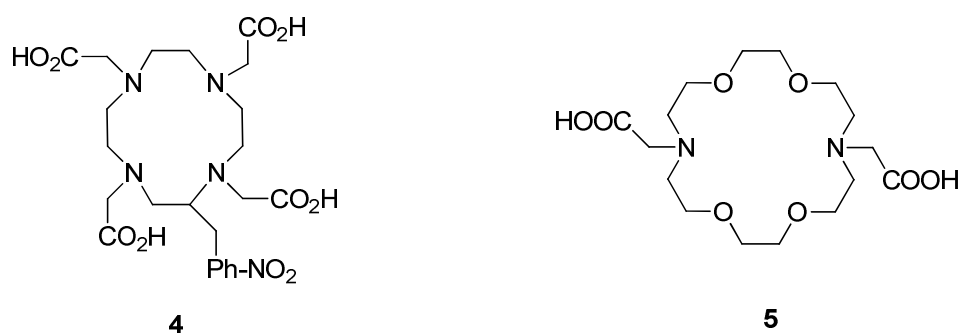


Figure 1.2 Macrocycles capable of binding with radioactive and paramagnetic metal ions.^{1,15}

Furthermore, macrocyclic ligands can be used in different microelectronic devices and sensors for the selective detection, amplification, and recognition of metal ions.¹ For example, macrocycles **6** and **7** can be used as sensor materials to detect Co^{2+} ions efficiently whereas macrocycle **8** has been used for the selective detection of Zn^{2+} ions in living systems (Figure 1.3).¹⁶⁻¹⁸

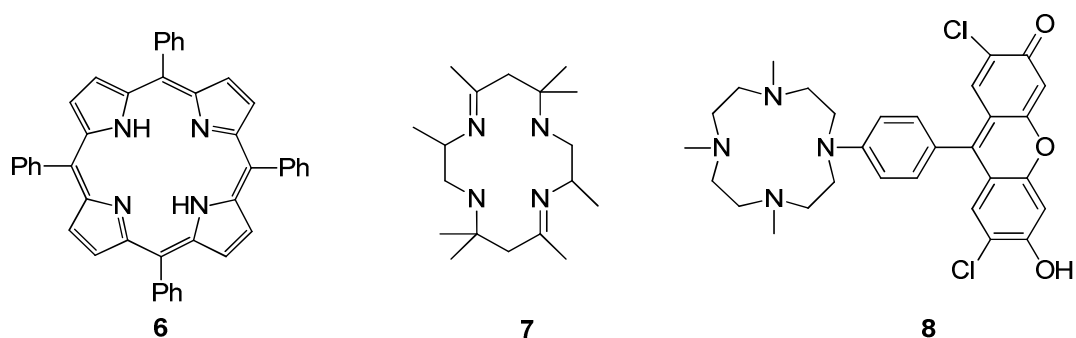


Figure 1.3 Example of macrocyclic sensor materials.

1.2.2 Biological aspect

Macrocyclic ligands and their complexes are ubiquitous in biological systems. In living systems, electron deficient metal ions, such as iron, magnesium and cobalt, can bind electron-rich bio-molecules to form metallobiomolecules which play an important role in biological systems.¹⁹ For instance, haemoglobin, also known as the iron metalloprotein, can be considered as the ‘molecular shuttle’ for electron transport, dioxygen transport and storage.¹ Besides, oxygen-based nonactin ligands are involved in alkali metal transportation as well as in ionic balances within the cell.¹

1.3 Types of macrocyclic ligands

A majority of ligands consist of oxygen, nitrogen, phosphorous or sulfur donor atoms. Depending on the nature and type of the donor atoms present, they can be classified into three major categories: oxygen-based macrocycles, nitrogen-based macrocycles, and macrocycles with donor atoms other than nitrogen and oxygen atoms.¹

1.3.1 Oxygen-based macrocycles

Cyclic polyethers are oxygen-based macromolecules that are well-known as the ‘crown ethers’. These are a large family of ligands with different ring sizes and varying number of the repeating ethyleneoxy (-CH₂CH₂O-) unit.¹ Macrocycles **9–11** are three different crown ethers of different ring sizes (Figure 1.4). Crown ethers are the accidental discovery by Charles Pedersen who was working at DuPont in 1967 and noticed the stronger affinity of crown ethers toward the alkali and alkaline earth metal ions.^{20,21} The complexation properties of crown ethers have been studied extensively and found to have had a large contribution towards the development of supramolecular host-guest chemistry.

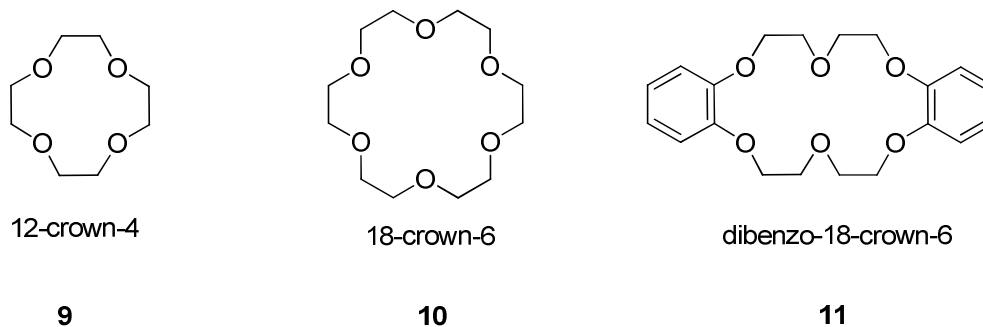


Figure 1.4 Crown ethers of different ring sizes.

Crown ethers with different ring sizes provide variable cavity sizes. For instance, the cavity sizes of [12]crown-4, [15]crown-5, and [18]crown-6 are 1.2–1.4 Å, 1.7–2.2 Å and 2.6–3.2 Å, respectively.² The different cavity sizes allow the crown ethers to bind metal ions with varying ionic radii to form stable complexes. Crown ethers can be used as scavengers to remove radioactive elements from the environment as well as extraction reagents to remove undesired elements in organic solvents.²² They also have potential applications in organic synthesis such as phase transfer catalysis and drug delivery.^{1,23}

1.3.2 Nitrogen-based macrocycles

1.3.2.1 Polyamine or imine macrocycles

The nitrogen atoms in a macrocyclic ring system coordinate with metal ions in a similar fashion as their open-chain analogues.¹ In terms of stability, however, they differ significantly. In general, a metal complex from a polydentate ligand is more stable in comparison to that from a monodentate ligand and this phenomenon is known as the *chelate effect*.^{24,25} Because of the effect, the stability of the complexes vary. Below is a series of copper(II) complexes that have different stability constants K (Figure 1.5).²⁴

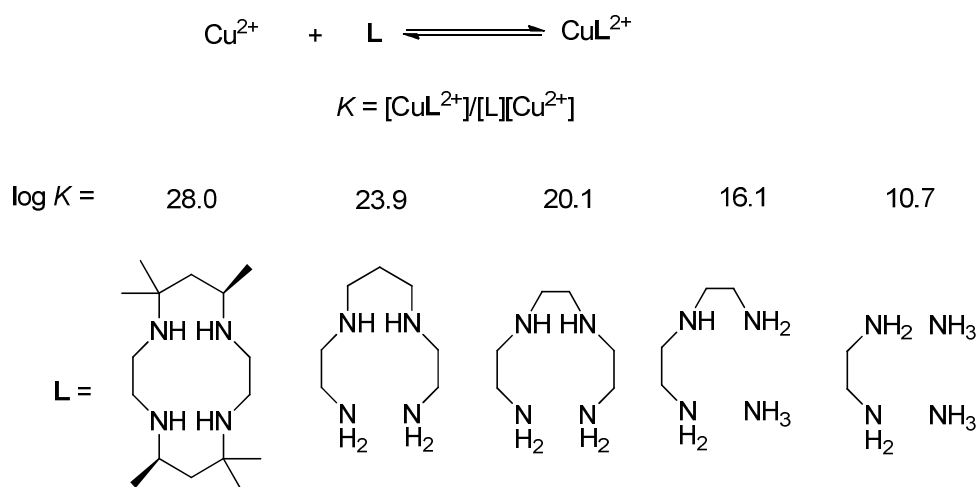
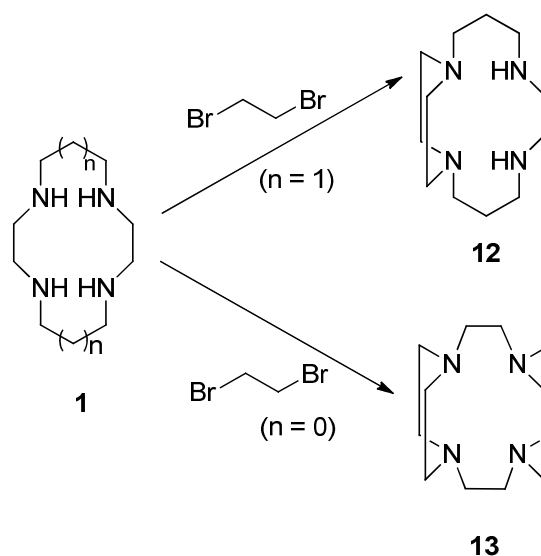


Figure 1.5 Variation of the stability of copper(II) complexes with different tetramines.

Construction of stable metal-ligand complexes depends on the complementarity between a metal ion and a ligand which includes the matching of their size, geometry and electronic environment.²⁶ Furthermore, by introducing topological constraints in a ligand, the affinity to a metal ion can be enhanced several fold.²⁶

Nitrogen-based macrocyclic ligands with a varying number of donor atoms, ring sizes and structural topologies have been synthesized. Among them, tetraazamacrocycles, commonly known as cyclams, are extensively studied.

The synthesis of topologically constrained tetraazamacrocycles can be classified into two synthetic routes: direct organic synthesis and metal-directed template synthesis.¹ In the direct organic synthetic approach, the tetraazamacrocyclic compounds of interest are obtained through organic transformations from smaller organic units. For example, Wainwright et al. synthesized bridged cyclam **12** and cyclen **13** through alkylation of **1** with 1,2-dibromoethane (Scheme 1.1).^{27,28}



Scheme 1.1 Synthesis of bridged cyclam **12** and cyclen **13**.

Although macrocyclic compounds can be synthesized by direct organic transformations, the instability of a reactant or the conformational changes required during macrocyclic ring closures can be a potential problem and, in some cases, can lead to undesired products.^{1,24} In order to circumvent these problems, metal-directed template approach is used. In this approach, a metal ion is attached to the coordination sites of a ligand, which can pre-organize and facilitate ring closures (Figure 1.6).¹

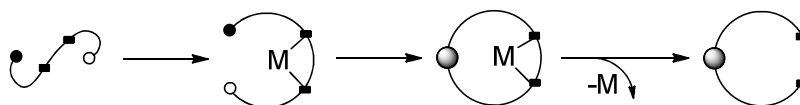
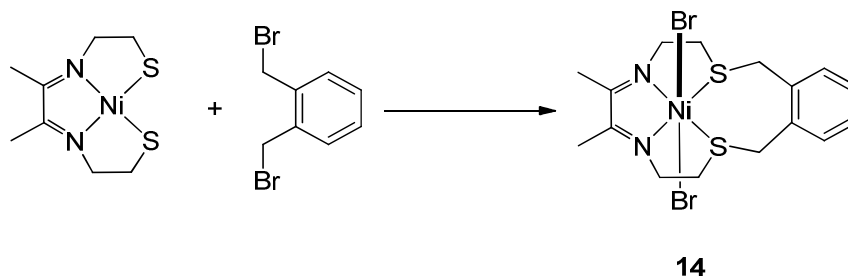


Figure 1.6 Schematic diagram of metal-directed template synthesis.¹

For example, nickel(II)- N_2S_2 complex **14**, can be easily synthesized by the template method but cannot be prepared using the direct method due to the instability of the metal-free N_2S_2 reactant (Scheme 1.2).¹

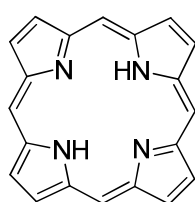


Scheme 1.2 Template synthesis of macrocyclic-nickel(II) complex **14**.

Although template synthesis has advantages such as conformational control on the desired products, the removal of metal ions from the highly stable metal complex can be a potential problem.²⁴

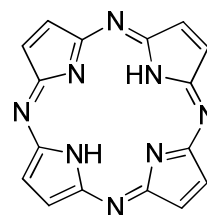
1.3.2.2 Porphyrins and phthalocyanines

Porphyrin **15** is a biologically important nitrogen-containing ligand because of its involvement in living systems (Figure 1.7).¹ In terms of structure, phthalocyanine **16** is an analog of porphyrin. Porphyrins have the ability to form complexes with iron(II) which are involved in dioxygen binding, transportation and metabolism.¹ Porphyrin- and phthalocyanine-based compounds are also of interest in dyes and pigments, molecular electronics, solar cells and supramolecular chemistry.²⁹⁻³¹



15

porphyrin



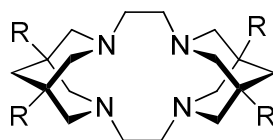
16

phthalocyanine

Figure 1.7 Structure of porphyrin **15** and phthalocyanine **16**.

1.3.2.3 Bis-bispidine-based tetraazamacrocycles

Bis-bispidine-based tetraazamacrocycles are new types of macrocycles with four nitrogen donor atoms in the structure (Figure 1.8). These ligands are highly rigid and pre-organized with no configurational flexibility.^{32,33} In addition, the four tertiary amino groups provide increased nucleophilicity in comparison to the secondary amino groups of cyclam.³² This, together with the steric hindrance around the cavity, is expected to facilitate metal-ion encapsulation to form highly stable complexes with interesting electronic properties such as charge transfer and redox properties.^{1,8,32,33}



(**17**, R = Ph)

(**18**, R = Me)

(**19**, R = H)

Figure 1.8 Example of bis-bispidine tetraazamacrocycles.

Although these macrocycles are interesting both in terms of structure and property, they have not been studied extensively because of synthetic challenges.^{32,34,35} Miyahara et al. synthesized the first tetraphenylbis-bispidine **17** (R = Ph) and found them to have very low solubility in organic solvents, which was a potential problem for further study of the compound.³⁶ Comba and coworkers prepared tetramethylbis-bispidine **18** (R = Me) and its Cu(II) complex which exhibited interesting optical properties, however, the characterization of the complex was minimal.³³ To date, this is the only bis-bispidine-metal complex that has been reported. Miyahara et al. also constructed bis-bispidine

tetraazamacrocycle **19** (R = H) which was found to be readily soluble in a wide range of solvents from nonpolar hexane to polar aqueous medium.³⁷

As part of the research interest in our group to make polytetraazamacrocycles, a modular synthetic protocol has been developed to give functionalized bis-bispidine tetraazamacrocyclic compounds **20** and **21** (Figure 1.9).³⁸

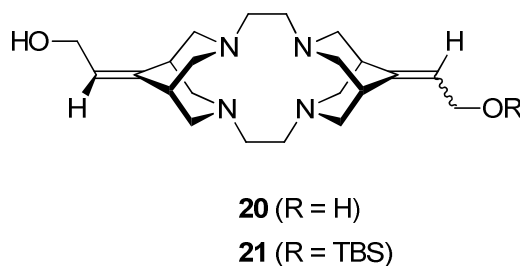
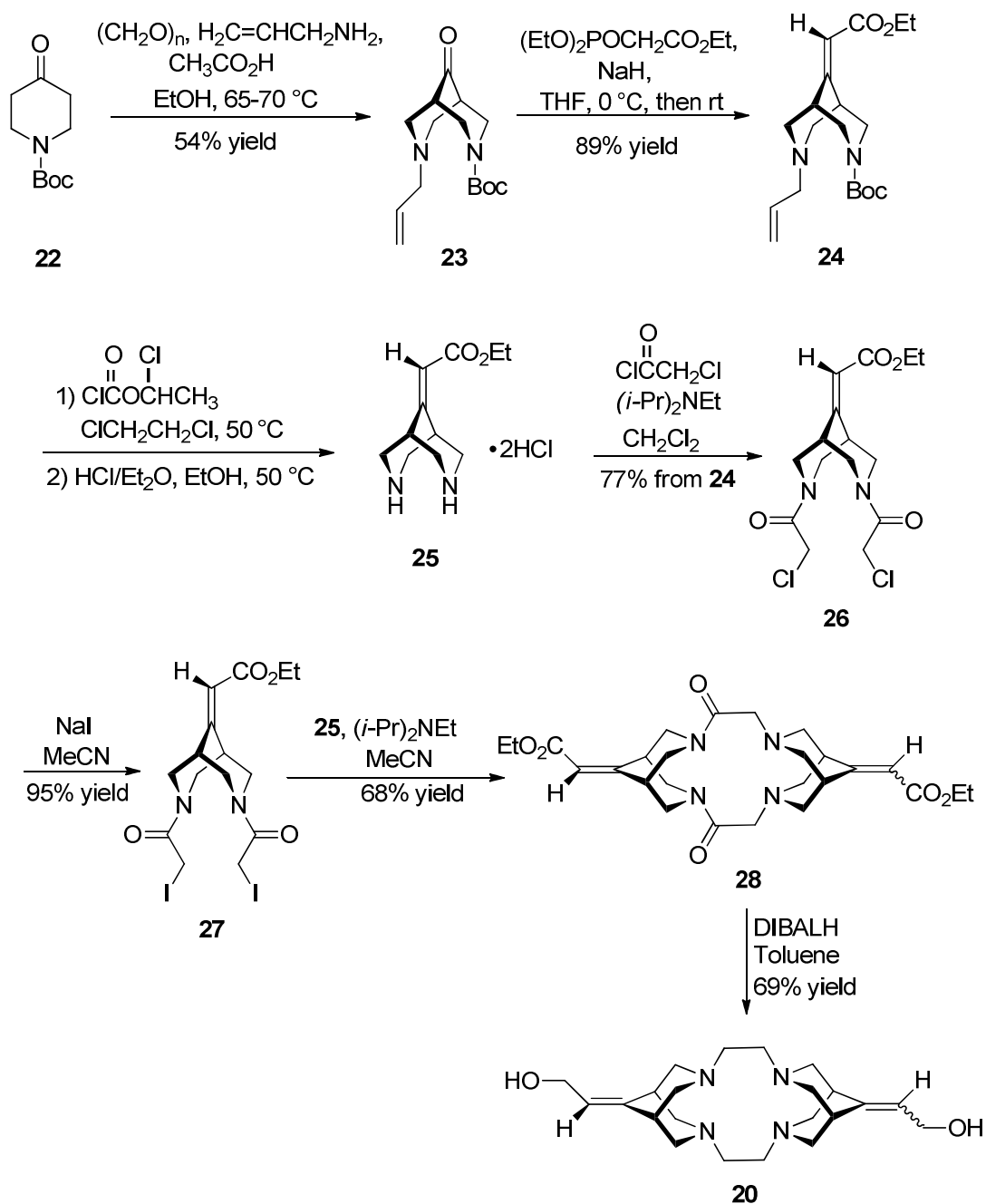


Figure 1.9 Functionalized bis-bispidine-based tetraazamacrocycles **20** and **21**.

In this synthetic protocol, double Mannich reaction of *N*-Boc-4-piperidone **22** with paraformaldehyde and allylamine gave *N*-Boc-*N'*-allylbispidinone **23** (Scheme 1.3). Reaction of triethyl phosphonoacetate with a strong base followed by the nucleophilic addition of the carbanion to bispidinone **23** yielded bispidine ester **24** under Horner-Wadsworth-Emmons conditions.³⁹ Removal of the allyl group on **24** in the presence of 1-chloroethyl chloroformate and the cleavage of the resulting carbamate group and the Boc protective group afforded bispidine hydrochloride **25**.

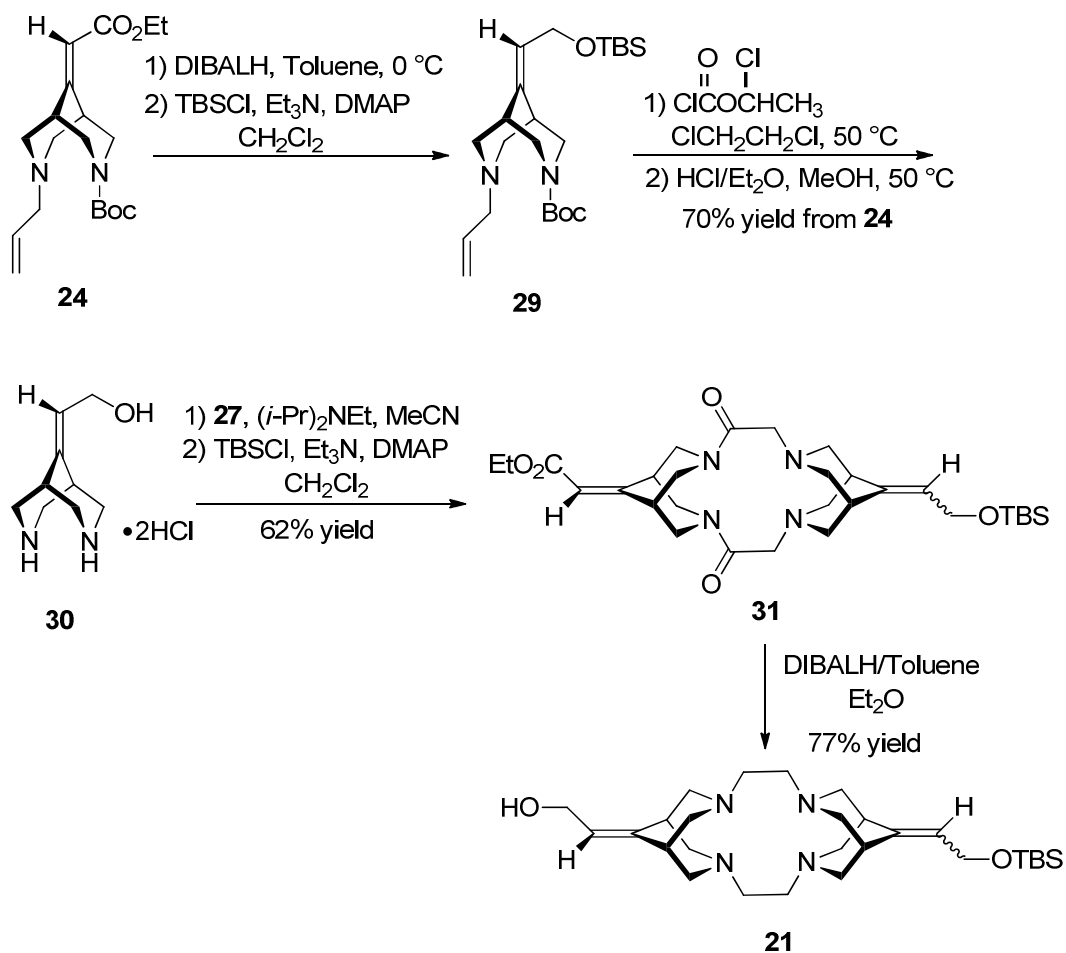
The acetylation reaction of bispidine hydrochloride **25** with chloroacetyl chloride was carried out to obtain bis(chloroacetamide) **26** which can be further transformed into bis(iodoacetamide) **27** upon treatment with sodium iodide. Cyclization of bispidine hydrochloride **25** and bis(iodoacetamide) **27** afforded macrocyclic bisamide **28** at

ambient temperature. DIBALH reduction of bisamide **28** in toluene was achieved to give functionalized bis-bispidine tetraazamacrocycle **20**.



Scheme 1.3 Synthesis of dihydroxy bis-bispidine tetraazamacrocycle **20**.

In order to make bis-bispidine tetraazamacrocycle **21** with different functional groups on each end of the macrocyclic framework, the functional groups were incorporated before the macrocycle formation. DIBALH reduction of bispidine ester **24** followed by TBS protection of the –OH group afforded silyl ether **29** (Scheme 1.4). Removal of the allyl, Boc and TBS groups in **29** through reaction with 1-chloroethyl chloroformate followed by treatment with HCl provided hydroxybispidine **30**. Macrocyclization of bis(iodoacetamide) **27** and hydroxybispidine **30** generated bisamide **31** which upon DIBAL reduction afforded bis-bispidine tetraazamacrocycle **21**.



Scheme 1.4 Synthesis of hydroxy bis-bispidine tetraazamacrocycle **21**.

The modular approach was a good starting point to obtain functionalized bis-bispidine-based macrocycles, especially for the independent incorporation of different functional groups to each end of the macrocyclic frameworks. However, this protocol was not applicable when identical labile functionalities, such as ester group, were desired on the macrocyclic framework. Therefore, in our pursuit to study the coordination chemistry of this type of compounds, a synthetic approach was needed which would allow the facile and concurrent incorporation of labile functional groups onto the bis-bispidine-based tetraazamacrocyclic framework.³⁴ This is discussed in detail in Chapter 2 of this thesis.

1.3.3 Macrocycles containing donor atoms other than nitrogen and oxygen

Macrocycles containing donor atoms other than nitrogen and oxygen are also known. Macrocyclic ligands **32**, **33** and **34** are examples of sulfur-, phosphorus- and selenium-based macrocycles, respectively (Figure 1.10).¹ Gellman et al. studied the structure and complexation properties of macrocycles consisting of phosphorous and sulfur.⁴⁰ However, the cumbersome syntheses of these ligands using toxic reagents limited their study in comparison to their nitrogen and oxygen analogues.

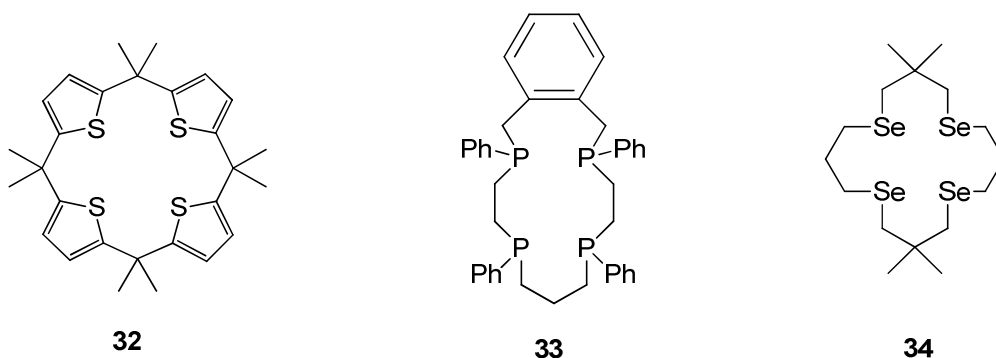
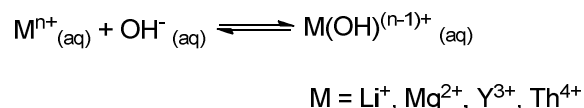


Figure 1.10 Example of sulfur-, phosphorous- and selenium-containing macrocycles.¹

1.4 Metal-ligand coordination

1.4.1 Metal ion dependence

Whether a metal ion can form a stable complex depends on criteria such as the ionic radius and charge density of the metal ions of interest.⁸ Complexation between a positively charged metal ion and an anionic or neutral ligand is an electrostatic interaction.⁷ For a particular ligand, the stability of its metal complexes vary with the charges on the metal cations. For example, when Li^+ , Mg^{2+} , Y^{3+} and Th^{4+} form complexes with OH^- , the stability constant $\log K$ are 0.3, 2.1, 7.0 and 10, respectively.⁷



Surface charge density also affects the stability of a complex. Surface charge density can be defined as “the ratio between the charge on a surface and the surface area”.⁷ When the ionic radius of the metal ion increases with a fixed charge on it, the effective attractive force of the metal ion for a ligand decreases. This can lead to a low stability constant of a complex. For instances, when divalent metal cations Be^{2+} , Mg^{2+} , Ca^{2+} and Ba^{2+} form complexes with OH^- in the above equation, the $\log K$ values are 7.0, 2.1, 1.5 and 0.6 respectively.⁷

1.4.2 Hole size of ligands and its consequences

The hole-size or cavity of a macrocyclic ligand can be defined as “the void which is occupied by a metal ion in a complex or is available to be occupied by a metal ion in the case of a free ligand”.⁴¹ The size of a cavity depends on several factors, such as the ring

size of the ligand, type and nature of the donor atoms, number of binding atoms, as well as conformational changes within the ligand.²⁴

The effective radius of cavity $r(H)$ can be determined from the distance between two diagonal donor atoms using molecular or computer-generated models or solid state X-ray crystallographic data.¹ In simple tetraazamacrocycles and crown ethers, it is calculated by subtracting the Pauling covalent radii of the donor atom $r(D)$ from the half distance between two diagonally located donor atoms, r (Figure 1.11).²⁴

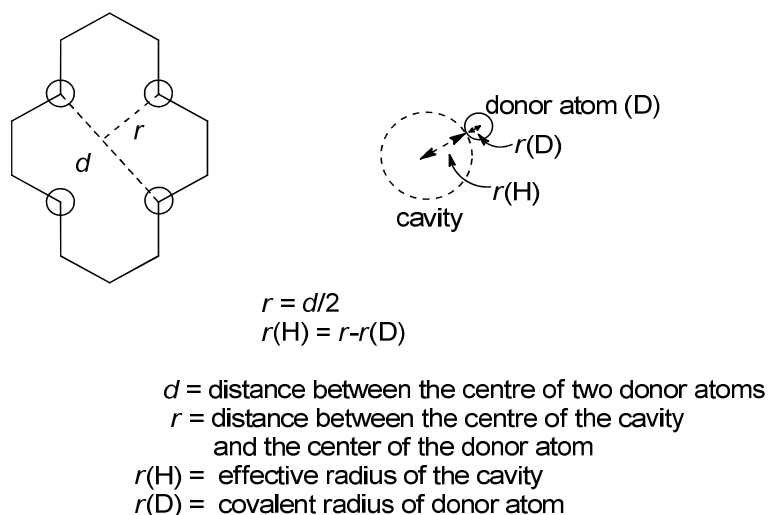


Figure 1.11 Determination of available cavity size.²⁴

The fit between the effective radius of a ligand cavity and the ionic radius of a metal ion determines the formation, stability and shape of the complex. The closer the fit, the more stable is the complex.³² A perfect matching of the size of metal ion and the ligand cavity can lead to the most stable complex, like a key and lock.⁴²

A slightly larger metal ion compared to the available cavity of the ligand can lead to a 1:1 complex where the metal ion occupies a position slightly above the mean plane of the

cavity.^{1,43} For example, in the pentagonal pyramid complex **35**, Na⁺ ion is larger than the cavity size of the crown ether benzo-15-crown-5 and sits 0.75 Å above the mean plane of the cavity (Figure 1.12).^{1,43}

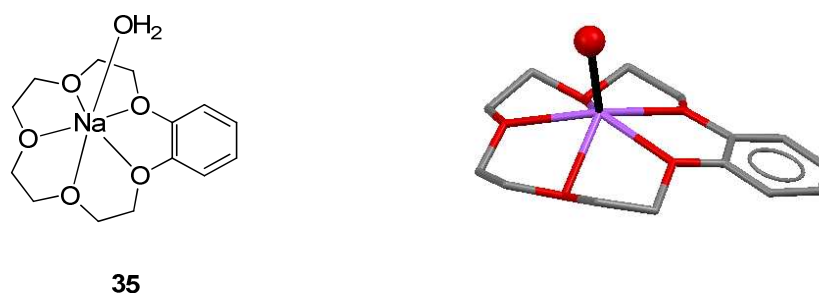


Figure 1.12 Structure of [Na(benzo-15-crown-5)(H₂O)]I **35**.^{1,43}

A cation too large to fit in a cavity can form a 2:1 sandwich complex where the metal ion sits in between the two ligands.⁴⁴ For instance, in structure **36**, Na⁺ is coordinated to two molecules of 12-crown-4 (Figure 1.13).^{1,45}

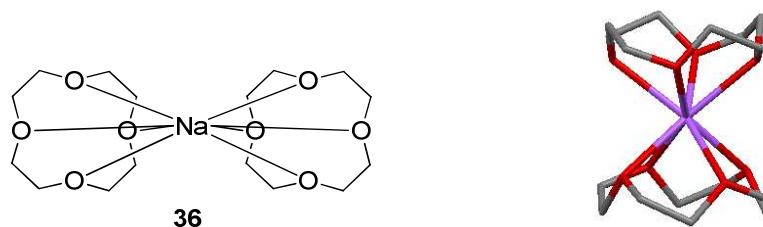


Figure 1.13 Structure of [Na(12-crown-4)₂][(ClO₄)] **36**.⁴⁵

In contrast, metal ions with an ionic radius smaller than the cavity of a ligand could induce a folding of the ligand. Formation of dinuclear complexes is also possible.⁴⁶⁻⁴⁸ An example is structure **37**, where the Na⁺ ion induces the folding of 18-crown-6 (Figure 1.14).⁴⁹



Figure 1.14 Structure of $[\text{Na}(18\text{-crown-6})]^+$ **37**.⁴⁹

1.4.3 Metal-bis-bispidine complexes

Due to their structural rigidity and the steric hindrance around the cavity, bis-bispidine-based tetraazamacrocycles are expected to encapsulate metal ions selectively and form highly stable complexes. Comba et al. synthesized tetramethylbis-bispidine **38** from diazaadamantane derivatives and studied its coordination with copper(II) ions (Figure 1.15).³³ However, no crystal structures of the complex **39** had been obtained.

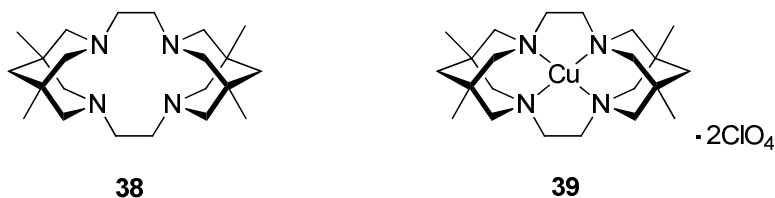


Figure 1.15 Tetramethylbis-bispidine **38** and its copper(II) complex **39**.³³

The UV-Visible spectra of the proposed copper(II) complex **39** showed a λ_{max} of 390 nm in nitromethane and 430 nm in water, which indicated that **38** had the highest ligand field strength for a tetraamine donor (Figure 1.16).^{32,33} Comba et al. stated that “In comparison with the parent $[\text{Cu}(\text{cyclam})]^{2+}$ compound there is a shift of the maximum by 110 nm (5740 cm^{-1} , 68 kJmol^{-1}) to lower wavelengths. This is the result of the increased nucleophilicity of the amines, a significant shortening of the Cu–N bonds, and the

shielding of the axial coordination sites''.³³ These results suggest that bis-bispidine-based metal complexes may have interesting optical and electronic properties worthy of further investigation.

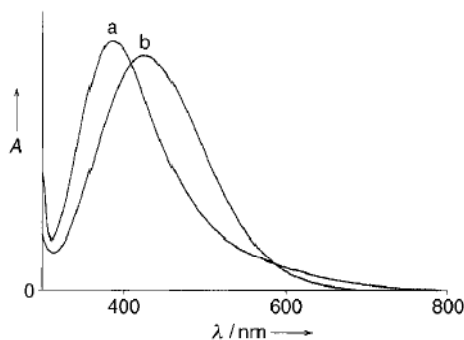
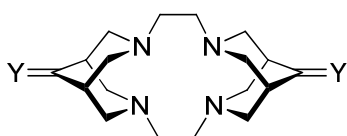


Figure 1.16 Electronic spectra of **39** in CH_3NO_2 (a) and in H_2O .³³

1.5 Scope of this thesis

This thesis illustrates the synthesis and coordination study of bis-bispidine-based tetraazamacrocycles. Chapter 2 includes the synthesis and characterization of bis-bispidine-based tetraazamacrocycles **40** (Figure 1.17).²⁵



40

($Y = \text{O}, [\text{OEt}]_2, \text{H}_2, \text{CHCO}_2\text{Et}$)

Figure 1.17 Functionalized bis-bispidine-based tetraazamacrocycles **40**.²⁵

In Chapter 3, attempts to obtain the metal complexes of bis-bispidine-based tetraazamacrocycles are discussed. Chapter 4 provides a summary of the research in this thesis and outlines suggested future work.

Reference

- (1) Constable, E. C. *Coordination Chemistry of Macrocyclic Compounds*; Oxford University Press: New York, 1999.
- (2) Melson, G. A. *Coordination Chemistry of Macrocyclic Compounds*; Plenum Press: New York, 1979.
- (3) Thompson, M. C.; Busch, D. H. *J. Am. Chem. Soc.* **1962**, *84*, 1762.
- (4) Curtis, N. F. *J. Chem. Soc.* **1960**, 4409.
- (5) Chandra, S. S., S. *J. Indian Chem. Soc.* **2006**, *83*, 988.
- (6) Chandra, S.; Pundir, M. *Spectrochim. Acta. A.* **2008**, *69*, 1.
- (7) Lawrance, G. A. *Introduction to Coordination Chemistry*; John Wiley & Sons Ltd, 2010.
- (8) Dietrich, B.; Viout, P.; Lehn, J.-M. *Macrocyclic Chemistry: Aspects of Organic and Inorganic Supramolecular Chemistry*; VCH Weinheim: New York, 1993.
- (9) Fenton, D. E. *Pure & Appl. Chem.* **1993**, *65*, 1493.
- (10) Gispert, J. R. *Coordination Chemistry*; Wiley-VCH Verlag: Weinheim, 2008.
- (11) Pollack, J. R.; Neilands, J. B. *Biochem. Biophys. Res. Commun.* **1970**, *38*, 989.
- (12) Fernandes, A. S.; Cabral, M. F.; Costa, J.; Castro, M.; Delgado, R.; Drew, M. G. B.; Felix, V. *J. Inorg. Biochem.* **2011**, *105*, 410.
- (13) Edelman, R. R.; Hesselink, J. R.; Zlatkin, M. B. *MRI: Clinical Magnetic Resonance Imaging*; W. B. Saunders, 1996.
- (14) DeNardo, G. L.; Mirick, G. R.; Kroger, L. A.; O'Donnell, R. T.; Meares, C. F.; DeNardo, S. J. *J. Nucl. Med.* **1996**, *37*, 451.

- (15) Burai, L.; Tóth, É.; Seibig, S.; Scopelliti, R.; Merbach, A. E. *Chem. Eur. J.* **2000**, *6*, 3761.
- (16) Bernhardt, P. V.; Moore, E. G. *Aust. J. Chem.* **2003**, *56*, 239.
- (17) Hirano, T.; Kikuchi, K.; Urano, Y.; Higuchi, T.; Nagano, T. *Angew. Chem. Int. Ed. Eng.* **2000**, *39*, 1052.
- (18) K. Jain, A.; K. Gupta, V.; P. Singh, L.; Khurana, U. *Analyst* **1997**, *122*, 583.
- (19) Storr, T.; Thompson, K. H.; Orvig, C. *Chem. Soc. Rev.* **2006**, *35*, 534.
- (20) Pedersen, C. J. *J. Am. Chem. Soc.* **1967**, *89*, 7017.
- (21) Pedersen, C. J. *J. Am. Chem. Soc.* **1967**, *89*, 2495.
- (22) McDowell, W. J. *Sep. Sci. Technol.* **1988**, *23*, 1251.
- (23) Rudkevich, D. M. *Bull. Chem. Soc. Jpn.* **2002**, *75*, 393.
- (24) Constable, E. C. *Metals and Ligand Reactivity* Chichester, West Sussex, England, 1990.
- (25) Hubin, T. J. *Coord. Chem. Rev.* **2003**, *241*, 27.
- (26) Busch, D. H. *Chem. Rev.* **1993**, *93*, 847.
- (27) Wainwright, K. P. *Inorg. Chem.* **1980**, *19*, 1396.
- (28) Ramasubbu, A.; Wainwright, K. P. *J. Chem. Soc., Chem. Commun.* **1982**, 277.
- (29) Yella, A.; Lee, H.-W.; Tsao, H. N.; Yi, C.; Chandiran, A. K.; Nazeeruddin, M. K.; Diau, E. W.-G.; Yeh, C.-Y.; Zakeeruddin, S. M.; Grätzel, M. *Science*, *334*, 629.
- (30) Walter, M. G.; Rudine, A. B.; Wamser, C. C. *J. Porphyrins Phthalocyanines*, *14*, 759.
- (31) Anderson, S.; Anderson, H. L.; Bashall, A.; McPartlin, M.; Sanders, J. K. M. *Angew. Chem. Int. Ed. Eng.* **1995**, *34*, 1096.

- (32) Comba, P.; Schiek, W. *Coord. Chem. Rev.* **2003**, *238* - 239, 21.
- (33) Comba, P.; Pritzkow, H.; Schiek, W. *Angew. Chem. Int. Ed. Eng.* **2001**, *40*, 2465.
- (34) Islam, M. J.; Miller, E. J.; Gordner, J. S.; Patel, D.; Wang, Z. *Tetrahedron Lett.* **2013**, *54*, 2133.
- (35) Galasso, V.; Goto, K.; Miyahara, Y.; Kovac , B.; Klasinc, L. *Chem. Phys.* **2002**, *277*, 229.
- (36) Miyahara, Y.; Goto, K.; Inazu, T. *Chem. Lett.* **2000**, *29*, 620.
- (37) Miyahara, Y.; Goto, K.; Inazu, T. *Tetrahedron Lett.* **2001**, *42*, 3097.
- (38) Wang, Z.; Miller, E. J.; Scalia, S. J. *Org. Lett.* **2011**, *13*, 6540.
- (39) Wadsworth, W. S.; Emmons, W. D. *J. Am. Chem. Soc.* **1961**, *83*, 1733.
- (40) Savage, P. B.; Holmgren, S. K.; Desper, J. M.; Gellman, S. H. *Pure Appl. Chem.* **1993**, *65*, 461.
- (41) Lippard, S. J. *Progress in Inorganic Chemistry*; Wiley, 2009.
- (42) Fischer, E. *Chem. Ber.* **1894**, *27*, 2985.
- (43) Bush, M. A.; Truter, M. R. *J. Chem. Soc. Perkin Trans 2* **1972**, 341.
- (44) Mallinson, P. R.; Truter, M. R. *J. Chem. Soc. Perkin Trans 2* **1972**, 1818.
- (45) Mason, E.; Eick, H. A. *Acta Crystallogr. Sec. B* **1982**, *38*, 1821.
- (46) Owen, J. D.; Truter, M. R.; Wingfield, J. N. *Acta Crystallogr., Sect. C* **1984**, *40*, 1515.
- (47) Bush, M. A.; Truter, M. R. *J. Chem. Soc. Perkin Trans 2* **1972**, 345.
- (48) Hughes, D. L. *J. Chem. Soc., Dalton Trans.* **1975**, 2374.
- (49) Doppelt, P.; Fischer, J.; Weiss, R. *Croat. Chem. Acta* **1984**, *57*, 507.

Chapter 2: Synthesis of Bis-bispidine-based Tetraazamacrocycles

2.1 Experimental

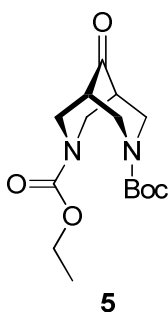
2.1.1 Materials and methods

All reagents and anhydrous solvents were used as received from the Aldrich Company unless otherwise indicated. Tetrahydrofuran, toluene, dichloromethane, hexane and diethyl ether were further purified on a MBraun solvent purification system through double column filtration of the anhydrous solvents (99.8%). 1,2-Dichloroethane (ACS grade) was distilled from calcium hydride and stored over 4 Å molecular sieves. *N*-Boc-*N'*-allylbispidinone **4** was synthesized according to the literature procedure.¹ All manipulations of air-sensitive materials were performed under a nitrogen atmosphere either in a MBraun glovebox or by standard Schlenk line techniques. Thin layer chromatography (TLC) was performed using silica gel (Whatman 250 µm-thick 60 Å F₂₅₄) plates with aluminum backing and followed under UV light and/or by staining with phosphomolybdic acid (PMA) solution in ethanol. Column chromatography was carried out using silica gel (SiliCycle, 60 Å, 40 – 63 µm, 230 – 400 mesh), reversed-phase silica gel (C18, Carbon 17%, 60 Å, 40 – 63 µm), or alumina (activated, basic, Brockmann I). ¹H, ¹³C, COSY and HSQC NMR spectra were recorded on 300 and 500 MHz spectrometers and referenced to residual protonated solvent (¹H) or deuterated solvent (¹³C) unless otherwise specified. High-resolution mass spectra were recorded on a Micromass Electrospray Ionization Time of Flight Mass Spectrometer operating in positive mode. Infrared (IR) spectra were obtained using a Bruker Alpha FT-IR spectrometer with a Platinum ATR module (single reflection diamond crystal). Melting

points were measured using an automated melting point apparatus (OptiMelt, Stanford Research Systems) and are uncorrected. As part of this M. Sc. research, synthesis and characterization of the compounds **7–10**, **12–13**, **16** and **17** (Method 1) had been published in the literature in 2013² and are reprinted below.

2.1.2 Synthesis and characterization

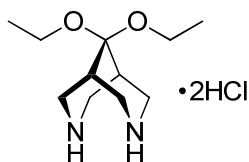
Synthesis of *N*-Boc-*N'*-ethoxycarbonylbispidinone (**5**)



To a clear solution of *N*-Boc-*N'*-allylbispidinone **4** (200 mg, 0.713 mmol) in anhydrous dichloroethane (3.5 mL) under N₂ atmosphere was added DMAP (18.0 mg, 0.143 mmol) followed by ethyl chloroformate (0.10 mL, 1.07 mmol). After stirring overnight at room temperature, the resulting clear reaction mixture was quenched with 15% NaOH (2mL). The organic layer was separated and the aqueous layer was re-extracted with dichloromethane (3 x 3 mL). The combined organic layers were washed with brine, dried over sodium sulfate, filtered, concentrated under reduced pressure, and purified by column chromatography (silica gel, hexanes → 25% EtOAc/hexanes) to give *N*-Boc-*N'*-ethoxycarbonylbispidinone **5** as a colourless solid. ¹H NMR (500 MHz, CDCl₃): δ 4.65 (m, 2H), 4.57 (d, *J* = 13.0 Hz, 1H), 4.50 (d, *J* = 12.5 Hz, 1H), 4.17 (m, 1H), 4.07 (q, *J* = 7.5 Hz, 1H), 3.36 – 3.23 (m, 4H), 2.41 (s, br, 1H), 1.45 (s, 9H), 1.26 (t, *J* = 7.0 Hz, 3H);

^{13}C NMR (125 MHz, CDCl_3): δ 212.0, 155.4, 154.3, 80.6, 61.8, 50.4, 50.3, 50.2, 49.6, 46.9, 28.1, 14.5.

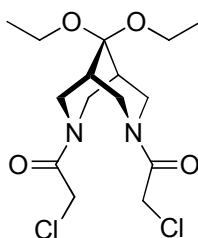
Synthesis of 9,9-Diethoxy-3,7-diazabicyclo[3.3.1]nonane hydrochloride (7)



7

To a solution of *N*-Boc- *N'*-allylbispidinone **4** (5.00 g, 17.8 mmol) in dry 1,2-dichloroethane (40 mL) was added 1-chloroethyl chloroformate (2.91 mL, 26.8 mmol) at ambient temperature under N_2 . The pale yellow reaction mixture was allowed to stir at 50 °C overnight. Upon solvent removal, the crude residue was dissolved in anhydrous ethanol (40 mL). To this solution was added HCl (45.0 mL of a 2.0 M solution in diethyl ether, 90.0 mmol) at ambient temperature and the reaction mixture was stirred at 50 °C for 1 h. Removal of ethanol under high vacuum (0.05 Torr) at 50 °C afforded the title product **7** as a pale yellow solid residue which was brought to the next step without any purification.

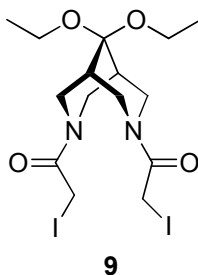
Synthesis of 3,7-Bis(chloroacetyl)-9,9-diethoxy-3,7-diazabicyclo[3.3.1]nonane (8)



8

To a suspension of bispidine diethyl ketal **7** obtained in the previous step in anhydrous dichloromethane (90.0 mL) at 0 °C under N₂ was added chloroacetyl chloride (3.55 mL, 44.6 mmol) dropwise followed by *N, N*-diisopropylethylamine (13.9 mL, 80.0 mmol). The resulting solution was stirred for 15 min at 0 °C before it was quenched with saturated aqueous NH₄Cl solution. The dichloromethane layer was separated and the aqueous layer was re-extracted with dichloromethane (3 x 50 mL). The combined organic layers were washed with brine, dried over sodium sulfate, filtered, concentrated under reduced pressure, and purified by column chromatography (silica gel, hexanes → 50% EtOAc/hexanes) to give bis(chloroacetamide) **8** as a white solid (4.18 g, 11.4 mmol, 64% yield from *N*-Boc-*N'*-allylbispidinone, **4**). mp: 184–186 °C. ¹H NMR (500 MHz, CDCl₃): δ 4.64 (d, *J* = 13.5 Hz, 2 H), 4.21 (d, *J* = 13.0 Hz, 2H), 3.95 (d, *J* = 13.0 Hz, 2H), 3.79 (d, *J* = 13.0 Hz, 2H), 3.67 (d, *J* = 13.5 Hz, 2H), 3.49 (q, *J* = 7.0 Hz, 4H), 3.14 (d, *J* = 14.0 Hz, 2H), 2.12 (s, 2H), 1.23 (t, *J* = 7.0 Hz, 6H); ¹³C NMR (125 MHz, CDCl₃): δ 166.3, 97.0, 55.0, 48.1, 43.6, 41.2, 34.8, 15.0; ¹H NMR (500 MHz, C₆D₆): δ 4.42 (d, *J* = 13.5 Hz, 2H), 4.06 (d, *J* = 13.0 Hz, 2H), 3.97 (d, *J* = 12.5 Hz, 2H), 3.19 (q, *J* = 13.5 Hz, 4H), 3.00 (m, 4H), 2.69 (d, *J* = 13.5 Hz, 2H), 1.32 (s, br, 2H), 0.95 (t, *J* = 7.0 Hz, 6H); ¹³C NMR (125 MHz, C₆D₆): δ 166.1, 97.4, 54.7, 47.9, 43.2, 41.8, 34.9, 15.0; IR (solid): 3001, 2975, 2887, 1642, 1443, 1115, 1056, 1027, 789 cm⁻¹; HRMS (ESI) calcd for C₁₅H₂₄N₂O₄Cl₂H⁺ [M+H⁺] 367.1191, found 367.1177. Colourless, plate-shaped crystals suitable for X-ray diffraction were grown by slow evaporation of a mixture of ethylacetate and hexanes solution.

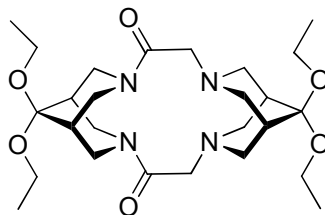
Synthesis of 3,7-Bis(iodoacetyl)-9,9-diethoxy-3,7-diazabicyclo[3.3.1]nonane (**9**)



To a solution of bis(chloroacetamide) **8** (4.62 g, 12.6 mmol) in anhydrous acetonitrile (40 mL) at ambient temperature was added a solution of sodium iodide (5.65 g, 37.7 mmol) in anhydrous acetonitrile (30 mL). After overnight stirring at ambient temperature, the reaction mixture was concentrated under reduced pressure, dissolved in dichloromethane and filtered. The filtrate was washed with 30 mL of water, separated, and the aqueous layer was re-extracted with dichloromethane (3 x 40 mL). The combined organic layers were dried over sodium sulfate, filtered, concentrated under reduced pressure and purified by column chromatography (silica gel, hexanes → 50% EtOAc/hexanes) to give bis(iodoacetamide) **9** as a white solid (6.35 g, 11.5 mmol, 92% yield). mp: 185–187 °C. ¹H NMR (500 MHz, CDCl₃): δ 4.62 (d, *J* = 14.0 Hz, 2H), 3.90 (d, *J* = 10.0 Hz, 2H), 3.74 (d, *J* = 13.0 Hz, 2H), 3.60 (d, *J* = 10.5 Hz, 2H), 3.55 (dm, *J* = 13.5 Hz, 2H), 3.50 (2q, *J* = 7.0 Hz, 4H), 3.09 (d, *J* = 14.0 Hz, 2H), 2.13 (s, br, 2H), 1.24 (t, *J* = 7.0 Hz, 6H); ¹³C NMR (75 MHz, CDCl₃): δ 167.3, 96.8, 55.0, 49.2, 43.7, 34.7, 15.0, -3.0; ¹H NMR (500 MHz, C₆D₆): δ 4.44 (d, *J* = 14.0 Hz, 2H), 3.76 (d, *J* = 10.5 Hz, 2H), 3.61 (d, *J* = 10.5 Hz, 2H), 3.19 (d, *J* = 13.0 Hz, 2H), 3.12 (d, *J* = 13.0 Hz, 2H), 3.00 (q, *J* = 7.0 Hz, 4H), 2.68 (d, *J* = 13.5 Hz, 2H), 1.32 (s, br, 2H), 0.94 (t, *J* = 7.0 Hz, 6H); ¹³C NMR (125 MHz, C₆D₆): δ 166.9, 97.3, 54.7, 49.0, 43.4, 34.9, 15.1, -1.7; IR (solid): 3007, 2966, 2878, 1625, 1437, 1053 cm⁻¹; HRMS (ESI) calcd for C₁₅H₂₄N₂O₄I₂H⁺ [M+H⁺] 550.9904, found

550.9920. Colourless, plate-shaped crystals suitable for X-ray diffraction were grown by slow evaporation of a mixture of ethylacetate and hexanes solution.

Synthesis of 9,9,18,18-Tetraethoxy-3,6,12,15 tetraazapentacyclo-
[13.3.1.1^{3,17}.1^{6,10}.1^{8,12}]docosane-4,14-dione (10)

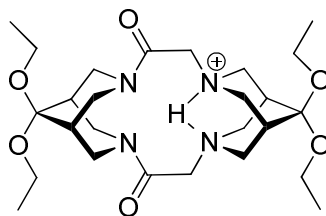


10

Bispidine diethyl ketal **7** was prepared from *N*-Boc-*N'*-allylbispidinone **4** (2.29 g, 8.18 mmol) according to the aforementioned procedure. To a suspension of **7** in anhydrous dichloromethane (50 mL) at ambient temperature was added a clear solution of bis(iodoacetamide) **9** (3.00 g, 5.46 mmol) in anhydrous dichloromethane (223 mL) followed by *N,N*-diisopropylethylamine (7.55 mL, 43.3 mmol). After overnight stirring, the clear reaction mixture was washed with saturated aqueous NaHCO₃ (30 mL) and separated. The aqueous layer was re-extracted with dichloromethane (3 x 50 mL) and the combined organic layers were washed with brine, dried over sodium sulfate, filtered, concentrated under reduced pressure and purified by column chromatography (basic alumina, hexanes → 50% THF/hexanes) to give bisamide **10** as a pale yellow solid (1.59 g, 3.12 mmol, 57 % yield). mp: 241–243 °C. ¹H NMR (500 MHz, CDCl₃): δ 4.04 (d, *J* = 13.5 Hz, 2H), 3.88 (d, *J* = 11.5 Hz, 2H), 3.55 (dd, *J* = 11.0, 4.0 Hz, 2H), 3.52 – 3.39 (m, 8H), 3.35 (d, *J* = 12.5 Hz, 2H), 3.24 (dd, *J* = 13.5, 4.0 Hz, 2H), 3.05 (dd, *J* = 10.0, 2.0 Hz, 2H), 2.89 (d, *J* = 10.5 Hz, 2H), 2.85 (d, *J* = 10.0 Hz, 2H), 2.62 (dd, *J* = 10.5, 2.5 Hz, 2H),

2.54 (d, $J = 12.5$ Hz, 2H), 2.27 (s, br, 1H), 2.15 (s, br, 1H), 1.96 (m, br, 1H), 1.91 (m, br, 1H), 1.20 (t, $J = 7.0$ Hz, 6H), 1.18 (t, $J = 7.0$ Hz, 6H); ^{13}C NMR (125 MHz, CDCl_3): δ 172.0, 97.7, 97.1, 59.5, 56.4, 54.9, 54.2, 54.1, 48.7, 45.1, 37.3, 35.6, 34.3, 33.7, 15.10, 15.07. ^1H NMR (500 MHz, C_6D_6): δ 4.33 (d, $J = 13.5$ Hz, 2H), 3.44 (d, $J = 11.0$ Hz, 2H), 3.27 – 3.16 (m, 14H), 3.03 (d, $J = 12.5$ Hz, 2H), 2.98 (dd, $J = 10.0, 2.5$ Hz, 2H), 2.73 (dd, $J = 10.5, 2.5$ Hz, 2H), 2.69 (d, $J = 12.5$ Hz, 2H), 2.44 (d, $J = 9.0$ Hz, 2H), 1.77 – 1.72 (m, 2H), 1.68 – 1.63 (m, 2H), 1.084 (t, $J = 7.0$ Hz, 6H), 1.076 (t, $J = 7.0$ Hz, 6H); ^{13}C NMR (125 MHz, C_6D_6): δ 171.0, 98.1, 97.9, 59.9, 56.6, 54.9, 54.6, 54.1, 48.7, 45.5, 37.7, 36.0, 34.8, 34.1, 15.32, 15.28; IR (solid): 2970, 2916, 2873, 2812, 1637, 1431, 1115, 1050 cm^{-1} ; HRMS (ESI) calcd for $\text{C}_{26}\text{H}_{44}\text{N}_4\text{O}_6\text{H}^+$ $[\text{M}+\text{H}^+]$ 509.3339, found 509.3339. Colourless block shaped crystals suitable for X-ray diffraction were grown by slow evaporation of a mixture of dichloromethane and hexanes solution.

Synthesis of protonated diketal bisamide (11)

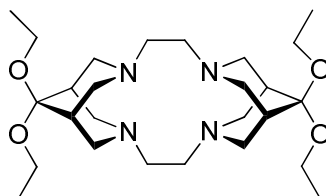


11

To a suspension of bispidine diethyl ketal **7**, prepared from *N*-Boc-*N'*-allylbispidinone **4** (0.77 g, 0.27 mmol) according to the aforementioned procedure, in anhydrous acetonitrile (3 mL) at ambient temperature was added a clear solution of diketal bis(iodoacetamide) **9** (0.100 g, 0.182 mmol) in anhydrous acetonitrile (6 mL) followed by *N,N*-diisopropylethylamine (0.25 mL, 1.45 mmol). After adding all the reagents, the initial clear solution became a white suspension in 15 min which was stirred overnight. After

overnight stirring at ambient temperature, the white precipitate was separated, washed with anhydrous acetonitrile (3 x 3 mL) and evaporated to dryness to give protonated bisamide **11** as a white solid. ^1H NMR (500 MHz, CDCl_3): δ 13.04 (br, 1H), 5.04 (d, $J = 10.5$ Hz, 2H), 4.79 (d, $J = 12.5$ Hz, 2H), 4.16 (m, $J = 12.5$ Hz, 4H), 3.65 (dd, $J = 12.5, 2.5$ Hz, 4H), 3.52 – 3.41 (m, 8H), 3.23 (dd, $J = 13.5, 3.5$ Hz, 4H), 3.11 (d, $J = 11.5$ Hz, 2H), 2.83 (dd, $J = 12.5, 5.5$ Hz, 2H), 2.65 (br, 1H), 2.45 (d, $J = 2.0$ Hz, 1H), 2.29 (br, 1H), 2.24 (d, $J = 2.0$ Hz, 1H), 1.22 (t, $J = 7.0$ Hz, 6H), 1.18 (t, $J = 7.0$ Hz, 6H); ^{13}C NMR (125 MHz, CDCl_3): δ 165.9, 96.4, 94.8, 57.0, 55.7, 55.5, 55.2, 49.5, 45.5, 34.9, 34.0, 33.8, 33.7, 15.0, 14.9; IR (solid): 3012, 2973, 2925, 2875, 2847, 1658, 1640, 1437, 1253, 1129, 1093, 1068, 1041 cm^{-1} .

Synthesis of 9,9,18,18-Tetraethoxy-3,6,12,15 tetraazapentacyclo[13.3.1.1^{3,17}.1^{6,10}.1^{8,12}]docosane (12)

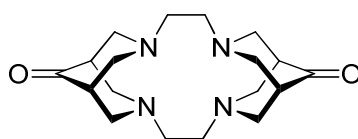


12

To a suspension of bisamide **10** (0.300 g, 0.590 mmol) in anhydrous diethyl ether (11.8 mL) at ambient temperature under N_2 was added DIBALH (3.54 mL of a 1.0 M solution in toluene, 3.54 mmol) dropwise. The resulting clear solution was stirred for 2.5 h before it was quenched with methanol (8 drops) followed by 15% aqueous NaOH (3 mL). After 15 min of stirring, the organic solvent was evaporated under a stream of air and the aqueous layer was extracted with benzene (3 x 3 mL). The combined organic layers were washed with brine, dried over sodium sulfate, filtered, concentrated under reduced

pressure, and purified by recrystallization in hexanes to afford **12** as a colourless crystalline product (0.124 g, 0.258 mmol, 44% yield). Sublimation of the crude product (0.041 g) at 150 °C under high vacuum (0.05 Torr) also afforded **12** as a white solid (0.023 g, 0.048 mmol, 56 % yield from the crude product). mp: 183–185 °C. ¹H NMR (500 MHz, CD₃OD): δ 3.50 (q, *J* = 7.0 Hz, 8H), 3.09 (d, *J* = 11.0 Hz, 8 H), 2.81 (d, *J* = 11.0 Hz, 8H), 2.66 (s, 8H), 2.20 (s, 4H), 1.21 (t, *J* = 7.0 Hz, 12 H); ¹³C NMR (125 MHz, CD₃OD): δ 98.3, 55.7, 55.6, 53.6, 37.0, 15.3; ¹H NMR (500 MHz, C₆D₆): δ 3.45 (q, *J* = 7.0 Hz, 8H), 2.81 (d, *J* = 9.5 Hz, 8H), 2.71 (d, *J* = 8.0 Hz, 8H), 2.42 (s, br, 8H), 1.97 (s, br, 4H), 1.17 (t, *J* = 7.0 Hz, 12H); ¹³C NMR (125 MHz, C₆D₆): δ 99.5, 54.7, 54.13, 54.08, 37.2, 15.5; IR (solid): 2943, 2749, 1445, 1354, 1300, 1267, 1115, 1088, 1051, 974, 904, 812 cm⁻¹; HRMS (ESI) calcd for C₂₆H₄₈N₄O₄H⁺ [M+H⁺] 481.3754, found 481.3741. Colourless block shaped crystals suitable for X-ray diffraction were grown by slow evaporation of a mixture of hexanes solution.

Synthesis of 3,6,12,15-Tetraazapentacyclo[13.3.1.1^{3,17}.1^{6,10}.1^{8,12}] docosane-9,18-dione (13)

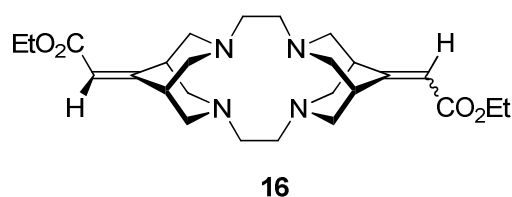


13

A solution of ketal **12** (0.362 g, 0.753 mmol) in 10% aqueous HCl (9.40 mL) was stirred at 60 °C overnight. The solvent was evaporated under a stream of air, and to the solid residue was added NaOH (120 mg, 3.01 mmol) and water (6 mL). After 3 h of stirring at ambient temperature, the reaction mixture was dried under a stream of air overnight and the solid residue was extracted with dichloromethane (4 x 4 mL). Filtration of the

dichloromethane extractions through Celite followed by solvent removal afforded **13** as a slightly pale yellow solid (0.179 g, 0.538 mmol, 71% yield). The product could be further purified by sublimation at 170 °C under high vacuum (0.05 Torr). mp:168–171 °C. ¹H NMR (500 MHz, CDCl₃): δ 3.45 (d, *J* = 10.5 Hz, 8H), 2.73 (dd, *J* = 10.5, 4.0 Hz, 8H), 2.52 (s, 8H), 2.46 (s, br, 4H); ¹³C NMR (125 MHz, CDCl₃): δ 216.3, 58.7, 52.9, 48.7; ¹H NMR (500 MHz, C₆D₆): δ 2.85 (d, *J* = 10.5 Hz, 8H), 2.36 (dd, *J* = 10.5, 4.0 Hz, 8H), 2.29 (m, br, 4H), 2.04 (s, 8H); ¹³C NMR (125 MHz, C₆D₆): δ 213.3, 58.4, 52.9, 48.8; IR (solid): 2930, 2739, 1728, 1359, 1146, 989 cm⁻¹; HRMS (ESI) calcd for C₁₈H₂₈N₄O₂H⁺ [M+H⁺] 333.2291, found 333.2278.

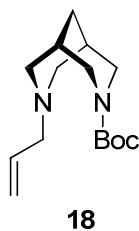
Synthesis of 2,2'-(3,6,12,15-Tetraazapentacyclo[13.3.1.1^{3,17}.1^{6,10}.1^{8,12}]docosane-9,18-diylidene**)bis(ethyl acetate) (**16**)**



To a suspension of sodium hydride (0.018 g, 0.75 mmol) in anhydrous THF (1 mL) at 0 °C under N₂ was added triethyl phosphonoacetate (0.15 mL, 0.75 mmol) dropwise. The resulting clear colourless solution was stirred for 5 min at 0 °C and added via a syringe to a slightly cloudy solution of bis-bispidinone **13** (0.050 g, 0.15 mmol) in anhydrous THF (4 mL) at 0 °C under N₂. The clear reaction mixture was allowed to stir for 15 min at 0 °C and then 1.5 h at ambient temperature. The reaction was quenched with 15% NaOH (0.5 mL) and stirred overnight. THF was evaporated and the resulting mixture was extracted with anhydrous dichloromethane (4 x 2 mL). The combined organic layers were

dried over sodium sulfate, filtered, concentrated under reduced pressure, and purified by column chromatography (reversed-phase silica gel, dichloromethane) to afford **16** as a slightly pale yellow solid (0.059 g, 0.12 mmol, 83% yield). ^1H NMR (500 MHz, CDCl_3): δ 5.67 (s, 2H), 4.14 (q, $J = 7.0$ Hz, 4H), 4.03 (m, br, 2H), 3.23–3.15 (m, 8 H), 2.45–2.34 (m, 18 H), 1.28 (t, $J = 7.0$ Hz, 6H); ^{13}C NMR (125 MHz, CDCl_3): δ 167.6, 166.7, 110.1, 59.5, 59.1, 59.0, 58.4, 58.3, 53.0, 43.3, 35.8, 14.3. IR (solid): 2921, 2853, 2762, 2740, 1705, 1651, 1227, 1147, 1034 cm^{-1} ; HRMS (ESI) calcd for $\text{C}_{26}\text{H}_{40}\text{N}_4\text{O}_4\text{H}^+$ [$\text{M}+\text{H}^+$] 473.3128, found 473.3116.

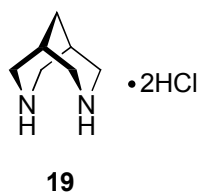
Synthesis of *N*-Boc-*N'*-allylbispidine (**18**)



To a reaction flask containing *N*-Boc-*N'*-allylbispidinone **4** (10.0 g, 35.7 mmol) and KOH (6.06 g 108 mmol) was added 71.0 mL of diethylene glycol followed by hydrazine monohydrate (4.32 mL, 89.2 mmol). The reaction mixture was stirred at 170 °C for 1 h. After cooling to ambient temperature, the resulting solution was washed with 15% NaOH aqueous solution (30 mL) followed by extraction with dichloromethane (100 mL). The dichloromethane layer was separated, and the aqueous layer was reextracted with dichloromethane (3 x 125 mL). The combined organic layers were washed with brine (50 mL), dried over sodium sulfate, filtered, concentrated under reduced pressure, and purified by column chromatography (silica gel, hexanes \rightarrow 10% EtOAc/hexanes) to afford *N*-Boc-*N'*-allylbispidine **18** as a colourless oil (6.09 g, 22.9 mmol, 64% yield). ^1H

NMR (500 MHz, CDCl₃): δ 5.69 (ddt, *J* = 17.0, 10.5, 6.5 Hz, 1H), 5.01 (dm, *J* = 17.5 Hz, 1H), 4.93 (dm, *J* = 10.5 Hz, 1H), 4.12 (dd, *J* = 13.0, 1.0 Hz, 1H), 3.99 (dd, *J* = 13.0, 1.0 Hz, 1H), 2.94 (dm, *J* = 13.0 Hz, 1H), 2.89 (d, *J* = 11.0 Hz, 1H), 2.86 – 2.81 (m, 2H), 2.77 (dd, *J* = 13.5, 5.5 Hz, 1H), 2.63 (dd, *J* = 13.5, 6.5 Hz, 1H), 2.08 (d, *J* = 11.0 Hz, 1H), 1.99 (d, *J* = 11.0 Hz, 1H), 1.68 (br, 1H), 1.64 (br, 1H), 1.56 (dm, *J* = 12.5 Hz, 1H), 1.48 (dm, *J* = 12.5 Hz, 1H), 1.35 (s, 9H); ¹³C NMR (125 MHz, CDCl₃): δ 155.4, 136.6, 116.5, 78.6, 62.5, 58.9, 58.4, 49.0, 47.9, 32.1, 29.5, 29.4, 28.8; IR (liquid): 3075, 3006, 2974, 2906, 2856, 2767, 1687, 1473, 1456, 1421, 1389, 1363, 1323, 1266, 1236, 1173, 1133, 1126, 1056, 999, 946, 901, 872, 835, 756, 623, 539 cm⁻¹; HRMS (ESI) calcd for C₁₅H₂₆N₂O₂H⁺ [M+H⁺] 267.2072, found 267.2073.

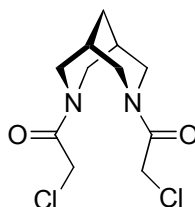
Synthesis of bispidine hydrochloride (**19**)



To a clear colourless solution of *N*-Boc-*N'*-allylbispidine **18** (7.16 g, 26.9 mmol) in dry 1,2-dichloroethane (53.0 mL) was added 1-chloroethyl chloroformate (4.40 mL, 40.3 mmol) at ambient temperature under nitrogen atmosphere. The reaction mixture was stirred at 50 °C overnight. Upon completion, the solvent was removed under high vacuum (0.05 Torr) at 50 °C. The crude brown residue was dissolved in methanol (53.0 mL). To this solution was added HCl (67.2 mL of a 2.0 M solution in diethyl ether, 134 mmol) at ambient temperature. The reaction mixture was stirred at 50 °C for 1 h. Removal of methanol under high vacuum (0.05 Torr) at 50 °C resulted a pale brown solid residue

which was washed with diethyl ether (3 x 50 mL). The residue was dried under high vacuum to afford **19** as a pale yellow solid (5.11 g, 25.7 mmol, 94% yield from *N*-Boc-*N'*-allylbispidine **18**). ¹H NMR (500 MHz, CD₃OD): δ 3.54 (d, *J* = 13.5 Hz, 4H), 3.41 (dd, *J* = 13.5, 4.5 Hz, 4H), 2.42 (br, 2H), 2.02 (br, 2H); ¹³C NMR (125 MHz, CD₃OD): δ 46.2, 26.3, 25.5; IR (solid): 2954, 2902, 2785, 2689, 2582, 2566, 2485, 2449, 2395, 1634, 1591, 1457, 1428, 1313, 1285, 1028, 1007, 958, 815, 562, 485; HRMS (ESI) calcd for C₁₄H₂₉N₄ClH⁺ [M₂+HCl+H⁺] 289.2159, found 289.2170.

Synthesis of bis(chloroacetamide) (**20**)

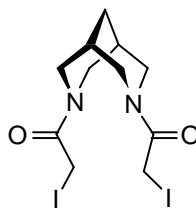


20

To a suspension of bispidine hydrochloride **19** (8.23 g, 41.5 mmol) in anhydrous dichloromethane (154 mL) at 0 °C under N₂ was added *N,N*-diisopropylethylamine (23.7 mL, 136 mmol) followed by chloroacetyl chloride (8.30 mL, 103 mmol) at 0 °C under N₂ atmosphere. The resulting slight orange clear solution was stirred for 15 min at 0 °C before it was quenched with saturated aqueous NH₄Cl solution. The dichloromethane layer was separated and the aqueous layer was re-extracted with dichloromethane (3 x 100 mL). The combined organic layers were washed with brine, dried over sodium sulfate, filtered, concentrated under reduced pressure, and purified by column chromatography (silica gel, hexanes → 75% EtOAc/hexanes) to give bis(chloroacetamide) **20** as a white solid (8.67 g, 31.1 mmol, 75% yield). mp: 201–202

°C. ^1H NMR (500 MHz, CDCl_3): δ 4.76 (d, $J = 13.5$ Hz, 2H), 4.22 (d, $J = 13.0$ Hz, 2H), 3.95 (d, $J = 12.5$ Hz, 2H), 3.94 (d, $J = 14.0$ Hz, 2H), 3.47 (d, $J = 13.5$ Hz, 2H), 2.92 (d, $J = 14.0$ Hz, 2H), 2.03 (br, 2H), 1.96 (br, 2H); ^{13}C NMR (125 MHz, CDCl_3): δ 166.5, 51.2, 46.5, 41.4, 31.9, 28.2; ^1H NMR (500 MHz, C_6D_6): δ 4.38 (d, $J = 14.0$ Hz, 2H), 4.01 (d, $J = 12.5$ Hz, 2H), 3.89 (d, $J = 13.0$ Hz, 2H), 3.19 (d, $J = 13.5$ Hz, 2H), 2.55 (d, $J = 13.5$ Hz, 2H), 2.08 (d, $J = 14.0$ Hz, 2H), 0.94 (br, 2H), 0.83 (br, 2H); ^{13}C NMR (125 MHz, C_6D_6): δ 166.0, 50.6, 45.7, 41.7, 31.6, 28.0; IR (solid): 3032, 2956, 2909, 2857, 1647, 1631, 1443, 1415, 1348, 1308, 1296, 1247, 1224, 1212, 1130, 1102, 990, 824, 783, 732, 594, 560, 467; HRMS (ESI) calcd for $\text{C}_{11}\text{H}_{16}\text{N}_2\text{O}_2\text{Cl}_2\text{H}^+$ $[\text{M}+\text{H}^+]$ 279.0667, found 279.0674.

Synthesis of bis(iodoacetamide) (**21**)

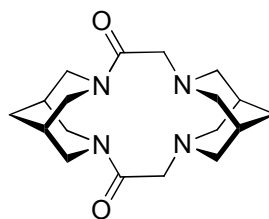


21

To a clear colourless solution of bis(chloroacetamide) **20** (5.68 g, 20.3 mmol) in acetone (300 mL) at ambient temperature was added a solution of NaI (12.2 g, 81.3 mmol) in acetone (100 mL). After stirring overnight at ambient temperature, the reaction mixture was concentrated under reduced pressure, dissolved in dichloromethane (150 mL) and filtered. The filtrate was washed with water (30 mL) and the aqueous layer was re-extracted with dichloromethane (4 x 150 mL). The combined organic layers were dried over sodium sulfate, filtered, concentrated under reduced pressure and purified by column chromatography (silica gel, hexanes \rightarrow 75% EtOAc/hexanes) to give bis(iodoacetamide) **21** as a white solid (8.52 g, 18.4 mmol, 91% yield). mp: 160–162 °C.

^1H NMR (500 MHz, CDCl_3): δ 4.73 (d, $J = 13.5$ Hz, 2H), 3.89 (d, $J = 10.5$ Hz, 2H), 3.87 (d, $J = 13.5$ Hz, 2H), 3.60 (d, $J = 10.5$ Hz, 2H), 3.34 (d, $J = 13.5$ Hz, 2H), 2.86 (d, $J = 14.0$ Hz, 2H), 2.04 (br, 2H), 1.92 (br, 2H); ^{13}C NMR (125 MHz, CDCl_3): δ 167.5, 52.2, 46.7, 31.6, 28.2, -2.8; ^1H NMR (500 MHz, C_6D_6): δ 4.40 (d, $J = 14.0$ Hz, 2H), 3.67 (d, $J = 10.5$ Hz, 2H), 3.53 (d, $J = 10.5$ Hz, 2H), 3.15 (d, $J = 13.5$ Hz, 2H), 2.50 (d, $J = 13.0$ Hz, 2H), 2.08 (d, $J = 13.5$ Hz, 2H), 0.94 (br, 2H), 0.87 (br, 2H); ^{13}C NMR (125 MHz, C_6D_6): δ 166.8, 51.6, 45.9, 31.4, 28.1, -1.7; IR (solid): 3043, 2992, 2917, 2866, 1621, 1459, 1443, 1404, 1343, 1251, 1233, 1161, 1084, 1064, 991, 594, 513, 472, 454; HRMS (ESI) calcd for $\text{C}_{11}\text{H}_{16}\text{N}_2\text{O}_2\text{I}_2\text{H}^+$ $[\text{M}+\text{H}^+]$ 462.9380, found 462.9377.

Synthesis of bisamide (**22**)

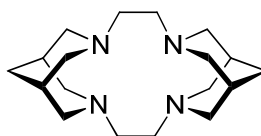


22

To a suspension of bispidine hydrochloride **19** (2.26 g, 11.4 mmol) in dichloromethane (100 mL) at ambient temperature was added *N,N*-diisopropylethylamine (9.90 mL, 56.8 mmol). A clear solution of bis(iodoacetamide) **21** (3.28 g, 7.09 mmol) in dichloromethane (260 mL) was added to the reaction flask. After stirring overnight at ambient temperature, the reaction mixture was washed with 10% Na_2CO_3 (150 mL). The dichloromethane layer was separated and the aqueous layer was re-extracted with dichloromethane (4 x 125 mL). The combined organic layers were washed with brine and dried over sodium sulfate, filtered and removal of the solvent afforded **22** as a pale yellow solid (3.30 g, 9.92 mmol, 96% yield). The crude product (1.467 g) could be

further purified by column chromatography (basic alumina, hexanes→ 75% THF/hexanes) to give **22** as a very pale yellow solid (1.095 g, 3.29 mmol, 75% yield from the crude product). ^1H NMR (500 MHz, CDCl_3): δ 4.14 (d, $J = 14.0$ Hz, 2H), 3.99 (d, $J = 11.5$ Hz, 2H), 3.32 (dd, $J = 11.5, 4.5$ Hz, 2H), 3.31 (d, $J = 12.5$ Hz, 2H), 3.03–2.97 (m, 6H), 2.73 (dd, $J = 10.0, 2.5$ Hz, 2H), 2.51 (d, $J = 13.0$ Hz, 2H), 2.32 (dd, $J = 11.0, 3.0$ Hz, 2H), 2.18 (br, 1H), 2.06 (br, 1H), 1.83 (br, 1H), 1.80 (br, 2H), 1.78 (br, 1H), 1.53 (br, 2H); ^{13}C NMR (125 MHz, CDCl_3): δ 172.4, 60.4, 59.5, 57.5, 50.6, 46.9, 32.1, 31.4, 29.6, 28.5, 27.9, 27.2; ^1H NMR (500 MHz, C_6D_6) δ 4.31 (d, $J = 13.5$ Hz, 2H), 3.39 (d, $J = 11.5$ Hz, 2H), 3.26 (d, $J = 11.5$ Hz, 2H), 2.91 (d, $J = 12.5$ Hz, 2H), 2.70 (dd, $J = 14.0, 4.5$ Hz, 2H), 2.58 (d, $J = 12.5$ Hz, 2H), 2.54 (dd, $J = 11.5, 4.5$ Hz, 2H), 2.42 (d, $J = 10.5$ Hz, 2H), 2.33 (dd, $J = 10.5, 2.5$ Hz, 2H), 2.19 (dd, $J = 11.0, 3.0$ Hz, 2H), 1.42 (br, 1H), 1.36–1.32 (m, 3H), 1.18 (br, 3H), 1.12 (br, 2H); ^{13}C NMR (125 MHz, C_6D_6): δ 171.1, 60.5, 59.4, 57.7, 50.3, 47.0, 32.4, 31.7, 29.9, 28.7, 28.1, 27.4; IR (solid): 2928, 2897, 2845, 2821, 2705, 1626, 1421, 1256, 1143, 1129, 1108, 1074, 1010, 984, 978, 847, 775, 738, 672, 619, 576, 529, 484, 473; HRMS (ESI) calcd for $\text{C}_{18}\text{H}_{28}\text{N}_4\text{O}_2\text{H}^+$ $[\text{M}+\text{H}^+]$ 333.2291, found 333.2291.

Synthesis of 3,6,12,15-Tetraazapentacyclo[13.3.1.1^{3,17}.1^{6,10}.1^{8,12}] docosane (**17**)



17

Method 1: To a reaction flask containing bis-bispidinone **13** (0.050 g, 0.15 mmol) and KOH (0.051 g 0.91 mmol) was added 1.0 mL of diethylene glycol followed by hydrazine

monohydrate (36 μ L, 0.75 mmol). The reaction mixture was allowed to stir at 170 $^{\circ}$ C for 1 h. After cooling down to ambient temperature, HCl (1.0 mL of a 2.0 M solution in diethyl ether, 2.0 mmol) was added, followed by THF (20 mL) under stirring. The solid precipitate was isolated, dissolved in 0.1 – 0.3 mL of water, and precipitated in THF (15 mL). This process was repeated two more times. To the residue was added 15% aqueous NaOH (1.0 mL) and THF (3.0 mL). The resulting mixture was stirred for 1.5 h before it was separated. The aqueous layer was re-extracted with dichloromethane (3 x 2 mL). The combined organic layers were dried over sodium sulfate, filtered, concentrated under reduced pressure, and purified by sublimation at 80 – 120 $^{\circ}$ C under high vacuum (0.05 Torr) to afford **17** as a white solid (0.019 g, 0.062 mmol, 42% yield). The structure of **17** was confirmed by comparing its NMR data with that reported in the literature³.

Method 2: To a pale brown suspension of bisamide **22** (300 mg, 0.902 mmol) in anhydrous diethyl ether (24 mL) at ambient temperature under nitrogen atmosphere was added diisobutylaluminum hydride (DIBALH) (9.0 mL of a 1.0 M solution in toluene, 9.00 mmol) dropwise. The pale yellow cloudy solution was stirred for 2 h under nitrogen atmosphere before it was quenched with 15% aq. NaOH (4.5 mL). The organic solvent was evaporated under a stream of air and the resulting mixture was extracted with CH₂Cl₂ (5 mL). The aqueous layer was re-extracted with CH₂Cl₂ (3 x 4.5 mL). The combined organic layers were dried over sodium sulfate for 1 h, filtered, concentrated under reduced pressure, evaporated under high vacuum overnight and purified by sublimation at 80 – 150 $^{\circ}$ C under high vacuum (0.05 Torr) to afford **17** as a white solid (125 mg, 0.411 mmol, 46% yield).

2.1.3 X-ray crystallography

2.1.3.1 General data collection and refinement

The X-ray crystal structure of compound **8–10** and **12** were obtained at -123 °C, where the crystals were covered in Paratone or Nujol and placed rapidly into the cold N₂ stream of the Kryo-Flex low-temperature device. The data was collected using the SMART⁴ software on a Bruker APEX CCD diffractometer using a graphite monochromator with Mo K α radiation ($\lambda = 0.71073 \text{ \AA}$). A hemisphere of data was collected using a counting time of 10 s per frame. Data reductions were performed using the SAINT⁵ software, and the absorption corrections of the raw data were performed using SADABS⁶. The structures were solved by direct methods using SHELX⁷ and refined by full-matrix least-squares on F^2 with anisotropic displacement parameters for the non-H atoms using SHELX-97⁸ and the WinGX⁹ software package, and thermal ellipsoid plots were evaluated by ORTEP3.2.¹⁰

2.1.3.2 Crystallographic data

Table 2.1 Crystallographic data for compound 8

Formula	C ₁₅ H ₂₄ Cl ₂ N ₂ O ₄
Formula weight (<i>g/mol</i>)	367.26
Crystal dimensions (<i>mm</i>)	0.2 × 0.2 × 0.05
Crystal colour and habit	Colourless, plate
Crystal system	Triclinic
Space group	P-1
Temperature, K	150
Unit cell dimensions	$a = 8.2504(11) \text{ \AA}$ $\alpha = 100.467(1)^\circ$ $b = 9.6655(13) \text{ \AA}$ $\beta = 91.120(1)^\circ$ $c = 11.6169(15) \text{ \AA}$ $\gamma = 107.542(1)^\circ$
V, \AA^3	865.9(2)

Number of reflections to determine final unit cell	5652
Min and max 2θ for cell determination, °	4.6, 56.8
Z	2
F(000)	388
ρ (g/cm)	1.409
λ, Å, (MoKα)	0.71073
μ, (mm ⁻¹)	0.40
Diffractometer type	Bruker APEX CCD
Scan types	ω and φ scans
Max 2θ for data collection, °	56.8
Measured fraction of data	0.924
Number of reflections measured	10253
Unique reflections measured	4007
R _{merge}	0.0331
Number of reflections included in refinement	4007
Cut off threshold expression	I > 2sigma(I)
Structure refined using	Full-matrix least-squares on F ²
Weighting scheme	w = 1/[σ ² (F _o ²) + (0.039P) ² + 0.4133P] where P = (F _o ² + 2F _c ²)/3
Number of parameters in least-squares	299
R ₁	0.0331
wR ₂	0.0820
R ₁ (all data)	0.0377
wR ₂ (all data)	0.0860
Goodness-of-fit, ^b S on F ²	1.055
Maximum shift/error	0.088
Min & max peak heights on final ΔF map (e ⁻ /Å)	-0.45, 0.47

Table 2.2 Crystallographic data for compound 9

Formula	C ₁₅ H ₂₄ I ₂ N ₂ O ₄
Formula weight (<i>g/mol</i>)	550.16
Crystal dimensions (<i>mm</i>)	0.20 × 0.20 × 0.05
Crystal colour and habit	Colourless, plate
Crystal system	Triclinic
Space group	P-1
Temperature, K	150
Unit cell dimensions	$a = 8.1367(11) \text{ \AA}$ $\alpha = 101.7470(10)^\circ$ $b = 9.9235(13) \text{ \AA}$ $\beta = 91.2460(10)^\circ$ $c = 12.2971(16) \text{ \AA}$ $\gamma = 108.1750(10)^\circ$
V, Å ³	919.7(2)
Number of reflections to determine final unit cell	3975
Min and max 2θ for cell determination, °	5.0, 55.6
Z	2
F(000)	532
ρ (<i>g/cm</i>)	1.987
λ, Å, (MoKα)	0.71073
μ, (<i>mm</i> ⁻¹)	3.439
Diffractionmeter type	Bruker APEX CCD
Scan types	ω and φ scans
Max 2θ for data collection, °	55.0
Measured fraction of data	0.974
Number of reflections measured	10572
Unique reflections measured	4112
R _{merge}	0.0261
Number of reflections included in refinement	3529
Cut off threshold expression	I > 2sigma(I)
Structure refined using	Full-matrix least-squares on F ²
Weighting scheme	$w = 1/[\sigma^2(F_o^2) + (0.0297P)^2 + 0.413P]$ where $P = (F_o^2 + 2F_c^2)/3$

Number of parameters in least-squares	210
R ₁	0.0323
wR ₂	0.0651
R ₁ (all data)	0.0404
wR ₂ (all data)	0.0688
Goodness-of-fit, ^b S on F ²	1.071
Maximum shift/error	0.001
Min & max peak heights on final ΔF map (e ⁻ /Å)	-0.538, 1.053

Table 2.3 Crystallographic data for compound 10•CH₂Cl₂

Formula	C ₂₆ H ₄₄ N ₄ O ₆ • CH ₂ Cl ₂	
Formula weight (g/mol)	593.58	
Crystal dimensions (mm)	0.26 × 0.18 × 0.08	
Crystal colour and habit	Colourless, plate	
Crystal system	Triclinic	
Space group	P-1	
Temperature, K	150	
Unit cell dimensions	$a = 8.4658(12) \text{ \AA}$	$\alpha = 75.041(2)^\circ$
	$b = 12.7598(18) \text{ \AA}$	$\beta = 89.508(2)^\circ$
	$c = 14.619(2) \text{ \AA}$	$\gamma = 87.310(2)^\circ$
V, Å ³	1523.9(4)	
Number of reflections to determine final unit cell	5169	
Min and max 2θ for cell determination, °	4.8, 49.4	
Z	2	
F(000)	636	
ρ (g/cm)	1.294	
λ, Å, (MoKα)	0.71073	
μ, (mm ⁻¹)	0.26	
Diffractometer type	Bruker APEX CCD	
Scan types	ω and φ scans	
Max 2θ for data collection, °	49.4	

Measured fraction of data	0.997
Number of reflections measured	14398
Unique reflections measured	5169
R_{merge}	0.050
Number of reflections included in refinement	3580
Cut off threshold expression	$I > 2\sigma(I)$
Structure refined using	Full-matrix least-squares on F^2
Weighting scheme	$w = 1/[\sigma^2(F_o^2) + (0.0592P)^2 + 0.6662P]$ where $P = (F_o^2 + 2F_c^2)/3$
Number of parameters in least-squares	352
R_1	0.0553
wR_2	0.1235
R_1 (all data)	0.0862
wR_2 (all data)	0.1386
Goodness-of-fit, χ^2 on F^2	1.018
Maximum shift/error	0.001
Min & max peak heights on final ΔF map ($e^-/\text{\AA}$)	-0.55, 0.47

Table 2.4 Crystallographic data for compound 12

Formula	$C_{26}H_{48}N_4O_4$	
Formula weight (g/mol)	480.68	
Crystal dimensions (mm)	$0.26 \times 0.18 \times 0.08$	
Crystal colour and habit	Colourless, block	
Crystal system	Triclinic	
Space group	P-1	
Temperature, K	150	
Unit cell dimensions	$a = 7.6273(8) \text{ \AA}$	$\alpha = 68.658(1)^\circ$
	$b = 9.0779(10) \text{ \AA}$	$\beta = 78.584(1)^\circ$
	$c = 10.6919(12) \text{ \AA}$	$\gamma = 83.150(1)^\circ$
$V, \text{ \AA}^3$	674.99(13)	
Number of reflections to determine final unit cell	5217	

Min and max 2θ for cell determination, °	4.8, 56.4
Z	1
F(000)	264
ρ (g/cm)	1.183
λ, Å, (MoKα)	0.71073
μ, (mm ⁻¹)	0.08
Diffractionmeter type	Bruker APEX CCD
Scan types	ω and φ scans
Max 2θ for data collection, °	56.4
Measured fraction of data	0.996
Number of reflections measured	6459
Unique reflections measured	2363
R _{merge}	0.018
Number of reflections included in refinement	2143
Cut off threshold expression	I > 2sigma(I)
Structure refined using	Full-matrix least-squares on F ²
Weighting scheme	w = 1/[σ ² (F _o ²) + (0.063P) ² + 0.2389P] where P = (F _o ² + 2F _c ²)/3
Number of parameters in least-squares	154
R ₁	0.0397
wR ₂	0.1075
R ₁ (all data)	0.0431
wR ₂ (all data)	0.1118
Goodness-of-fit, ^b S on F ²	0.984
Maximum shift/error	0.001
Min & max peak heights on final ΔF map (e ⁻ /Å)	-0.21, 0.27

^aR1(F) = {Σ(|F_o| - |F_c|)/Σ|F_o|} for reflections with F_o > 4(σ(F_o)). wR2(F²) = {Σw(|F_o|² - |F_c|²)/Σw(|F_o|²)²}^{1/2}, where 'w' denotes the weight given each reflection.

^bS = [Σw(|F_o|² - |F_c|²)²]/(n-p)^{1/2}, hence, 'n' is the number of reflections and 'p' is the number of parameters used.

2.2 Results and discussion

Due to the high rigidity of their macrocyclic framework and the steric hindrance around the cavity, semi-cage like bis-bispidine-based tetraazamacrocycles can be used to encapsulate transition metal ions selectively to form stable complexes.^{11,12} Bis-bispidinone **1** (Y = O) has a pair of carbonyl groups at each end of the macrocyclic framework and could be used as a versatile substrate for facile difunctionalization to prepare diester **1** (Y = CHCO₂Et) and bis-bispidine **1** (Y = H₂) (Figure 2.1). The former could be utilized in polymer synthesis through condensation reaction with different types of diols. The latter is the simplest tetraazamacrocyclic structure without any extra functional groups and could be used as an ideal ligand for metal-coordination studies.

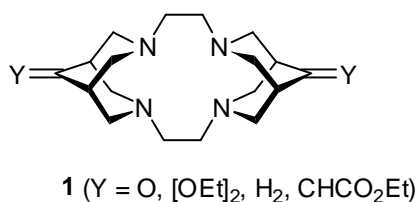
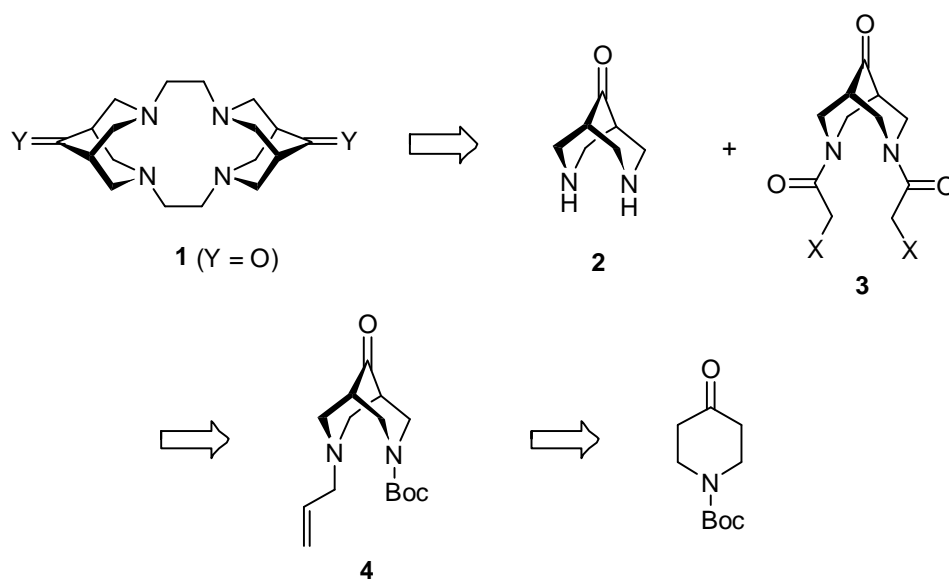


Figure 2.1. Bis-bispidine-based tetraazamacrocycles.

2.2.1 Retrosynthetic plan for bis-bispidinone **1**

The target bis-bispidinone **1** would be prepared by the cyclization of bispidinone **2** and its derivative **3** (Scheme 2.1). Both building blocks **2** and **3** could be derived from *N*-Boc-*N'*-allylbispidinone **4** which can be synthesized from *N*-Boc-4-piperidone via double Mannich reaction by following the literature procedure.^{1,13}

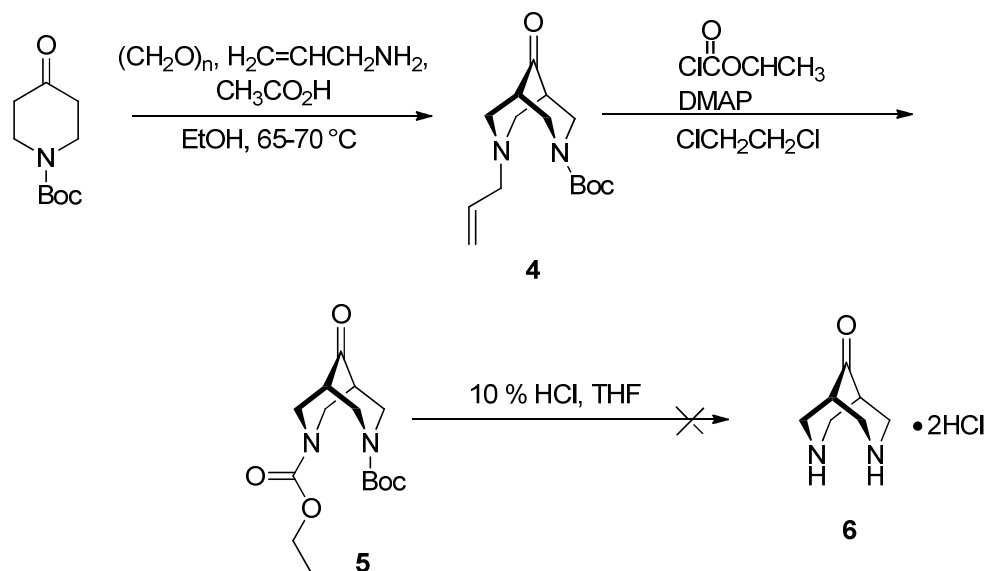


Scheme 2.1 Retrosynthetic plan.

2.2.2 Synthesis of bis-bispidine hydrochloride **6**

N-Boc-*N'*-allylbispidinone **4** was synthesized according to the literature procedure from *N*-Boc-4-piperidone via a double Mannich reaction (Scheme 2.2).¹ It had been observed that the subsequent deprotection of the allyl group on **4** with 1-chloroethyl chloroformate did not go to completion.¹⁴ This was probably due to the presence of a trace amount of acid present either in the solvent or in 1-chloroethyl chloroformate.¹⁴ To remove any protonated **4** in the reaction medium which might interfere in the subsequent transformations, *N*-Boc-*N'*-ethoxycarbonylbispidinone **5** was synthesized using ethyl chloroformate in the presence of catalytic amount (0.2 equiv) of 4-dimethylaminopyridine (DMAP) (Scheme 2.2). The resulting ethyl carbamate could be purified by column chromatography using silica gel. In comparison, although the removal of allyl group can be achieved by using 1-chloroethyl chloroformate,¹⁴ due to the

instability of 1-chloroethyl carbamate group, the resulting product cannot be purified by column chromatography to remove protonated **4**.



Scheme 2.2 Synthesis of *N*-Boc-*N'*-ethoxycarbonylbispidinone **5**.

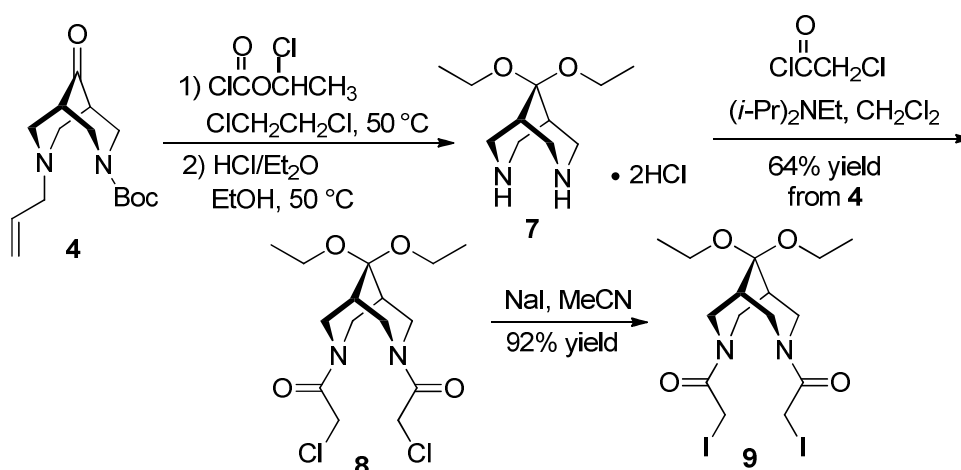
The formation of **5** was confirmed by ^1H and ^{13}C NMR. The ^1H NMR of **5** in deuterated chloroform shows the disappearance of vinyl protons (5.03-5.76 ppm) in **4**. The ^1H NMR also indicates the incorporation of the ethyl formate group which shows a quartet at 4.07 ppm and a triplet at 1.26 ppm corresponding to the ethoxy group. In addition, the ^{13}C NMR indicates the disappearance of the allyl carbons at 134.9 and 117.5 ppm in **4**¹ and the appearance of the newly formed amide group with a carbon resonance at 155.4 ppm, indicating that compound **5** was formed successfully.

The transformation of **5** to bispidinone **6** was carried out under mild acidic conditions using 10% HCl in THF. Although the Boc protective group was cleaved cleanly, the removal of ethyl carbamate was not successful under this condition.

2.2.3 Synthesis and characterization of bis(iodoacetamide) **9**

2.2.3.1 Synthesis and Characterization¹⁴

In a separate study by Erin Miller in our group, it was found that bispidinone **6** was unstable in the presence of a base such as *N,N*-diisopropylethylamine. However, bispidine diethyl ketal **7** was stable when treated with *N,N*-diisopropylethylamine and could be successfully converted to bis(iodoacetamide) **9**.¹⁴ Therefore, compounds **7** – **9** were synthesized according to the newly established procedures (Scheme 2.3).^{2,14} The allyl group in **4** was removed upon treatment with 1-chloroethyl chloroformate at 50 °C. procedure.^{1,15,16} The resulting 1-chloroethyl carbamate was treated with HCl in anhydrous ethanol to afford bispidine diethyl ketal **7**. Bis(chloroacetamide) **8** was synthesized via acetylation of **7** in the presence of chloroacetyl chloride in 64% overall yield from *N*-Boc-*N'*-allylbispidinone **4**.^{1,2,14} Further transformation of **8** to bis(iodoacetamide) **9** was achieved in high yield in a reaction with sodium iodide. The formation of **8** and **9** was confirmed by ¹H and ¹³C NMR.^{2,14} HSQC, IR, mass spectrometry and single crystal X-ray analysis have also been used to further validate the structure of **8** and **9**.



Scheme 2.3 Synthesis of bis(iodoacetamide) **9**.

2.2.3.2 Crystallographic data analysis of **8**

Bis(chloroacetamide) **8** was analyzed by single crystal X-ray diffraction and the ORTEP plot is shown in Figure 2.2. The crystal structure of **8** indicates that the bispidine backbone consists of a chair-chair conformation (Figure 2.2). The nonbonding N4...N8 distance was 2.84 Å, similar to the distances observed (2.85 – 3.07 Å) for neutral bispidine compounds.^{17,18}

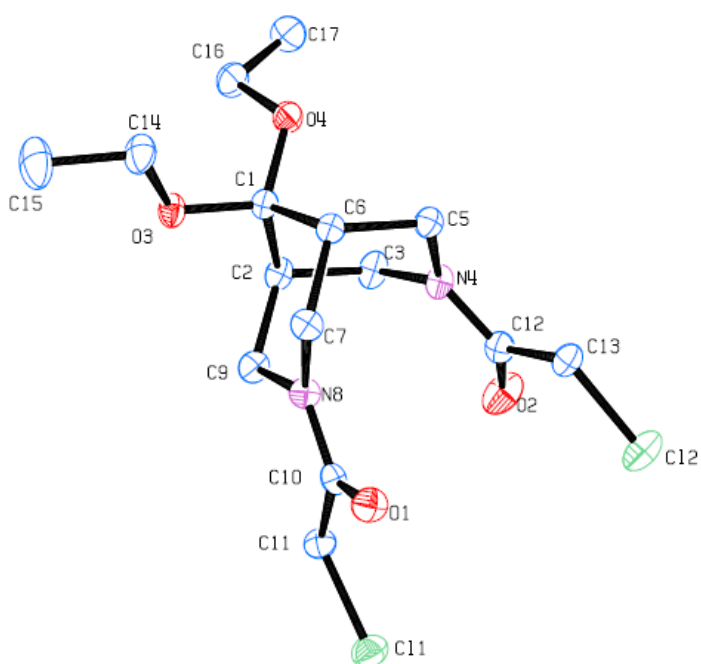


Figure 2.2 Crystallographic structure of bis(chloroacetamide) **8**. Ellipsoids are at the 50% probability level and hydrogen atoms were omitted for clarity. Selected bond distances (Å) and a nonbonding distance (Å): C11–C11 = 1.7715(15), C13–C12 = 1.7761(14), C10–O1 = 1.2248(17), C12–O2 = 1.2306(14), C1–O4 = 1.4163(19), C1–O3 = 1.4128(18), N1...N2 = 2.84.

2.2.3.3 Crystallographic data analysis of **9**

Bis(iodoacetamide) **9** was analyzed by single crystal X-ray diffraction and the ORTEP plot is shown in Figure 2.3. The structure shows a chair-chair bispidine conformation similar to that in **8**, with an N4···N8 distance of 2.84 Å. However, the torsional angles of I2–C13–C12–O2 (8.5°) and I1–C11–C10–O1 (13.4°) in **9** are significantly larger than the C12–C13–C12–O2 and C11–C11–C10–O1 torsional angles of 1.69 and 6.21° in **8**, respectively. This can be attributed to the larger size of iodine atoms in comparison to chlorine atoms, leading to a higher degree of oxygen–iodine repulsion.¹⁹

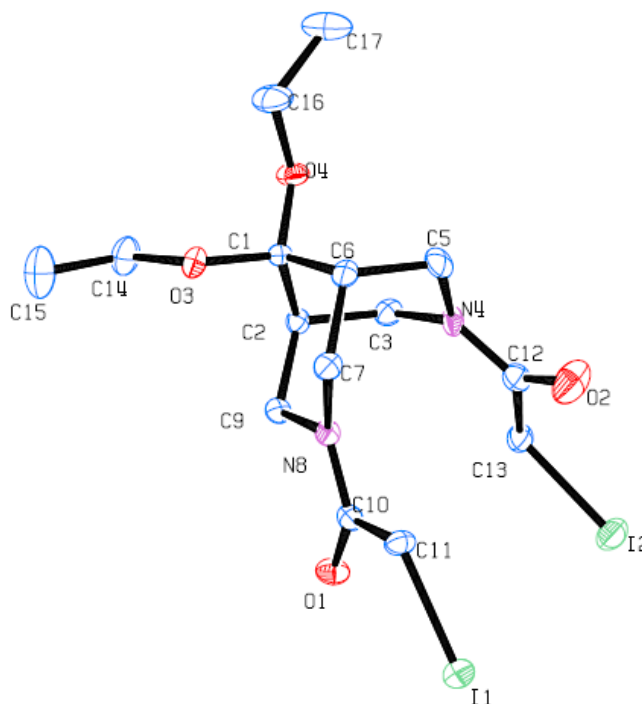
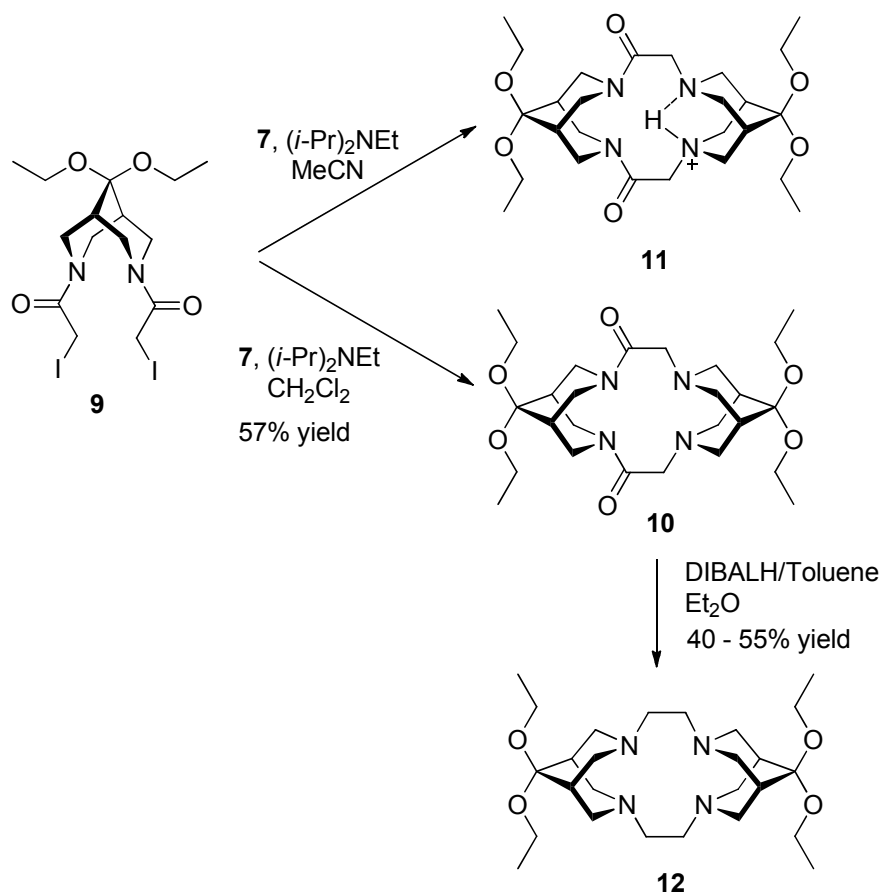


Figure 2.3 Crystallographic structure of bis(iodoacetamide) **9**. Ellipsoids are at the 50% probability level and hydrogen atoms were omitted for clarity. Selected bond distances (Å); nonbonding distance (Å); and torsion angles (°): C11–I1 = 2.1300(14), C13–I2 = 2.1209(37), C12–O2 = 1.2234(46), C10–O1 = 1.2288(37), C1–O3 = 1.4162(53), C1–O4 = 1.4100(48); N4···N8 = 2.84.

2.2.4 Synthesis and characterization of diketal bis-bispidine 12

2.2.4.1 Synthesis and characterization

Diketal bisamide **10** was successfully synthesized by the cyclization of bis(iodoacetamide) **9** and bispidine diethyl ketal **7** at ambient temperature in satisfactory yield (Scheme 2.4).^{1,2}



Scheme 2.4 Synthesis of diketal bis-bispidine tetraazamacrocycle **12**.

Interestingly, this cyclization reaction seemed to be influenced by the solvent and the concentration of the reactants in the reaction mixture. When acetonitrile was used as a solvent and the reactant concentration was higher than 0.013 mol/L, a white solid

precipitated from the reaction mixture.^{2,14} The reaction, however, went smoothly to give **10** in the same solvent with concentration below 0.013 mol/L. When dichloromethane was used as the solvent, the reaction proceeded efficiently even if the reactant concentration was 0.02 mol/L. Treatment of **10** with 2.0 M HCl in ether gave the same compound as the white precipitate in the acetonitrile reaction medium and was confirmed as **11**, the protonated product of **10**, by ¹H NMR in deuterated chloroform.

The crude pale yellow solid bisamide **10** was purified by column chromatography using silica gel or basic alumina. In this case, purification of the crude product on basic alumina was found to be more effective, which afforded a better yield (57%) in comparison to silica gel (30%). The compound was studied by NMR spectroscopy, such as ¹H, ¹³C NMR, HSQC, and COSY, as well as by single crystal X-ray diffraction analysis. The ¹H NMR spectrum of **10** in deuterated chloroform shows that the relatively broad singlet peaks at 2.27, 2.15, 1.96 and 1.91 ppm are the resonances of the four bridgehead protons. The ¹³C NMR exhibited four bridgehead carbon resonances at 37.3, 35.6, 34.3 and 33.7 ppm along with two quaternary ketal carbons at 97.7 and 97.1 ppm. The ¹³C NMR in C₆D₆ also exhibited four bridgehead carbons at 37.7, 36.0, 34.8 and 34.0 ppm as well as the two quaternary ketal carbons at two ends of the macrocyclic bisamide. The high rigidity of **10** imposed by both the bispidine units and the amide functional groups can restrict the bond rotation in the macrocycle, which likely results in the complex proton NMR spectra in which each of the bridgehead protons or carbons exhibits a distinctive chemical shift.

The ¹H NMR of **11** in CDCl₃ shows a broad peak (δ = 13.0 ppm) which can be assigned as the proton in the macrocyclic cavity. In addition, the ¹H NMR in CDCl₃ indicates a

downfield shift of bridgehead protons from 2.27, 2.15, 1.96 and 1.91 in **10** to 2.65, 2.45, 2.29 and 2.24 ppm, respectively. ^{13}C NMR also indicates the downfield shift of the resonances corresponding to the bridgehead carbons from 37.3, 35.5, 34.3 and 33.7 ppm in **10** to 34.9, 34.0, 33.8 and 33.7 ppm in **11**, respectively, due to the protonation.

Reduction of the amide groups in bisamide **10** was carried out in diethyl ether²⁰ with DIBAL in toluene.^{1,2} This afforded diketal bis-bispidine tetraazamacrocyclic **12** (Scheme 2.4). The ^1H and ^{13}C NMR indicated the conversion was complete under the reaction condition. As expected, tetraazamacrocyclic **12** possesses a highly basic tetramine core which could bind to normal-phase silica gel, and prevent the product from being purified effectively on the column. Purification by column chromatography using basic alumina was also found to be unsuccessful because the highly basic tetramine core could potentially bind to the polar Al-OH groups as well as the unsaturated aluminum ions on the column. However, purification of the crude product could be achieved by sublimation at 150 °C under high vacuum (0.05 Torr) or recrystallization in hexanes at ambient temperature. The NMR spectra indicate the crude product was pure which was routinely brought to the next step without any further purification.

2.2.4.2 Crystallographic data analysis of 10

The structure of diketal bisamide **10** was determined by single crystal X-ray diffraction. Its ORTEP plot indicates the presence of a dichloromethane solvent molecule along with **10** (Figure 2.4). The structure shows two bispidine units of chair-chair conformations which are connected by two ethylene bridges.

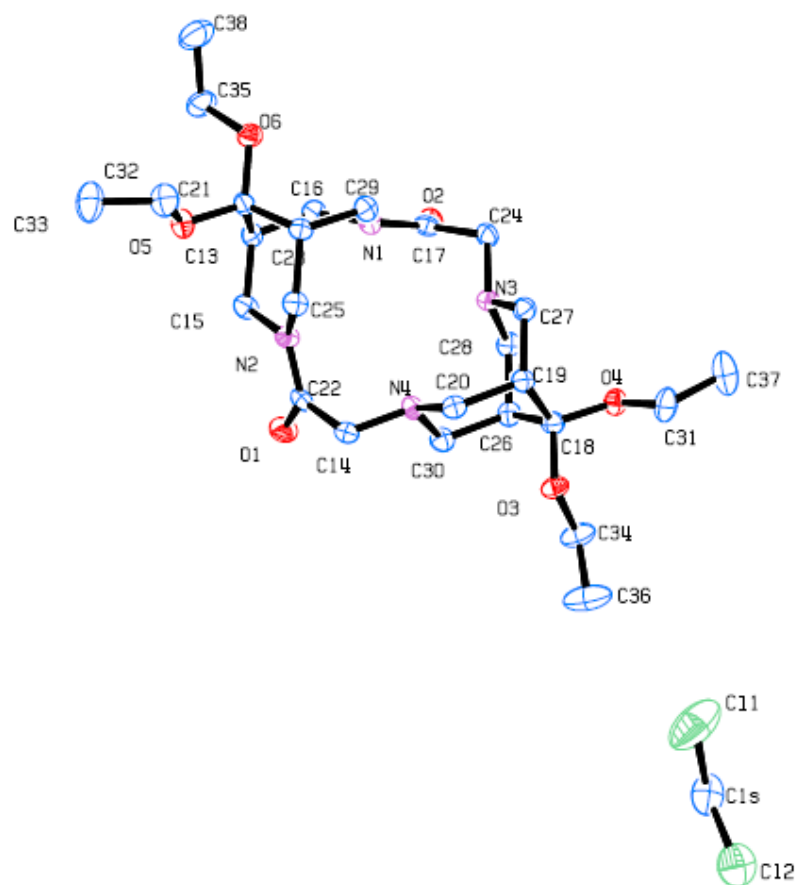


Figure 2.4 Crystallographic structure of macrocyclic bisamide **10**·CH₂Cl₂. Ellipsoids are at the 50% probability level and hydrogen atoms were omitted for clarity. Selected bond distances and nonbonding distances (Å): C22–O1 = 1.2303(32), C17–O2 = 1.2337(37), C21–O5 = 1.4082(35), C21–O6 = 1.4164(28), C18–O3 = 1.4122(29), C18–O4 = 1.4177(33); N1···N2 = 3.09, N3···N4 = 2.84.

2.2.4.3 Crystallographic data analysis of **12**

The compound diketal bis-bispidine tetraazamacrocycle **12** was analyzed by single crystal X-ray diffraction and the ORTEP plot is shown in Figure 2.5. The solid state structure of **12** indicates the nonbonding N1···N2 distance is 2.87 Å on each of the

bispidine units of **12**, which is in good agreement with other bispidine-based compounds (2.85–3.07 Å).¹⁷

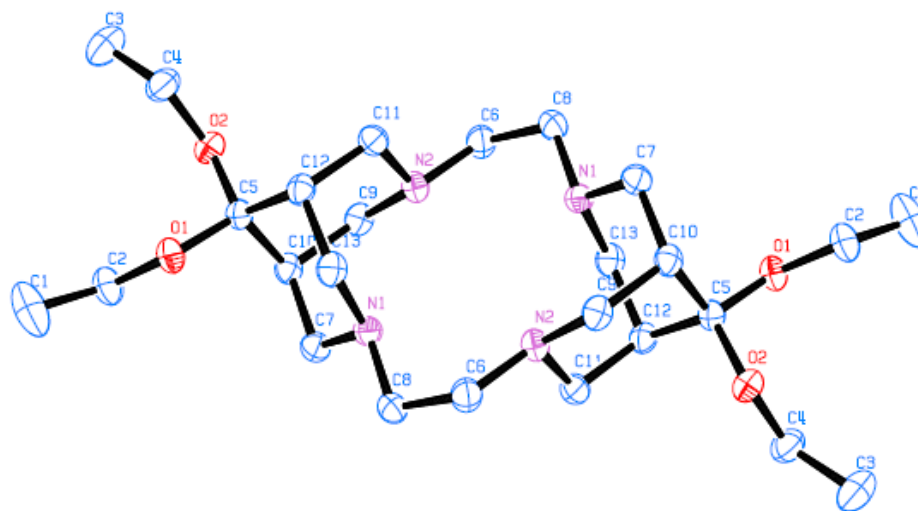


Figure 2.5 Crystallographic structure of diketal tetraazamacrocycle **12**. Ellipsoids are at the 50% probability level and hydrogen atoms were omitted for clarity. Selected bond distances (Å); nonbonding distances (Å) and angle (°): C5–O1 = 1.4184(14), C5–O2 = 1.4215(14); N1···N2 = 2.87 and O1–C5–O2 = 110.16(9).

The distances between the two diagonal nitrogen atoms in the bis-bispidine core are 4.009 Å (N1···N1) and 4.075 Å (N2···N2). Using the Pauling covalent radius for nitrogen atoms (0.72 Å), the radius of the cavity $r(\text{H})$ can be calculated as 1.285 and 1.318 Å, respectively. It should be noted that the cavity size of **12** is comparable to that of cyclam derivatives (1.18–1.38 Å).²¹

In addition, the crystal packing of **12** exhibited channels of the tetramine cores (Figure 2.6).

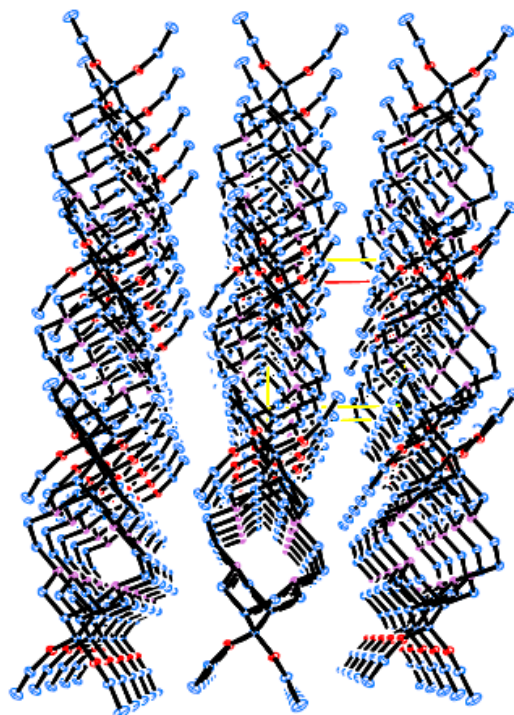
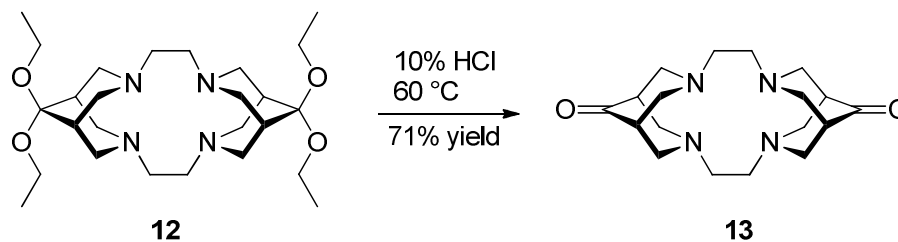


Figure 2.6 Molecular view of bis-bispidine tetraazamacrocycle **12** showing channels of the tetraamine cores. Ellipsoids are at the 50% probability level and hydrogen atoms are omitted for clarity.

2.2.5 Synthesis and characterization of bis-bispidinone **13**^{2,22}

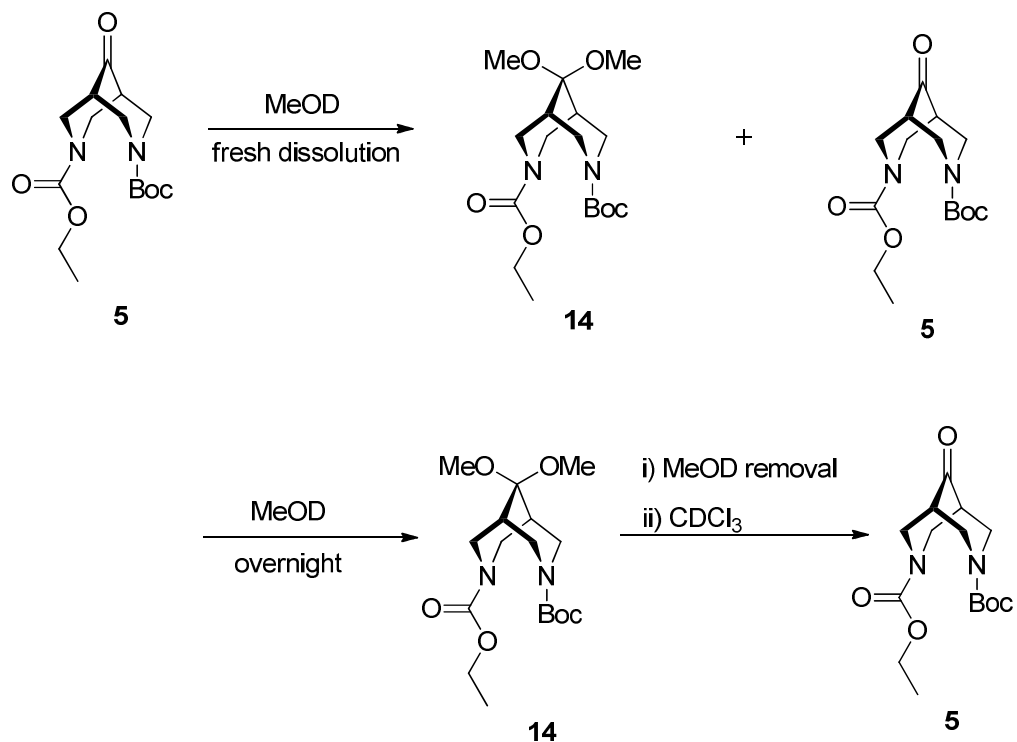
Synthesis of bis-bispidinone **13** was achieved by the hydrolysis of diketal tetraazamacrocycle **12** using 10% aqueous HCl at 60 °C (Scheme 2.5). Both the ¹H and ¹³C NMR spectra of the crude product (in deuterated methanol) indicated that the ethyl groups of the diketal macrocycle **12** were cleaved cleanly. However, the ¹³C NMR did not exhibit any carbonyl carbon resonance of **13** in the 200–220 ppm region. Instead, a distinctive peak at 90–100 ppm was observed which suggests the existence of a ketal or ketone hydrate carbon. Although the protons in the tetramine cavity could be removed by an aqueous sodium hydroxide solution, extraction of the aqueous solution with different

solvents, such as dichloromethane, benzene and THF, did not provide the desired compound **13**. Analysis of the aqueous layer by ^{13}C NMR indicated the presence of a characteristic ketal or ketone hydrate carbon peak at 90-100 ppm. Again, there was no carbonyl peak.

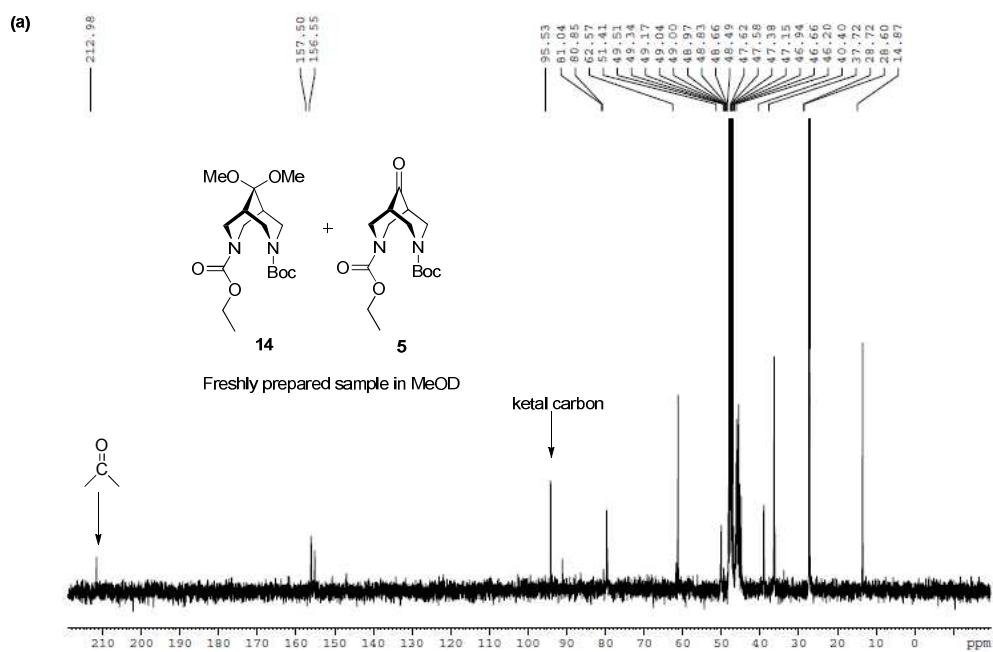


Scheme 2.5 Synthesis of bis-bispidinone **13**.

In order to have more insights on the bispidinone carbonyl group, *N*-Boc-*N'*-ethoxycarbonylbispidinone **5** was studied by ^{13}C NMR in deuterated methanol (Scheme 2.6). When the solution was freshly prepared, the compound was found to exist as a mixture of both dimethyl ketal **14** and ketone **5** with the carbon resonances in the 90–100 ppm and 200–220 ppm regions, respectively (Figure 2.7(a)). However, ketone **5** was completely converted to ketal **14** after the NMR sample was kept overnight in deuterated methanol (Figure 2.7(b)). Interestingly, when the methanol solvent was completely evaporated to dryness followed by dissolution of the residue in deuterated chloroform, only ketone **5** was detected in the ^{13}C NMR (Figure 2.7(c)).



Scheme 2.6 Transformation of *N*-Boc-*N'*-ethoxycarbonylbispidinone **5** to dimethyl ketal.



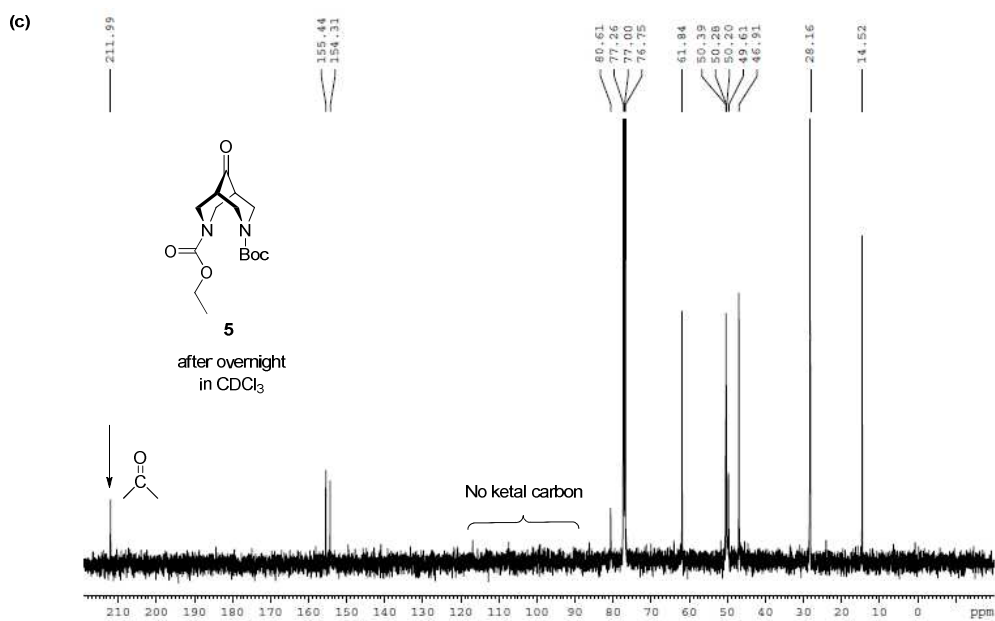
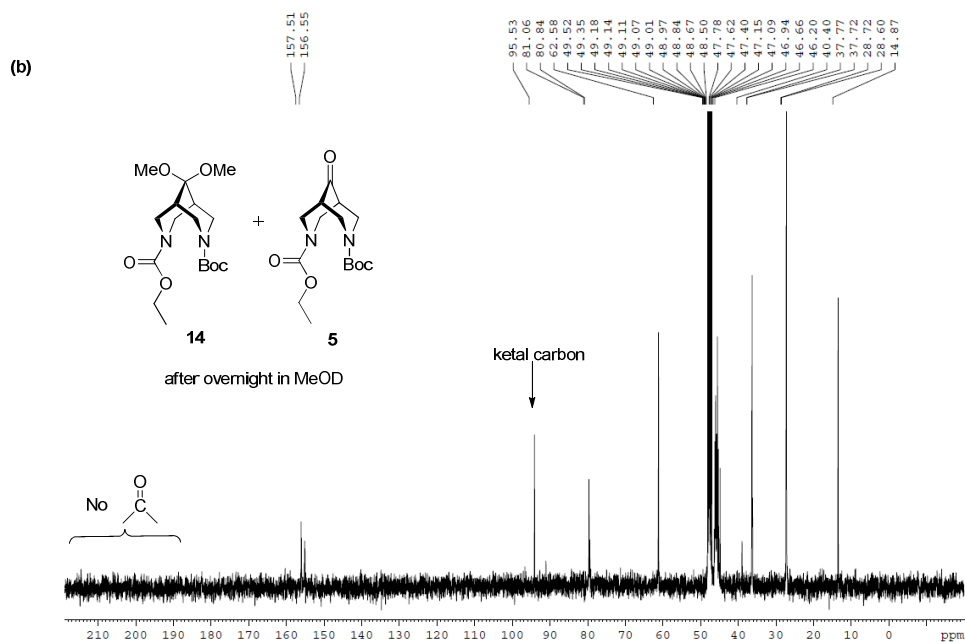


Figure 2.7 ¹³C NMR sample of (a) a freshly prepared sample of *N*-Boc-*N'*-ethoxycarbonylbispidinone **5** in MeOD. (b) the sample after overnight in MeOD. (c) the sample after evaporation of MeOD followed by dissolution in CDCl₃.

These observations suggested that the bispidinone carbonyl group exhibited an unusual reactivity toward the methanol solvent. Dimethyl ketal **14**, unlike diethyl ketal **8** and **9**, was found to be labile and converted easily to ketone **5** in the absence of methanol. It should be noted that as ketone **5** was not miscible with water, it could be extracted with dichloromethane or ether during an aqueous workup.

Based on the results obtained from compound **5**, it could be reasoned that in contrast to typical ketones, bis-bispidinone **13** preferred to exist as ketone hydrate **15** rather than ketone **13** in an aqueous medium (Figure 2.8).^{23,24} Moreover, the dissolution of **13** in aqueous media was enhanced further by the hydrophilic tetramine cavity. Therefore, the extraction of bis-bispidinone **13** from an aqueous solution was tremendously difficult.

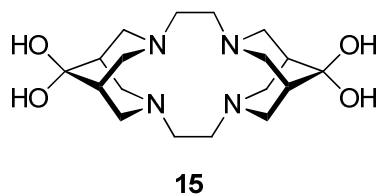


Figure 2.8 Formation of ketone hydrate **15** in aqueous medium.

In order to isolate the desired product, it was necessary to first convert ketone hydrate **15** to ketone **13**.² This was achieved by removing water from the aqueous mixture. Repeated extraction of the solid residue with dichloromethane afforded the desired product. The non-aqueous isolation process thus developed was found to be very effective and practical for the isolation of bis-bispidinone **13**.

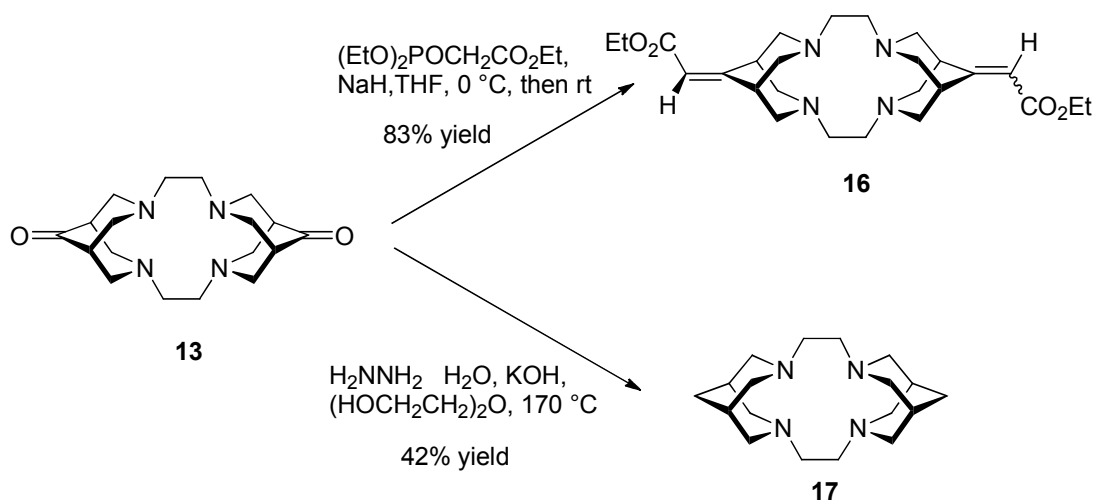
It should be mentioned that crude bis-bispidinone **13** can be purified by sublimation under high vacuum (0.05 Torr). However, a significant amount of the crude product did not sublime even after overnight heating at 170 °C. This was probably due to the strong

intermolecular dipole–dipole interaction between the carbonyl groups. As the ^1H and ^{13}C NMR indicated, the crude product obtained through the aforementioned non-aqueous extraction method was pure, and it was routinely used in other reactions without any further purification.

2.2.6 Synthesis and characterization of diester **16** and bis-bispidine **17**

Bis-bispidinone **13** can serve as a viable substrate from which various types of functional groups could be introduced onto the bis-bispidine tetraazamacrocyclic framework. For instance, diester **16** can be synthesized by the installation of ester groups onto bis-bispidinone **13**, and could be further employed in polymer synthesis through condensation with different diols (Scheme 2.7). On the other hand, the simplest tetraazamacrocycle, bis-bispidine **17** can be prepared by the reduction of bis-bispidinone **13** and is an ideal substrate for metal-coordination studies.

Derivatization of bis-bispidinone **13** was carried out to prepare **16** under Horner–Wadsworth–Emmons reaction conditions^{2,25,26} through the generation of triethyl phosphonoacetate carbanion in the presence of a strong base followed by nucleophilic addition of the carbanion to bis-bispidinone **13**. It should be noted that under the reaction conditions, the tetraazamacrocyclic framework was found to remain intact. After the incorporation of α,β -unsaturated ester groups on **13**, the resulting diester **16** was isolated by conventional aqueous workup and extraction using organic solvents, such as dichloromethane or THF. Purification of the crude product was achieved by column chromatography using reversed-phase silica gel which afforded **16** in 83% yield. Both the ^1H and ^{13}C NMR spectra indicated that the resulting diester **16** had formed successfully.



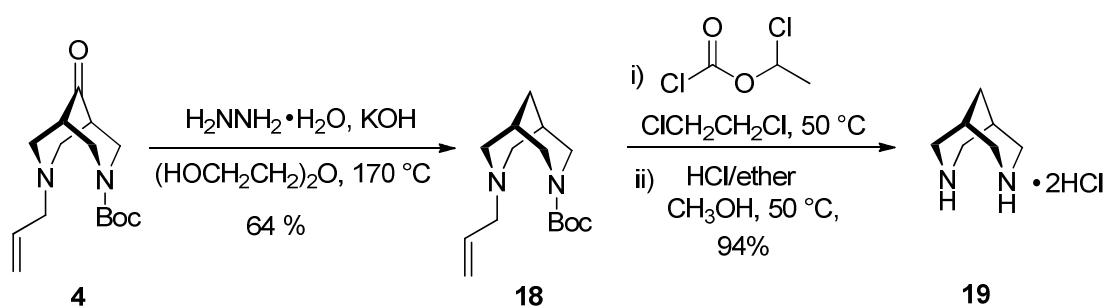
Scheme 2.7 Synthesis of bis-bispidine diester **16** and bis-bispidine **17**.

Bis-bispidinone **13** was subjected to the Wolff–Kishner–Huang–Minlon reduction in the presence of hydrazine monohydrate and potassium hydroxide at 170 °C to afford bis-bispidine **17** in a satisfactory yield.^{2,27,28} It should be mentioned that under these harsh reaction conditions, the tetraazamacrocyclic framework remained intact and the reaction went to completion after 1 h. The purification of the crude product was achieved by sublimation at 80–120 °C under high vacuum (0.05 Torr). The synthesis described herein was found to be efficient in terms of shortened reaction time, straightforward workup procedure as well as lowered reagent toxicity in comparison to the previous literature procedures.^{17,29}

2.2.7 Synthesis and characterization of bispidine hydrochloride **19**

To obtain bis-bispidine tetraazamacrocycle **17** in a more efficient pathway, *N*-Boc-*N'*-allylbispidinone **4** can be reduced to its bispidine derivative **18** before the macrocycle formation.

Thus, reduction of *N*-Boc-*N'*-allylbispidinone **4** under the Wolff–Kishner–Huang–Minlon conditions in the presence of hydrazine monohydrate and potassium hydroxide at 170 °C for 1 h afforded *N*-Boc-*N'*-allylbispidine **18** (Scheme 2.8).^{17,28} The crude product could be isolated by aqueous workup and further purified by column chromatography using silica gel (64% yield). The synthetic protocol could be employed both for large and small scale reactions.



Scheme 2.8 Synthesis of bispidine hydrochloride **19**.

The ^1H and ^{13}C NMR spectra indicate that the desired product **18** was synthesized successfully. The ^1H NMR spectrum of **18** in deuterated chloroform displayed resonances at 1.56 and 1.48 ppm which were assigned to the methylene protons generated by the reduction of the carbonyl group. In addition, the upfield shift of bridgehead protons from 2.31 and 2.28 ppm in **4** to 1.68 and 1.64 ppm in **18**, respectively, was due to the reduction of the carbonyl group.¹ Comparison of the ^{13}C NMR spectra of **4** and **18** indicated the resonance of the carbonyl carbon in **4** at 213.6 ppm was not present in **18** but the newly generated methylene carbon was detected at 32.1 ppm in **18**. The bridgehead carbons also shifted upfield from 48.0 and 47.9 ppm in **4** to 29.5 and 29.4 ppm in **18**, respectively.

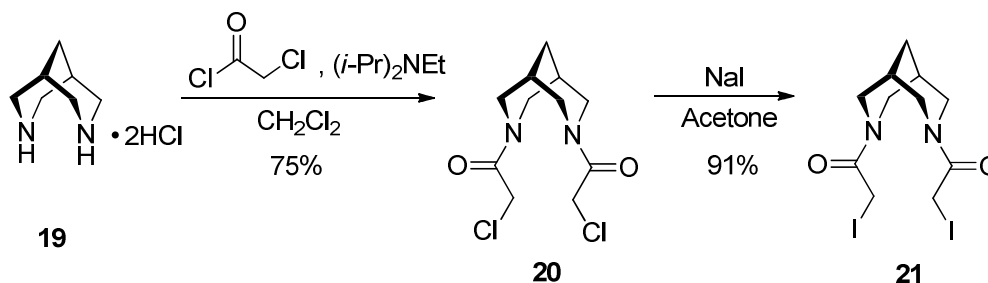
The removal of the allyl group in **18** was straightforward as described previously for **4**.^{1,2,14} Together with the Boc protective group, the 1-chloroethyl carbamate group in the

resulting intermediate was cleaved with HCl in methanol to afford bispidine hydrochloride **19** as a pale yellow residue (Scheme 2.8). The crude residue could be further purified by washing with diethyl ether to give a pale yellow solid **19** in 94% yield.

^1H and ^{13}C NMR displayed straightforward and well resolved peaks confirming the successful formation of **19**. The ^1H NMR of **19** in deuterated methanol exhibited the resonances of the methylene protons between the bridgeheads at 2.02 ppm and the bridgehead protons at 2.42 ppm. In addition, the four equatorial protons on the methylene carbons next to the nitrogen atoms exhibited resonances at 3.54 ppm, whereas the four axial protons appeared at 3.41 ppm. The ^{13}C NMR was also straightforward with the resonances of the carbons adjacent to the nitrogen atoms at 46.2 ppm, the bridgehead carbons at 26.3 ppm, and the methylene carbon at 25.5 ppm.

2.2.8 Synthesis and characterization of bis(iodoacetamide) **21**

Conversion of bispidine hydrochloride **19** to bis(chloroacetamide) **20** was achieved through acetylation of **19** using chloroacetyl chloride in the presence of *N,N*-diisopropylethylamine. Further reaction of **20** with sodium iodide in acetone resulted in bis(iodoacetamide) **21** in excellent yield (Scheme 2.9).



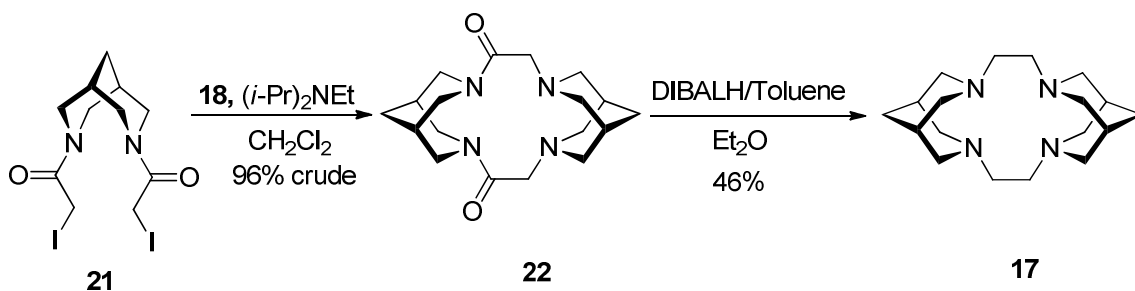
Scheme 2.9 Synthesis of bis(chloroacetamide) **20** and bis(iodoacetamide) **21**.

Both the ^1H and ^{13}C NMR spectra suggested that bis(chloroacetamide) **20** had formed successfully. The ^1H NMR of **20** indicated that the protons on the α -carbon next to the carbonyl group appeared at 4.22 ppm and 3.95 ppm, respectively. In addition, the bridgehead protons and the methylene protons between the bridgeheads exhibited resonances at 2.03 and 1.96 ppm, respectively. The ^{13}C NMR displayed the characteristic amide carbonyl peak at 166.5 ppm and the α -carbon next to the carbonyl group at 41.4 ppm. The peak at 31.9 ppm indicated the bridgehead carbons, while the peak at 28.2 ppm corresponded to the methylene carbon between the bridgehead carbons.

The formation of bis(iodoacetamide) **21** was confirmed by ^1H and ^{13}C NMR. A comparison of the ^1H NMR spectra of **20** and **21** in deuterated chloroform indicated the doublets at 4.22 and 3.95 ppm in **20** which corresponds to the protons on the α -carbons next to the carbonyl group, shifted upfield to 3.87 and 3.60 ppm in **21**, respectively. The upfield shift could be due to the substitution of the chlorine atom by the less electronegative iodine atom. The ^{13}C NMR displayed the characteristic amide carbonyl carbon peak at 167.5 ppm, while the α -carbon next to the carbonyl group exhibited a resonance at -2.8 ppm.

2.2.9 Synthesis and characterization of bisamide **22** and bis-bispidine **17**

Macrocyclization of bis(iodoacetamide) **21** and bispidine hydrochloride **19** in the presence of *N,N*-diisopropylethylamine at ambient temperature in dichloromethane resulted in macrocyclic bisamide **22** in high yield (Scheme 2.10).



Scheme 2.10. Synthesis of macrocyclic bisamide **22** and bis-bispidine **17**.

The cyclization reaction went smoothly to completion in dichloromethane, with a reactant concentration of 0.02 mol/L. After the aqueous workup, the desired pale yellow solid **25** was obtained in 96% yield. Although the crude product could be further purified by column chromatography using basic alumina (75% yield), it was routinely used in subsequent transformations without the need of any further purification.

The structure of **22** was confirmed by ^1H and ^{13}C NMR analysis. The ^1H NMR spectrum in CDCl_3 exhibited broad singlet peaks at 2.18, 2.06, 1.83 and 1.78 ppm corresponding to the four bridgehead protons. In addition, the resonances of the methylene protons on each end of the bisamide **22** were displayed at 1.80 and 1.53 ppm, corresponding to those on the amide and amine side of the macrocycle, respectively. The ^{13}C NMR also indicated well-resolved resonances for all bridgehead carbons and the methylene carbons on each end. This suggested that **22** had a rigid structure due to the presence of the amide functional groups and the bispidine units which can restrict bond rotations.

Reduction of bisamide **22** with DIBAL in diethyl ether²⁰ afforded tetraazamacrocycle **17** (Scheme 2.10). Purification of the crude product was achieved by sublimation as described before (Scheme 2.8). Both ^1H and ^{13}C NMR data indicated that the conversion

of bisamide **22** to bis-bispidine **17** was complete under the reaction conditions. The structure of **17** was confirmed by comparing its ^1H and ^{13}C NMR data with that reported in the literature.³

2.3 Conclusion

The bis-bispidine-based tetraazamacrocyclic compounds have been synthesized effectively and characterized by ^1H , ^{13}C , and IR spectroscopy, as well as by high resolution mass spectrometry. Some of the compounds have also been characterized by single crystal X-ray analysis. Effective synthesis and isolation of bis-bispidinone **13** has been achieved and further functionalizations provide diester **16** and bis-bispidine **17**. Bis-bispidine-based tetraazamacrocycles **12** and **17** have been used for coordination studies which are discussed in Chapter 3.

Reference

- (1) Wang, Z.; Miller, E. J.; Scalia, S. J. *Org. Lett.* **2011**, *13*, 6540.
- (2) Islam, M. J.; Miller, E. J.; Gordner, J. S.; Patel, D.; Wang, Z. *Tetrahedron Lett.* **2013**, *54*, 2133.
- (3) Miyahara, Y.; Goto, K.; Inazu, T. *Tetrahedron Lett.* **2001**, *42*, 3097.
- (4) SMART; Bruker AXS Inc.: Madison, WI, 2001.
- (5) SAINTPlus; Bruker AXS Inc.: Madison, WI, 2001.
- (6) SADABS; Bruker AXS Inc.: Madison, WI, 2001.
- (7) Sheldrick, G. *Acta Crystallogr. Sec. A* **2008**, *64*, 112.
- (8) Sheldrick, G. M. *Universitat Gottingen: Gottingen*, 1997.
- (9) Farrugia, L. *J. Appl. Crystallogr.* **1999**, *32*, 837.
- (10) Farrugia, L. *J. Appl. Crystallogr.* **1997**, *30*, 565.
- (11) Comba, P.; Pritzkow, H.; Schiek, W. *Angew. Chem. Int. Ed.* **2001**, *40*, 2465.
- (12) Comba, P.; Schiek, W. *Coord. Chem. Rev.* **2003**, *238 - 239*, 21.
- (13) Ruenitz, P. C.; Smisman, E. E. *J. Heterocycl. Chem.* **1976**, *13*, 1111.
- (14) Miller, E. J. B.Sc. Thesis, University of Windsor, 2012.
- (15) Tidwell, J. H.; Buchwald, S. L. *J. Am. Chem. Soc.* **1994**, *116*, 11797.
- (16) Olofson, R. A.; Martz, J. T.; Senet, J. P.; Piteau, M.; Malfroot, T. *J. Org. Chem.* **1984**, *49*, 2081.
- (17) Cui, H.; Goddard, R.; Porschke, K.-R. *Organometallics* **2011**, *30*, 6241.
- (18) Bleiholder, C.; Borzel, H.; Comba, P.; Ferrari, R.; Heydt, M.; Kerscher, M.; Kuwata, S.; Laurency, G.; Lawrance, G. A.; Lienke, A.; Martin, B.; Merz, M.; Nuber, B.; Pritzkow, H. *Inorg. Chem.* **2005**, *44*, 8145.

- (19) McKenna, A. G.; McKenna, J. F. *J. Chem. Educ.* **1984**, *61*, 771.
- (20) Taniguchi, T.; Ogasawara, K. *Angew. Chem. Int. Ed.* **1998**, *37*, 1136.
- (21) Constable, E. C. *Coordination Chemistry of Macrocyclic Compounds*; Oxford University Press: New York, 1999.
- (22) Most of the discussion in this section has been taken from our previously published paper: Islam, M. J.; Miller, E. J.; Gordner, J. S.; Patel, D.; Wang, Z., *Tetrahedron Lett.* **2013**, *54*, 2133.
- (23) Comba, P.; Lopez de Laorden, C.; Pritzkow, H. *Helv. Chim. Acta* **2005**, *88*, 647.
- (24) Comba, P.; Haaf, C.; Wadepohl, H. *Inorg. Chem.* **2009**, *48*, 6604.
- (25) Wadsworth, W. S.; Emmons, W. D. *J. Am. Chem. Soc.* **1961**, *83*, 1733.
- (26) Wadsworth, W. S. *Org. React.* **2004**, *73*.
- (27) Huang, M. *J. Am. Chem. Soc.* **1949**, *71*, 3301.
- (28) Murray, R. K.; Babiak, K. A. *J. Org. Chem.* **1973**, *38*, 2556.
- (29) Miyahara, Y.; Goto, K.; Inazu, T. *Synthesis* **2001**, *2001*, 0364.

Chapter 3: Coordination Studies of Bis-bispidine-based Tetraazamacrocycles

3.1 Experimental

3.1.1 Materials and methods

All reagents and anhydrous solvents were used as received from the Aldrich Company unless otherwise indicated. All manipulations of air-sensitive materials were performed under a nitrogen atmosphere either in an MBraun glovebox or by standard Schlenk line techniques. NMR spectra were recorded on 300 and 500 MHz spectrometers and referenced to residual protonated solvent (^1H) or deuterated solvent (^{13}C) unless otherwise specified.

3.1.2 Synthesis and characterization

3.1.2.1 Synthesis of diketal bis-bispidine-copper(II) complexes (Table 3.3)

Reaction of diketal bis-bispidine and copper(II) triflate (Entry 1-1)

To a clear colourless refluxing solution of **1** (50 mg, 0.10 mmol) in anhydrous THF/ CH_3CN (3 mL, 4:1, v/v) was added a pale blue clear solution of $\text{Cu}(\text{CF}_3\text{SO}_3)_2$ (60 mg, 0.17 mmol) in THF/ CH_3CN (1.1 mL, 4:1, v/v) under N_2 atmosphere. After 24 h of reflux, the resulting blueish-green reaction mixture became a pale pink suspension which was completely evaporated to dryness under a stream of air. To the greenish residue, hot distilled water was added and stirred for 1h. In the resulting mixture, the clear purple supernatant was pipetted out and the orange precipitate was dried completely. To the orange precipitate, methanol was added and stirred overnight. The resulting pale yellow clear solution was filtered through a celite pad. Colourless, block-shaped crystals suitable

for X-ray diffraction were grown by the slow evaporation of methanol solution at room temperature. The crystals were characterized as $[(\mathbf{1})\text{H}_2](\text{CF}_3\text{SO}_3)_2$ (**5**) by single crystal X-ray analysis.

Reaction of diketal bis-bispidine and copper(II) chloride dihydrate (Entry 1-2)

To a clear very pale yellow solution of **1** (5.0 mg, 0.01 mmol) in 1 mL of methanol was added a clear very pale green solution of $\text{CuCl}_2 \cdot 2\text{H}_2\text{O}$ (2.0 mg, 0.011 mmol) in 1 mL of methanol. The reaction mixture became a dark purple clear solution immediately, which was stirred at ambient temperature overnight. ^1H NMR analysis of the crude reaction mixture after overnight stirring indicated the complete conversion of **1** to protonated **5**.

Reaction of diketal bis-bispidine and copper(II) acetate (Entry 1-3)

To a very pale yellow clear solution of **1** (15 mg, 0.031 mmol) in 2 mL of methanol was added a cloudy dark blue suspension of $\text{Cu}(\text{OAc})_2$ (7.0 mg, 0.034 mmol) in 1.5 mL of methanol at ambient temperature. After overnight reflux, the reaction mixture remained blue cloudy. ^1H NMR analysis of the crude reaction mixture indicated the presence of **1** and no other product.

3.1.2.2 Synthesis of diketal bis-bispidine-nickel(II) complex

Reaction of diketal bis-bispidine and nickel(II) acetate (Entry 1-4)

To a clear colourless solution of **1** (50.0 mg, 0.104 mmol) in 2 mL of MeOH was added a pale greenish clear solution of $\text{Ni}(\text{OAc})_2 \cdot 4\text{H}_2\text{O}$ (29.0 mg, 0.114 mmol) in 1.5 mL of MeOH. The resulting clear pale greenish solution was refluxed overnight and cooled to room temperature. ^1H NMR analysis of the clear solution indicated the presence of **5**.

3.1.2.3 Synthesis of diketal bis-bispidine-cobalt(II) complex

Reaction of diketal bis-bispidine and cobalt(II) nitrate (Entry 1-5)

To a pale pink clear solution of $\text{Co}(\text{NO}_3)_2 \cdot 6\text{H}_2\text{O}$ (13 mg, 0.046 mmol) in 1 mL of THF/ CH_3CN (4:1, v/v) was added a clear colourless solution of **1** (20 mg, 0.042 mmol) in 1 mL of THF/ CH_3CN (4:1, v/v). The reaction mixture became a pale brown cloudy suspension and was stirred at ambient temperature for 2 days. The crude reaction mixture was then analyzed by ^1H NMR, which indicated the complete conversion of **1** to the protonated **5**.

3.1.2.4 Synthesis of bis-bispidine-copper complex (Table 3.4)

Reaction of bis-bispidine and copper(II) acetate (Entry 2-1)

To a clear pale greenish-blue solution of $\text{Cu}(\text{OAc})_2$ (31 mg, 0.17 mmol) in 14 mL anhydrous ethanol was added a very pale yellow clear solution of **2** (47 mg, 0.15 mmol) in 2.0 mL of anhydrous ethanol at room temperature. The green clear reaction mixture was refluxed for 1 h and the resulting dark green clear solution was evaporated completely to dryness under a stream of air. To the green residue was added 8 mL of 0.22 M NaClO_4 and the mixture was stirred for 2 h at room temperature. The brownish-red clear solution was separated, filtered through a celite pad and evaporated slowly at room temperature and yellow prism crystals were obtained. The crystals were characterized as **7** by single crystal X-ray analysis.

Reaction of bis-bispidine and copper(II) triflate (Entry 2-2)

To a clear colourless solution of **2** (50 mg, 0.16 mmol) in 4.0 mL of anhydrous THF/ CH_3CN (4:1, v/v) was added a pale blue clear solution of $\text{Cu}(\text{CF}_3\text{SO}_3)_2$ (95 mg, 0.26 mmol) in 2.0 mL THF/ CH_3CN (4:1, v/v) under N_2 atmosphere at ambient temperature.

The cloudy green solution was refluxed for 24 h. The resulting pale green suspension was completely evaporated to dryness under a stream of air before hot distilled water (6 mL) was added. After 2 h of stirring, the clear pale pink aqueous layer was separated, filtered through a celite pad and evaporated slowly at room temperature until colourless block shaped crystals formed. ^1H NMR analysis of the reaction mixture indicated the presence of **2** and **7** (**2:7** = **1: 8**).

Reaction of bis-bispidine and copper(II) perchlorate hexahydrate (Entry 2-3)

To a white suspension of **2** (30 mg, 0.099 mmol) in 4 mL of anhydrous acetonitrile was added a clear pale blue solution of $\text{Cu}(\text{ClO}_4)_2 \cdot 6\text{H}_2\text{O}$ (44 mg, 0.12 mmol) in 2 mL of anhydrous acetonitrile at ambient temperature. After overnight stirring at ambient temperature, the dark purple cloudy reaction mixture was evaporated completely to dryness under a stream of air. To the residue, water (2 mL) was added, stirred for 1h and the resulting clear purple solution was separated and analyzed by ^1H NMR, which indicated the complete conversion of **1** to **7**.

Reaction of bis-bispidine and copper(II) chloride dihydrate (Entry 2-4)

To a very pale yellow clear solution of **2** (30 mg, 0.099 mmol) in 1.5 mL of methanol was added a clear dark green solution of $\text{CuCl}_2 \cdot 2\text{H}_2\text{O}$ (18.5 mg, 0.108 mmol) in 1.5 mL of methanol. The slightly cloudy reaction mixture was stirred for 2 h at ambient temperature, let settle, and the pale blue clear supernatant was separated. ^1H NMR analysis of the supernatant indicated the presence of **2** and protonated **7** (**2:7** = 1:6).

Reaction of bis-bispidine and copper(II) acetate in DMSO (Entry 2-5)

To a clear pale greenish-blue solution of $\text{Cu}(\text{OAc})_2$ (31 mg, 0.17 mmol) in 14 mL anhydrous ethanol was added a very pale yellow clear solution of **2** (47 mg, 0.15 mmol) in 2.0 mL of anhydrous ethanol at room temperature. The green clear reaction mixture was refluxed for 1 h and the resulting dark green clear solution was evaporated completely to dryness under a stream of air. To the green residue was added 8 mL of 0.22 M NaClO_4 and the mixture was stirred for 2 h at room temperature. The brownish-red clear solution was separated, filtered through a celite pad, and evaporated slowly at room temperature and yellow prism crystals were obtained. The crystals were characterized as **7** by single crystal X-ray analysis.

3.1.2.5 Synthesis of bis-bispidine-nickel(II) complex

Reaction of bis-bispidine and nickel(II) acetate (Entry 2-6)

To a hot clear colourless solution of **2** (50 mg, 0.16 mmol) in 3 mL of MeOH was added a pale greenish clear solution of $\text{Ni}(\text{OAc})_2 \cdot 4\text{H}_2\text{O}$ (45 mg, 0.18 mmol) in 8 mL of MeOH. The resulting pale yellow clear solution was refluxed for 48 h and then cooled to ambient temperature. The clear pale yellow solution was analyzed by ^1H NMR, which indicated the presence of **2** and protonated **7** (**2:7** = 9:1).

Reaction of bis-bispidine and nickel(II) acetate in DMSO (Entry 2-7)

To a suspension of **2** (20 mg, 0.066 mmol) in 2 mL of anhydrous DMSO was added a pale green clear solution of $\text{Ni}(\text{OAc})_2 \cdot 4\text{H}_2\text{O}$ (18 mg, 0.072 mmol) in 0.5 mL anhydrous DMSO. After stirring for 10 min, the suspension became a clear solution and was heated at 80 °C overnight. ^1H NMR analysis of the pale brown clear solution indicated that there was no **2** left in the reaction medium.

Reaction of bis-bispidine, nickel(II) acetate and DBU in DMSO (Entry 2-8)

To anhydrous DMSO (2 mL) was added DBU and stirred for 30 min followed by **2** (20 mg, 0.066 mmol). To the resulting cloudy suspension was added solid Ni(OAc)₂·4H₂O (18 mg, 0.072 mmol). After 2 days of stirring at room temperature, the clear pale green solution was analyzed by ¹H NMR which indicated the presence of **2** and DBUH⁺. Gradual increase of heating from 50 to 80 °C for 4 days indicated presence of DBUH⁺ and **2**, but no desired nickel complex.

3.1.2.6 Synthesis of bis-bispidine-cobalt(II) complexes

Reaction of bis-bispidine and cobalt(II) nitrate (Entry 2-9)

To a dark pink clear solution of Co(NO₃)₂·6H₂O (29 mg, 0.099 mmol) in 1 mL of MeOD was added a clear colourless solution of **2** (10 mg, 0.033 mmol) in 1 mL of MeOD. After 2 h of stirring at ambient temperature, the cloudy pale brown reaction mixture was settled, filtered through filter paper, and analyzed by ¹H NMR. ¹H NMR analysis of the supernatant indicated the presence of **2** and protonated **7** (**2:7** = 1:14).

3.1.3 X-ray crystallography

3.1.3.1 Data collection and refinement of compound 5

The X-ray crystal structure of compound **5** was obtained at -123 °C, where the crystals were covered in Paratone or Nujol and placed rapidly into the cold N₂ stream of the Kryoflex low-temperature device. The data was collected using the SMART¹ software on a Bruker APEX CCD diffractometer using a graphite monochromator with Mo K α radiation ($\lambda = 0.71073 \text{ \AA}$). A hemisphere of data was collected using a counting time of 10 s per frame. Data reductions were performed using the SAINT² software, and the absorption correction of the raw data were performed using SADABS³. The structures

were solved by direct methods using SHELX⁴ and refined by full-matrix least-squares on F^2 with anisotropic displacement parameters for the non-H atoms using SHELX-97⁵ and the WinGX⁶ software package, and thermal ellipsoid plots were evaluated by ORTEP3.2⁷.

3.1.3.2 Data collection and refinement for compound 7

The X-ray crystal structure of compound 7 was mounted on a Mitegen polyimide micromount with a small amount of Paratone N oil. All X-ray measurements were made on a Bruker Kappa Axis Apex diffractometer at a temperature of -163 °C. The unit cell dimensions were determined from a symmetry constrained fit of 9945 reflections with $4.88^\circ < 2\theta < 75.42^\circ$. The data collection strategy was a number of ω and ϕ scans, which collected data up to 79.19° (2θ). The frame integration was performed using SAINT.⁸ The resulting raw data were scaled and absorption corrected using a multi-scan averaging of symmetry equivalent data using SADABS.⁹ The structure was solved by direct methods using the SIR2011 program.¹⁰ All non-hydrogen atoms were obtained from the initial solution. The hydrogen atoms were introduced at idealized positions and were allowed to ride on the parent atom. The structural model was fit to the data using full matrix least-squares based on F^2 . The calculated structure factors included corrections for anomalous dispersion from the usual tabulation. The structure was refined using the SHELXL-2013 program.⁴ Graphic plots were produced using the NRCVAX program.¹¹

3.1.3.3 Crystallographic data

Table 3.1. Crystallographic data for compound 5

Formula	$C_{26}H_{50}N_4O_4 \cdot (CF_3SO_3)_2$	
Formula weight (<i>g/mol</i>)	780.84	
Crystal dimensions (<i>mm</i>)	$0.26 \times 0.18 \times 0.08$	
Crystal colour and habit	Colourless, block	
Crystal system	Triclinic	
Space group	P-1	
Temperature, K	150	
Unit cell dimensions	$a = 8.126(3) \text{ \AA}$	$\alpha = 104.734(4)^\circ$
	$b = 8.167(3) \text{ \AA}$	$\beta = 95.430(4)^\circ$
	$c = 13.517(4) \text{ \AA}$	$\gamma = 91.032(4)^\circ$
$V, \text{ \AA}^3$	862.8(5)	
Number of reflections to determine final unit cell	3187	
Min and Max 2θ for cell determination, $^\circ$	5.2, 56.2	
Z	1	
F(000)	412	
ρ (<i>g/cm</i>)	1.503	
$\lambda, \text{ \AA}$, (MoK α)	0.71073	
$\mu, (mm^{-1})$	0.25	
Diffractometer type	Bruker APEX CCD	
Scan types	ω and ϕ scans	
Max 2θ for data collection, $^\circ$	57.0	
Measured fraction of data	0.993	
Number of reflections measured	3975	
Unique reflections measured	3974	
R_{merge}	0.0576	
Number of reflections included in refinement	3247	
Cut off threshold expression	$I > 2\sigma(I)$	
Structure refined using	Full-matrix least-squares on F^2	
Weighting scheme	$w = 1/[\sigma^2(F_o^2) + (0.1017P)^2 + 0.1212P]$	

	where $P = (F_o^2 + 2F_c^2)/3$
Number of parameters in least-squares	326
R ₁	0.0576
wR ₂	0.1486
R ₁ (all data)	0.0725
wR ₂ (all data)	0.1674
Goodness-of-fit, ^b S on F^2	1.095
Maximum shift/error	0.039
Min & max peak heights on final ΔF map ($e^-/\text{\AA}$)	-0.65, 1.01

Table 3.2. Crystallographic data for compound 7

Formula	$C_{18}H_{34}N_4 \cdot (ClO_4)_2$	
Formula weight (g/mol)	505.39	
Crystal dimensions (mm)	$0.342 \times 0.175 \times 0.124$	
Crystal colour and habit	Yellow prism	
Crystal system	Monoclinic	
Space group	P 2 ₁ /c	
Temperature, K	110	
Unit cell dimensions	$a = 7.6275(17) \text{\AA}$	$\alpha = 90^\circ$
	$b = 14.438(4) \text{\AA}$	$\beta = 110.363(7)^\circ$
	$c = 10.889(4) \text{\AA}$	$\gamma = 90^\circ$
V, \AA^3	1124.2(5)	
Number of reflections to determine final unit cell	9945	
Min and max 2θ for cell determination, $^\circ$	4.88, 75.42	
Z	2	
F(000)	536	
ρ (g/cm)	1.493	
λ , \AA , (MoK α)	0.71073	
μ , (cm^{-1})	0.342	
Diffractionmeter type	Bruker Kappa Axis Apex2	
Scan types	ω and ϕ scans	

Max 2θ for data collection, °	79.19
Measured fraction of data	0.998
Number of reflections measured	69262
Unique reflections measured	6771
R _{merge}	0.0353
Number of reflections included in refinement	6771
Cut off threshold expression	I > 2sigma(I)
Structure refined using	Full matrix least-squares using F ²
Weighting scheme	w=1/[σ ² (Fo ²)+(0.0622P) ² +0.5029P] where P=(Fo ² +2Fc ²)/3
Number of parameters in least-squares	256
R ₁	0.0497
wR ₂	0.1247
R ₁ (all data)	0.0792
wR ₂ (all data)	0.1414
Goodness-of-fit, ^b S on F ²	1.035
Maximum shift/error	0.000
Min & max peak heights on final ΔF map (e ⁻ /Å)	-0.822, 1.281

^aR₁(F) = {Σ(|F_o| - |F_c|)/Σ|F_o|} for reflections with F_o > 4(σ(F_o)).

wR₂(F²) = {Σw(|F_o|² - |F_c|²)²/Σw(|F_o|²)²}^{1/2}, where 'w' denotes the weight given each reflection.

^bS = GOF = [Σw(|F_o|² - |F_c|²)²]/(n-p)^{1/2}, hence, 'n' is the number of reflections and 'p' is the number of parameters used.

3.2 Results and discussion

Bis-bispidine-based tetraazamacrocycles **1** and **2** ($R = H$) are anticipated to be effective ligands which can bind metal ions such as Cu^{2+} , Ni^{2+} and Co^{2+} selectively and form stable complexes (Figure 3.1).¹² Comba et al. studied the coordination reaction of **3** ($R = Me$) with $Cu(CF_3SO_3)_2$ at reflux in CH_3CN/THF for 24 h under an argon atmosphere.¹³ The complex was characterized by UV-Visible spectroscopy and elemental analysis. The electronic spectra showed that **3** had the highest ligand field strength for a tetraamine donor. This is the only instance where a metal-bis-bispidine complex has been reported. To date, no crystal structure has been obtained from the complex.

The calculated available cavity $r(H)$ of **1** is 1.29-1.32 Å and the ionic radii of Cu^{2+} , Ni^{2+} and Co^{2+} are 0.75 Å, 0.69 Å and 0.75 Å, respectively. The half distance r between the two diagonal donor nitrogen atoms in **1** is 2.00-2.04 Å, comparable to the Cu-N distance of ca. 1.98 Å in the calculated structure of the copper(II)-**3** complex.¹³ It is expected that Cu^{2+} , Ni^{2+} and Co^{2+} ions would fit well into the cavity of bis-bispidine-based tetraazamacrocycles **1** and **2** and form stable complexes.

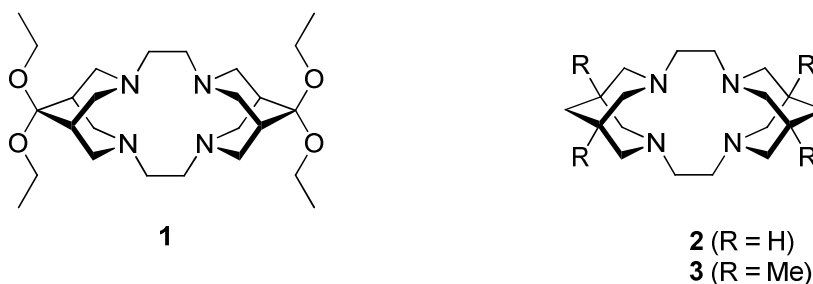
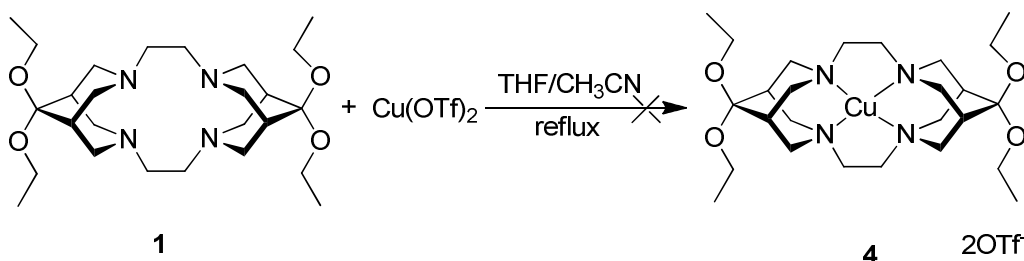


Figure 3.1 Bis-bispidine tetraazamacrocycles **1–3**

3.2.1 Synthesis towards metal-diketal bis-bispidine complexes

3.2.1.1 Attempted synthesis of **4**

The reaction of diketal bis-bispidine tetraazamacrocyclic **1** and copper(II) triflate was carried out by refluxing a mixture of **1** and copper(II) triflate in anhydrous THF/CH₃CN under nitrogen atmosphere for 3 h according to literature procedures used by Comba et al. (Scheme 3.1).¹³ This afforded a cloudy green suspension and the analysis of the reaction mixture by ¹H NMR in deuterated methanol indicated the peaks corresponding to the bridgehead protons and the ethylene bridge protons shifted from 2.20 ppm and 2.66 ppm in **1** to 2.52 and 3.10 ppm, respectively. The equatorial and axial methylene protons adjacent to the nitrogen atoms shifted downfield to 3.50 and 3.21 ppm from 3.09 and 2.81 ppm in **1**, respectively. By comparing the ¹H NMR spectrum of the reaction mixture and the spectrum obtained from the protonated **1**, it was confirmed that protonation of ligand **1** had occurred during the coordination reaction.



Scheme 3.1 Coordination reaction of **1** with copper(II) triflate.

Further refluxing of the reaction mixture under a nitrogen atmosphere for a total of 24 h resulted in a pale pink suspension without any change in the ¹H NMR spectrum. Evaporation of the solvents followed by washing the green residue with hot distilled water gave an orange solid. The ¹H NMR of the orange solid in deuterated methanol

showed a resonance at 9.6 ppm which was characteristic of the protons in the tetramine core. Slow evaporation of the NMR solution at ambient temperature resulted in colourless block-shaped crystals.

3.2.1.2 Crystallographic data analysis of **5**

Single crystal X-ray diffraction analysis of the colourless block-shaped crystals confirmed the formation of protonated diketal bis-bispidine tetraazamacrocycle **5** with triflate as the counter ions (Figure 3.2).

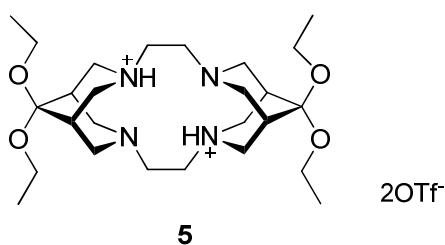


Figure 3.2 Protonated diketal bis-bispidine tetraazamacrocycle **5**.

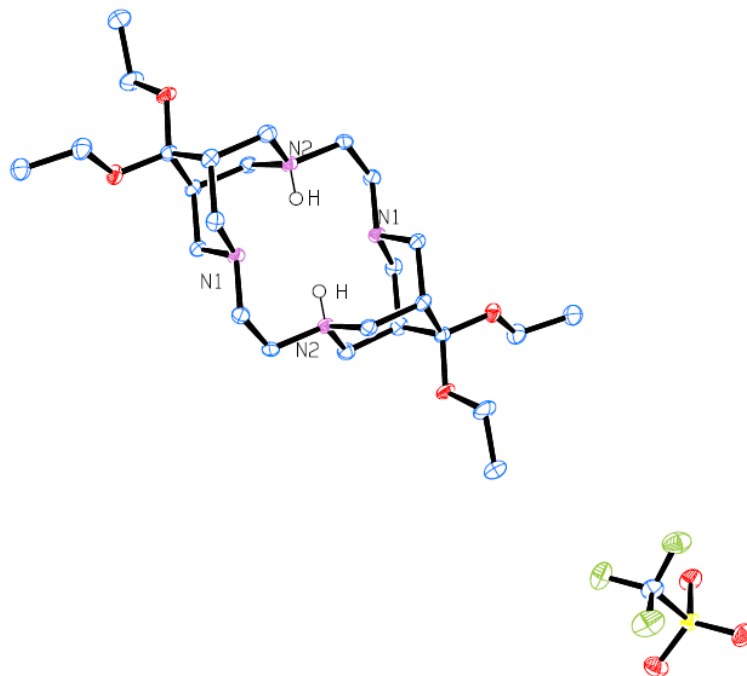


Figure 3.3 Crystallographic ORTEP plot of protonated diketal bis-bispidine **5**. Ellipsoids are at the 50% probability level.

The ORTEP plot of **5** is shown in Figure 3.3. It is observed that the nonbonding N1...N2 distance between the two nitrogen atoms on the same side of a bispidine unit is reduced from 2.87 Å in **1** to 2.71 Å in **5**. The shortening of the N1...N2 distance could be due to the minimization of the repulsion between the lone pairs of electrons on the nitrogen atoms as a result of the protonation. It should be mentioned that this phenomenon is common for protonated bispidine compounds as well as their metal-complexes.¹⁴⁻¹⁶ Moreover, the bonding and nonbonding distances N2-H and N1...H were observed as 0.87 and 2.11 Å, respectively, which are in good agreement with the reported values for protonated bis-bispidine.¹⁷ Although anhydrous acetonitrile and THF were used for the reaction under a nitrogen atmosphere, the protonation of **1** may be due to the presence of trace amounts of acids, either in the solvents or in copper(II) triflate.

3.2.1.3 Coordination of **1** with Cu²⁺, Ni²⁺ and Co²⁺ ions

Different reaction conditions have been tested in an attempt to achieve the desired complex (Table 3.3). The reaction of **1** and CuCl₂·2H₂O in methanol at ambient temperature resulted in a clear dark purple solution. After overnight stirring, the solution was analysed by ¹H NMR in deuterated methanol, which indicated the complete conversion of **1** to its protonated species **5** (Entry 1-2). When the reaction was carried out using **1** and Cu(OAc)₂ in methanol under overnight reflux, the ¹H NMR in deuterated methanol showed the presence of only **1** and no other product (Entry 1-3). Attempts had also been made to coordinate diketal bis-bispidine **1** with other metal ions, such as Co²⁺ and Ni²⁺, because their ionic radii are close to that of the Cu²⁺ ion (Co²⁺ = 0.75 Å, Ni²⁺ = 0.69 Å, Cu²⁺ = 0.75 Å).

The reaction of Ni(OAc)₂·4H₂O and **1** in methanol upon overnight reflux resulted in **1** and no other product (Entry 1-4), whereas the reaction of **1** with Co(NO₃)₂·6H₂O in THF/CH₃CN under reflux for 48 h gave no desired product (Entry 1-5).

Table 3.3 Reaction conditions of **1** with metal ions

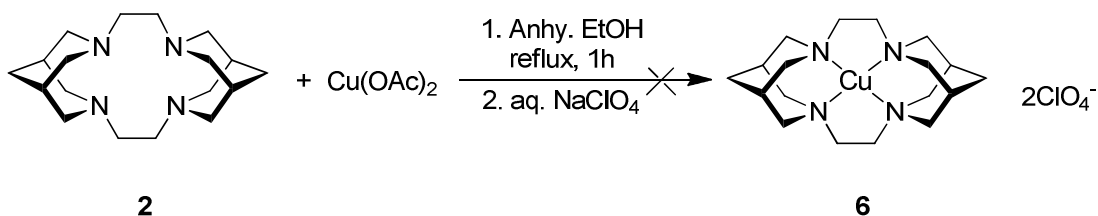
Entry	Metal salt	Solvent	Temperature °C	Reaction time	Outcome*
1-1	Cu(CF ₃ SO ₃) ₂	THF/CH ₃ CN	reflux	24 h	5
1-2	CuCl ₂ ·2H ₂ O	MeOH	rt	overnight	5
1-3	Cu(OAc) ₂	MeOH	reflux	overnight	No reaction
1-4	Ni(OAc) ₂ ·4H ₂ O	MeOH	reflux	overnight	No reaction
1-5	Co(NO ₃) ₂ ·6H ₂ O	THF/CH ₃ CN	rt	48 h	No reaction

*Results are based on ¹H NMR

3.2.2 Synthesis towards metal-bis-bispidine complexes

3.2.2.1 Attempted synthesis of **6**

Bis-bispidine tetraazamacrocycle **2** was used in the coordination reaction with copper(II) acetate in anhydrous ethanol (Scheme 3.2).



Scheme 3.2 Coordination reaction of **2** with copper(II) acetate.

After 1 h of reflux, the clear green reaction mixture was analysed by ^1H NMR in deuterated chloroform and displayed an inconclusive spectrum with broad peaks. Although the ^1H NMR in deuterated methanol did not show any new peaks besides the proton resonances of **2**, it was thought that the desired copper complex might not show in the NMR spectrum due to the paramagnetic property of the copper(II) species.¹⁸ The green reaction mixture was evaporated. Addition of 0.22 M NaClO_4 aqueous solution to the green residue gave a clear pale orange-yellow solution. Slow evaporation of the solution at ambient temperature yielded yellow prism crystals, which were analysed by single crystal X-ray diffraction. The structure was that of protonated bis-bispidine tetraazamacrocycle **7** (Figure 3.4).

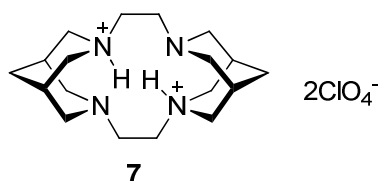


Figure 3.4 Protonated bis-bispidine tetraazamacrocycle **7**.

3.2.2.2 Crystallographic data analysis of **7**

The crystal structure of **7** is disordered (Figure 3.5). The normalized occupancy for the major disorder fraction in the diprotonated cation was refined to a value of 0.80 (Figure 3.6). It exhibits a $\text{N1}\cdots\text{N2}$ distance of 2.72 Å. This is consistent with that in **5** (Figure 3.2 and Figure 3.3) and $(\text{D}^+)_2\cdot(\text{Cl}^-)_2\cdot 4\text{CHCl}_3$ which had been reported previously.¹⁷ Although the N2-H distance of 1.00 Å is slightly longer than the values in **5** (0.87 Å) and $(\text{D}^+)_2\cdot(\text{Cl}^-)_2\cdot 4\text{CHCl}_3$ (0.86 Å), it is comparable to the value obtained from DFT calculations for diprotonated bis-bispidine tetraazamacrocycle (1.04 Å).¹⁴

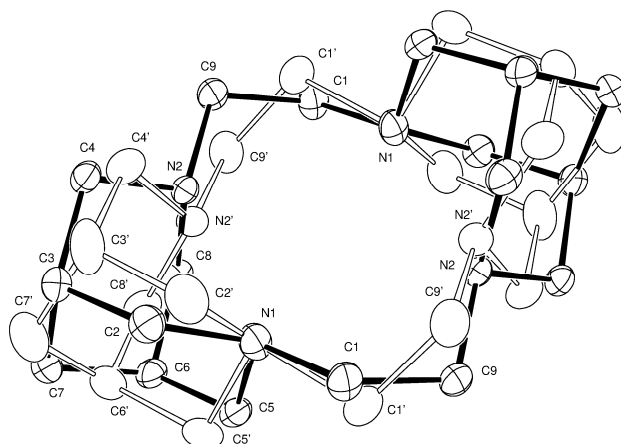


Figure 3.5. ORTEP diagram of protonated cation of **7**. Ellipsoids are at the 50% probability level and hydrogen atoms are omitted for clarity. Major and minor components are depicted with solid and open bonds, respectively.

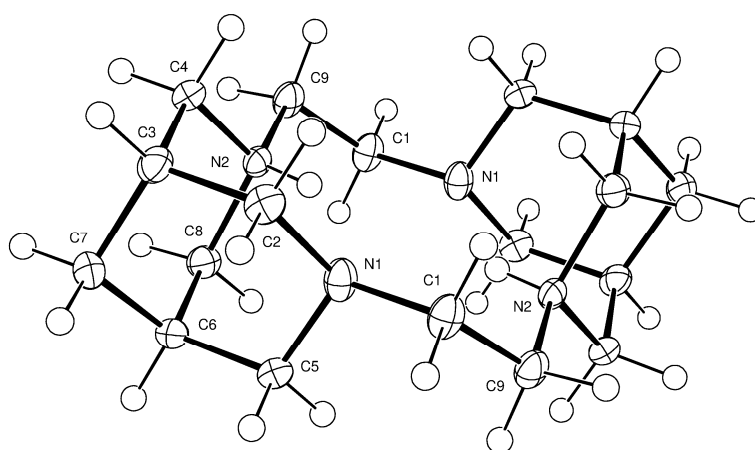


Figure 3.6 ORTEP drawing for the cation of **7** (major component). Ellipsoids are at the 50% probability level.

In addition, the perchlorate anion also exhibits a disordered structure with CL1, O1, and O2 maintaining their positions, while O3 and O4 have secondary positions at O3' and O4' (Figure 3.7). The normalized occupancy for the major disorder component in the anion was refined to a value of 0.59.

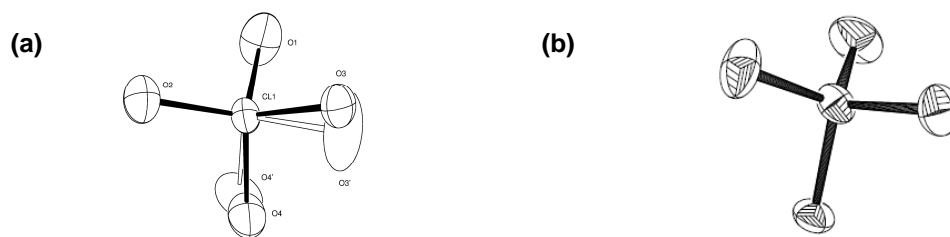


Figure 3.7 ORTEP diagram of **(a)** disordered perchlorate anion of **7**, major and minor component are depicted with solid and open bonds, respectively. **(b)** major component of perchlorate anion. In both cases, ellipsoids are at the 50% probability level.

3.2.2.3 Coordination of **2** with Cu^{2+} , Ni^{2+} and Co^{2+} ions

The coordination of **2** with different metal ions is summarized in Table 3.4. Reaction of bis-bispidine **2** with $\text{Cu}(\text{CF}_3\text{SO}_3)_2$ in anhydrous acetonitrile/methanol at reflux for 24 h resulted in a pale green suspension.¹³ Analysis of the reaction mixture by ^1H NMR in MeOD indicated the conversion of **2** to its protonated species **7** with a **2:7** ratio of 1:8 (Entry 2-2). The reaction was also carried out in anhydrous acetonitrile with $\text{Cu}(\text{ClO}_4)_2 \cdot 6\text{H}_2\text{O}$ at room temperature. ^1H NMR analysis of the reaction mixture indicates the conversion of **2** to its protonated species, **7** (Entry 2-3).

The reaction of **2** with $\text{Co}(\text{NO}_3)_2 \cdot 6\text{H}_2\text{O}$ in methanol at room temperature yielded a cloudy pale brown suspension. ^1H NMR analysis of the reaction mixture showed that **2** had converted to the protonated species **7** (Entry 2-9).

Based on the above results, it was thought that the protonation of ligand **2** in the reaction medium might be due to the presence of a trace amount of protons in either the protic solvents or the metal ion reagents. Therefore, aprotic anhydrous DMSO was chosen as a solvent for the coordination reaction. Heating $\text{Cu}(\text{OAc})_2$ in anhydrous DMSO for 66 h

resulted in broad peaks in the ^1H NMR spectrum which showed no starting material **2** nor protonated compound **7** (Entry 2-5). Reaction of **2** with $\text{Ni}(\text{OAc})_2 \cdot 4\text{H}_2\text{O}$ in DMSO indicated the conversion of **2** to **7** (Entry 2-7).

Table 3.4 Reaction conditions of **2** with metal ions

Entry	Metal ion source	Solvent	Temperature °C	Reaction time	Outcome*
2-1	$\text{Cu}(\text{OAc})_2$	EtOH	reflux	1 h	7
2-2	$\text{Cu}(\text{CF}_3\text{SO}_3)_2$	Anhy THF/ CH_3CN	reflux	24 h	2 and 7
2-3	$\text{Cu}(\text{ClO}_4)_2 \cdot 6\text{H}_2\text{O}$	Anhy. CH_3CN	rt	12h	7
2-4	$\text{CuCl}_2 \cdot 2\text{H}_2\text{O}$	MeOH	rt	2 h	2 and 7
2-5	$\text{Cu}(\text{OAc})_2$	Anhy. DMSO	rt to 100 °C	66 h	No 2 or 7
2-6	$\text{Ni}(\text{OAc})_2 \cdot 4\text{H}_2\text{O}$	MeOH	reflux	48 h	2 and 7
2-7	$\text{Ni}(\text{OAc})_2 \cdot 4\text{H}_2\text{O}$	Anhy. DMSO	rt to 80 °C	4 d	7
2-8	$\text{Ni}(\text{OAc})_2 \cdot 4\text{H}_2\text{O}$	Anhy. DMSO + DBU	rt to 80 °C	4 d	inconclusive
2-9	$\text{Co}(\text{NO}_3)_2 \cdot 6\text{H}_2\text{O}$	MeOH	rt	2 h	7

* Results are based on ^1H NMR

The reaction mixture in Entry 2-1 was analyzed by UV-Visible spectroscopy in H_2O and in CH_3NO_2 and no absorption peak was detected. To understand the reaction better, bis-bispidine macrocycle **2** in dry DMSO was heated at 80 °C overnight. It was observed that some of **2** were converted to its protonated species **7**. Prolonged heating at 80 °C for 2 days resulted in the complete conversion of **2** to its protonated species. This indicated that the bis-bispidine macrocycle **2** could be protonated even in anhydrous DMSO.

It was thought that addition of a strong base, such as DBU, could abstract the trace amount of protons in DMSO and **2** would undergo coordination with metal ions without being protonated. However, reaction of **2** and Ni(OAc)₂·6H₂O in dry DMSO in the presence of excess DBU at ambient temperature for 48 h gave **2** and DBU·H⁺ but no desired product. Gradual heating of the reaction mixture from 50 to 80 °C again gave **2** and DBU·H⁺ but no desired metal complex (Entry 2-7).

3.3 Conclusion

Attempts to obtain metal complexes using bis-bispidine-based tetraazamacrocycles and different metal ions such as Cu²⁺, Ni²⁺ and Co²⁺ were unsuccessful. No desired complex was formed under the reaction conditions, including those reported by Comba et al. To accomplish the desired metal-bis-bispidine complexes, therefore, requires more systematic study. A possible method can be template synthesis.

Reference

- (1) SMART; Bruker AXS Inc.: Madison, WI, 2001.
- (2) *SAINTPlus*; Bruker AXS Inc.: Madison, WI, 2001.
- (3) *SADABS*; Bruker AXS Inc.: Madison, WI, 2001.
- (4) Sheldrick, G. *Acta Crystallogr., Sect. A* **2008**, *64*, 112.
- (5) Sheldrick, G. M. *Universitat Gottingen: Gottingen*, 1997.
- (6) Farrugia, L. *J. Appl. Cryst.* **1999**, *32*, 837.
- (7) Farrugia, L. *J. Appl. Cryst.* **1997**, *30*, 565.
- (8) Bruker-Nonius; SAINT version 2012.12 ed. Bruker-Nonius, Madison, WI 53711, USA, 2012.
- (9) Bruker-Nonius; SADABS version 2012.1 ed. Bruker-Nonius, Madison, WI 53711, USA, 2012.
- (10) Burla, M. C.; Caliandro, R.; Camalli, M.; Carrozzini, B.; Cascarano, G. L.; Giacovazzo, C.; Mallamo, M.; Mazzone, A.; Polidori, G.; Spagna, R. *J. Appl. Cryst.*, *45*, 357.
- (11) Gabe, E. J.; Le Page, Y.; Charland, J. P.; Lee, F. L.; White, P. S. *J. Appl. Cryst.* **1989**, *22*, 384.
- (12) Comba, P.; Schiek, W. *Coord. Chem. Rev.* **2003**, *238 - 239*, 21.
- (13) Comba, P.; Pritzkow, H.; Schiek, W. *Angew. Chem. Int. Ed.* **2001**, *40*, 2465.
- (14) Galasso, V.; Goto, K.; Miyahara, Y.; Kovac, B.; Klasinc, L. *Chem. Phys.* **2002**, *277*, 229.

- (15) Bleiholder, C.; Borzel, H.; Comba, P.; Ferrari, R.; Heydt, M.; Kerscher, M.;
Kuwata, S.; Laurency, G.; Lawrance, G. A.; Lienke, A.; Martin, B.; Merz, M.;
Nuber, B.; Pritzkow, H. *Inorg. Chem.* **2005**, *44*, 8145.
- (16) Comba, P.; Haaf, C.; Wadepohl, H. *Inorg. Chem.* **2009**, *48*, 6604.
- (17) Miyahara, Y.; Goto, K.; Inazu, T. *Tetrahedron Lett.* **2001**, *42*, 3097 and 9097
(corrigendum).
- (18) Black, D. S. C.; Deacon, G. B.; Rose, M. *Tetrahedron* **1995**, *51*, 2055.

Chapter 4: Conclusion and Future Work

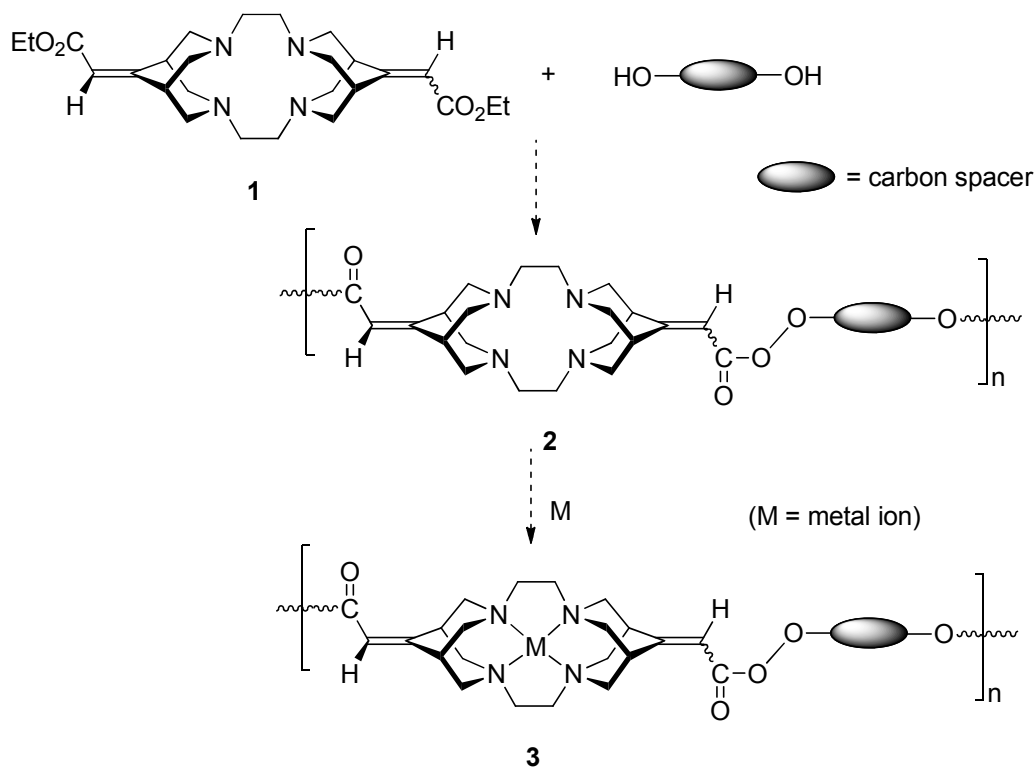
4.1 Conclusion

Bis-bispidine-based tetraazamacrocycles with various functional groups have been synthesized (Chapter 2). The macrocyclic bisamide **10** was prepared through the cyclization reaction of an unusually stable bispidine diethyl ketal **7** and bis(iodoacetamide) **9**. Both **7** and **9** were constructed from *N*-Boc-*N'*-allylbispidinone **4**. Successful reduction of bisamide **10** followed by the cleavage of ethyl groups afforded bis-bispidinone **13**. This versatile bis-bispidinone substrate **13** was used to obtain bis-bispidine-based tetraazamacrocycles **16** and **17**. Chapter 2 also includes an alternative pathway to obtain bis-bispidine tetraazamacrocycle **17**.

Attempts have been taken to achieve the Cu²⁺, Ni²⁺ and Co²⁺ complexes of bis-bispidine-based tetraazamacrocycles **12** and **17** (Chapter 3). No desired metal complexes of bis-bispidine-based tetraazamacrocycles have been obtained.

4.2 Future Work

To achieve the desired metal complexes of bis-bispidine-based tetraazamacrocycles, more systematic study using various transition metal ions under different reaction conditions is required. Once formed, the optical and electronic properties of the complexes will be studied. Furthermore, as part of the research interest in our group to prepare polymetallomacrocycles, bis-bispidine tetraazamacrocycle **1** can be incorporated into a polymer backbone through step-growth polymerization with different diols which have aliphatic or aromatic carbon spacers (Scheme 4.1). These types of polymers could be used to incorporate metal ions to form polymetallomacrocycles **3** which are expected to have interesting optical and electronic properties.



Scheme 4.1 Proposed synthesis of polymacrocycle **2** and polymetallomacrocycle **3**.

Appendices

Appendix A: Copyright Permissions



RightsLink®

Home Account Info Help



Title: Effective synthesis of bis-bispidonone and facile difunctionalization of highly rigid macrocyclic tetramines
Author: Md. Jahirul Islam, Erin J. Miller, Jacob S. Gordner, Deep Patel, Zhuo Wang
Publication: Tetrahedron Letters
Publisher: Elsevier
Date: 24 April 2013
Copyright © 2013, Elsevier

Logged in as:
Jahirul Islam
Account #:
3000669938

LOGOUT

Order Completed

Thank you very much for your order.

This is a License Agreement between Jahirul Islam ("You") and Elsevier ("Elsevier"). The license consists of your order details, the terms and conditions provided by Elsevier, and the [payment terms and conditions](#).

[Get the printable license.](#)

License Number	3236840481078
License date	Sep 26, 2013
Licensed content publisher	Elsevier
Licensed content publication	Tetrahedron Letters
Licensed content title	Effective synthesis of bis-bispidonone and facile difunctionalization of highly rigid macrocyclic tetramines
Licensed content author	Md. Jahirul Islam, Erin J. Miller, Jacob S. Gordner, Deep Patel, Zhuo Wang
Licensed content date	24 April 2013
Licensed content volume number	54
Licensed content issue number	17
Number of pages	4
Type of Use	reuse in a thesis/dissertation
Portion	full article
Format	both print and electronic
Are you the author of this Elsevier article?	Yes
Will you be translating?	No
Order reference number	
Title of your thesis/dissertation	Synthesis and Characterization of Bis-bispidine-based Tetraazamacrocycles and Their Coordination Studies
Expected completion date	Oct 2013
Estimated size (number of pages)	130
Elsevier VAT number	GB 494 6272 12
Permissions price	0.00 USD
VAT/Local Sales Tax	0.00 USD / 0.00 GBP
Total	0.00 USD

ORDER MORE...

CLOSE WINDOW

Copyright © 2013 Copyright Clearance Center, Inc. All Rights Reserved. [Privacy statement](#). Comments? We would like to hear from you. E-mail us at customercare@copyright.com

Vita Auctoris

Name	Md. Jahirul Islam
Place of birth	Chandpur, Bangladesh
Education	University of Windsor, Department of Chemistry and Biochemistry, M. Sc, 2011 – 2013 Shahjalal University of Science & Technology, M. Sc., Sylhet, Bangladesh, 2004 – 2005. Shahjalal University of Science & Technology, B.Sc. (Hons.), Sylhet, Bangladesh, 2001 – 2004.
Scholarships/ Awards	University of Windsor Master's International Entrance (Tuition) Scholarship, 2011 – 2013. University of Windsor Master's International Excellence Scholarship, 2011 – 2012. Graduate Student Society (GSS) Scholarship, 2011 – 2012. International Student Society (ISS) Bursary Award, 2012.
Professional Work History	Research and Teaching Assistant University of Windsor, Windsor, Ontario, Canada Sept 2011 – Sept 2013. Council Representative, Department of Chemistry & Biochemistry, Graduate Student Society (GSS), Sept 2011 – Aug 2012.
Publication	Islam, M. J.; Miller, E. J.; Gordner, J. S.; Patel, D.; Wang, Z. <i>Tetrahedron Lett.</i> 54, 2013 , 2133–2136.

Islam, M. J.; Subhan, M. A. *Proc. Pakistan Acad. Sci.* 47(2), **2010**, 87–93.

Shahed, S. M. F., **Islam, M. J.;** Choudhuri, M. M. R.; Susan, M. A. B. H. *J. Bangladesh Chem. Soc.*, 22, **2009**, 123-130.

Islam, M. J.; Choudhuri, M. M. R.; Shahed, S. M. F.; Subhan, M. A. *Proc. Pakistan Acad. Sci.* 46(2), **2009**, 91–95.

**Conference
Posters**

Synthesis and Property Studies of Bis-bispidine-based Tetraazamacrocycles, **Islam, M. J.;** Miller, E. J.; Gordner, J. S.; Patel, D.; Wang, Z. *96th Canadian Chemistry Conference* , Quebec City, Quebec, Canada , May 26-30, **2013**.

Synthesis and Characterization of Funtionalized Bis-bispidine Tetraazamacrocycles, **Islam, M. J.;** Miller, E. J.; Gordner, J. S.; Patel, D.; Wang, Z. *Quebec Ontario Minisymposium in Synthetic and Bioorganic Chemistry (QOMSSOC)*, Windsor, ON, Canada, Nov 9-11, **2012**.

Effect of Some Biologically Important Compounds on the Critical Micelle Concentration of Sodium Dodecyl Sulfate in Aqueous Solution”, **Islam, M, J.;** Subhan, M, A. *31st Annual Conference of Bangladesh Chemical Society*, Dhaka, Bangladesh, Jan 30-Feb 1, **2009**.